

Universität Bonn

Physikalisches Institut

Non-perturbative aspects of string theory from elliptic curves

Jonas Reuter

We consider two examples for non-perturbative aspects of string theory involving elliptic curves. First, we discuss F-theory on genus-one fibered Calabi-Yau manifolds with the fiber being a hypersurface in a toric fano variety. We discuss in detail the fiber geometry in order to find the gauge groups, matter content and Yukawa couplings of the corresponding supergravity theories for the four examples leading to gauge groups $SU(3) \times SU(2) \times U(1)$, $SU(4) \times SU(2) \times SU(2)/\mathbb{Z}_2$, $U(1)$ and \mathbb{Z}_3 . The theories are connected by Higgsings on the field theory side and conifold transitions on the geometry side. We extend the discussion to the network of Higgsings relating all theories stemming from the 16 hypersurface fibrations. For the models leading to gauge groups $SU(3) \times SU(2) \times U(1)$, $SU(4) \times SU(2) \times SU(2)/\mathbb{Z}_2$ and $U(1)$ we discuss the construction of vertical G_4 fluxes. Via the D3-brane tadpole cancelation condition we can restrict the minimal number of families in the first two of these models to be at least three.

As a second example for non-perturbative aspects of string theory we discuss a proposal for a non-perturbative completion of topological string theory on local B-model geometries. We discuss in detail the computation of quantum periods for the examples of local \mathbb{F}_1 , local \mathbb{F}_2 and the resolution of $\mathbb{C}^3/\mathbb{Z}_5$. The quantum corrections are calculated order by order using second order differential operators acting on the classical periods. Using quantum geometry we calculate the refined free energies in the Nekrasov-Shatashvili limit. Finally we check the non-perturbative completion of topological string theory for the geometry of local \mathbb{F}_2 against numerical calculations.

Physikalisches Institut der
Universität Bonn
Nussallee 12
D-53115 Bonn



BONN-IR-2015-07
August 2015
ISSN-0172-8741

Non-perturbative aspects of string theory from elliptic curves

Dissertation
zur
Erlangung des Doktorgrades (Dr. rer. nat.)
der
Mathematisch-Naturwissenschaftlichen Fakultät
der
Rheinischen Friedrich-Wilhelms-Universität Bonn

von
Jonas Reuter
aus
Bonn

Bonn, 2015

Dieser Forschungsbericht wurde als Dissertation von der Mathematisch-Naturwissenschaftlichen Fakultät der Universität Bonn angenommen und ist auf dem Hochschulschriftenserver der ULB Bonn http://hss.ulb.uni-bonn.de/diss_online elektronisch publiziert.

1. Gutachter: Prof. Dr. Albrecht Klemm
2. Gutachter: PD Dr. Stefan Förste

Tag der Promotion: 11.08.2015
Erscheinungsjahr: 2015

Acknowledgements

First, I would like to thank my supervisor Prof. Dr. Albrecht Klemm for introducing me to string theory and mathematical physics and for giving me the opportunity to work on these subjects. I also thank PD. Dr. Stefan Förste for being my second advisor.

Futhermore I am deeply indepted to Prof. Dr. Mirjam Cvetič, Jie Gu, Prof. Dr. Min-xin Huang, Prof. Dr. Marcos Mariño, Dr. Damian Mayorga, Paul Oehlmann, Hernan Piragua and Dr. Marc Schiereck for interesting discussions and the fruitful collaborations. Especially I would like to express my deep gratitude to Dr. Denis Klevers for teaching me countless things about physics in general and in particular F-theory and geometry.

For proofreading I thank Jie Gu, Dr. Hans Jockers, Dr. Denis Klevers, Paul Oehlmann and Elisabeth Theobald.

I also thank the other current and former members of our group for the nice atmosphere and many interesting discussions about physics and beyond.

Last, this work was partially supported by the Bonn-Cologne Graduate School of Physics and Astronomy.

Contents

1	Introduction	1
2	F-theory	7
2.1	F-theory: Geometry and physics	7
2.1.1	Type IIB/F-theory duality	7
2.1.2	M/F-theory duality	9
2.1.3	Non-Abelian gauge groups and Cartan divisors	10
2.1.4	Elliptic fibrations and Abelian gauge groups	11
2.1.5	Matter and singularities in F-theory	13
2.1.6	Vertical fluxes and compactifications to 4D	15
2.2	Toric varieties	17
2.3	Examples: Fibers for the standard model and Pati-Salam	20
2.3.1	Polyhedron F_{11} : $SU(3) \times SU(2) \times U(1)$	20
2.3.2	Polyhedron F_{13} : $SU(4) \times SU(2)^2/\mathbb{Z}_2$	27
2.4	The toric Higgs network	32
2.4.1	Higgs connection	33
2.4.2	Higgs network	37
2.5	Genus-one fiber with discrete symmetries	38
2.5.1	Polyhedron F_3 : non-toric $U(1)$	39
2.5.2	Higgsing to X_{F_1} with \mathbb{Z}_3	43
3	Topological string theory	47
3.1	Topological string construction	47
3.1.1	Topological field theories	47
3.1.2	Coupling to gravity: Topological string theory	51
3.2	Quantum mirror curves	54
3.2.1	Refinement and Nekrasov-Shatashvili limit	55
3.2.2	Quantum geometry	56
3.2.3	Example 1: local \mathbb{F}_1	62
3.2.4	Example 2: local \mathbb{F}_2	67
3.2.5	Example 3: $\mathbb{C}^3/\mathbb{Z}_5$	68
3.3	Non-perturbative completion	71
3.3.1	Quantum mechanics of spectral curves	71
3.3.2	Connecting topological strings and quantum mechanics: Spectral determinants	72
3.3.3	The quantization condition	76
3.3.4	The maximally supersymmetric case	77
3.3.5	Example: local \mathbb{F}_2	78

4 Conclusion	87
A Appendix	91
A.1 Addition law on elliptic curves	91
A.2 Nagell algorithm	92
A.3 Calculation of quantum operators	95
A.4 Refined matrix models	96
Bibliography	99
List of Figures	107
List of Tables	109
Acronyms	111

Introduction

In the last centuries physics was mainly confined to perturbative calculations of observables as a series in a small parameter x . For example the calculation of corrections by Feynman graphs in quantum electrodynamics (QED) is a perturbative series in the small parameter $\alpha \sim \frac{1}{137}$. Nevertheless in QED and many other examples the occurring series expansions are not convergent but only asymptotic. This means that the difference between the series expansion and the real physical value does not necessarily goes to zero by taking higher and higher order contributions. As a result there is an optimal expansion order \tilde{N} where the difference between the physical quantity and its approximation is minimal and where the series needs to be truncated [1]. In QED the effects of the asymptotic nature of the series expansion are usually small due to the small value of α .

Trans-series

One possibility to find the non-perturbative effects are trans-series. They have been developed as a systematic treatment of non-perturbative contributions starting in the 1980s with the work of Jean Écalte [2]. In this setup the perturbative Taylor series is replaced by a trans-series expansion which also includes non-perturbative contributions for example of the form $e^{-A/x}$ where x is the small parameter

$$f(x) = \sum_{n,k=0}^{\infty} x^n e^{-kA/x} f_n^{(k)}. \quad (1.1)$$

Here $f(x)$ is an arbitrary function and A is the so-called instanton-action. For the example of a quantum field theory (QFT) it is given by the value of the action at additional saddle points in the expansion of the path integral.

Trans-series have been studied in quantum mechanical toy models, simple models in QFT (for both see for example [1]) and recently also string theory [3, 4].

In the following we want to concentrate on non-perturbative aspects of string theory. Hence let us introduce string theory.

String theory

In the construction of string theory [5] the one dimensional worldline of a point particle in Minkowski space is replaced by a two dimensional worldsheet. The bosonic parts of superfields on the worldsheet embed the string into the higher dimensional target space. Quantization of the two dimensional supersymmetric field theory reveals a conformal anomaly which needs to be canceled for a consistent theory. This cancelation requires the dimensionality of the target space and thus physical spacetime to be ten.

Interestingly the calculation of the field content of the target space field theory leads to a massless particle with spin two which are exactly the properties of a graviton. Thus string theory naturally

contains gravity and is a candidate for quantum gravity.

To bring the requirement of ten spacetime dimensions into line with the observed four dimensional spacetime one comes back to an idea of Kaluza and Klein [6, 7]. They proposed to compactify additional dimensions on a “small” manifold. Here small means that the effects are smaller than the latest experimental bounds on them and thus evade detection. Consistency and the demand for $\mathcal{N} = 1$ supersymmetry in four dimensions leads to the fact that the compactification manifolds have to be complex three dimensional Calabi-Yau (CY) manifolds.

$\mathcal{N} = 1$ supersymmetry [8] is phenomenologically interesting in four dimensions since it provides possible solutions to open problems of the standard model of particle physics. For example the lightest supersymmetric partner is a candidate for dark matter, supersymmetry automatically cancels loop contributions to the Higgs mass and can thus explain the Higgs mass of $m_H \sim 125\text{GeV}$ without fine tuning and last but not least it modifies the running of coupling constants such that they meet much better at a scale of $\sim 10^{16}\text{GeV}$.

Besides the dimensionality the compactification manifold also determines the physical properties of the resulting field theory as for example the spectrum or the couplings. Unfortunately there are numerous different CY manifolds which weakens the predictive power of the theory.

The replacement of point particles with one dimensional strings corresponds to an effective renormalization of field theory since the string length automatically introduces a cutoff in the theory. This can be envisioned in terms of Feynman graphs as a thickening of the lines. As in the case of QFT the string graphs indicate that string theory is still a perturbative theory.

Perturbative string theory has five different manifestations: Type I, type IIA, type IIB, heterotic $\text{SO}(32)$ and heterotic $E_8 \times E_8$ string theories. In the 1990s it was found that these five different theories are connected by a web of string dualities and can be interpreted as the limits of a central eleven dimensional non-perturbative theory called M-theory [9]. The fundamental degrees of freedom in M-theory are M2- and M5-branes which are higher dimensional generalizations of strings. The low energy limit of M-theory is known to be eleven dimensional supergravity. For an illustration of the web of string theories see Figure 1.1.

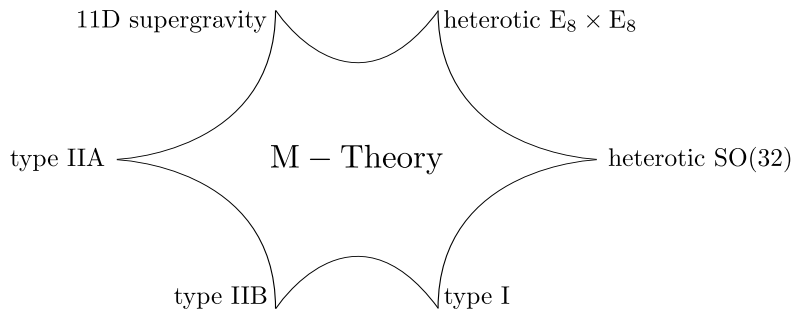


Figure 1.1: The M-Theory star indicating the string theory dualities between type I, type IIA, type IIB, heterotic $\text{SO}(32)$ and heterotic $E_8 \times E_8$ string theories as well as eleven dimensional supergravity. These theories can all be interpreted as being limits of a central M-theory.

Dualities

We already mentioned dualities between string theories. Dualities are descriptions of the same physical situation in two different ways. The classical example of a duality is the 2D Ising model. The 2D Ising model describes a macroscopic magnet by a lattice of spins which can point up and down. A statistical treatment of the spins leads to an unordered phase for high temperatures and an ordered phase for low

temperatures. The two solutions for the partition function in the ordered and unordered phase can be mapped to each other by a duality transformation [10]. This does not mean that the high- and low-temperature solutions are equal but that there exists a dictionary to describe the low temperature physics in the language of the high temperature framework and vice versa by identifying the observables in an appropriate way.

One particular important class of dualities in string theory are gauge/gravity correspondences [11]. In these theories a d dimensional gravity theory can also be described as a gauge theory on its $d - 1$ dimensional boundary which is called the *holographic principle*. Gauge/gravity dualities map weak coupling in the gauge theory to strong coupling in the gravity theory and weak coupling in the gravity theory to strong coupling in the gauge theory. The two benefits of these dualities are first that it is possible to describe the same physical problem either by gravity or by a gauge theory and second that they allow the calculation of non-perturbative effects in one theory by making a perturbative calculation in another theory. A famous example for a gauge/gravity correspondence is the AdS/CFT correspondence [12]. This duality maps type IIB string theory on the background $AdS_5 \times S^5$ to a supersymmetric conformal field theory (CFT) on the four dimensional boundary of AdS_5 .

In current research gauge/gravity dualities are for example used to calculate properties of the non-perturbative quark gluon plasma occurring at the LHC or shortly after the big bang (for a review see [13]) as well as in calculations of strongly correlated systems in condensed matter physics (for a review see [14]).

Topological string theory

Another interesting setup to study gauge/gravity correspondences involves topological string theory [15, 16]. Topological string theory is a subsector of the physical string with less degrees of freedom: As the target space it only has the compactified part of the physical string. It comes in two variants: The A-model and the B-model.¹

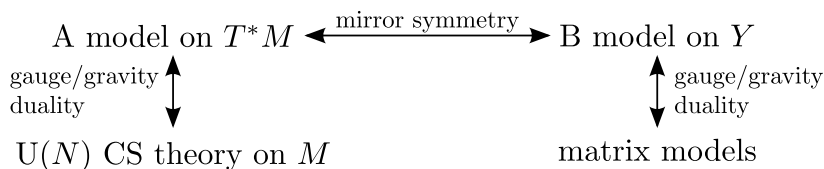


Figure 1.2: Illustration of the duality chain of topological string theory [17].

There are two gauge/gravity correspondences connected with topological string theory as illustrated in Figure 1.2. First the topological A-model on the cotangent bundle T^*M of a real three dimensional manifold M is dual to Chern-Simons (CS) theory on M in the large N limit [18]. Here CS theory is a gauge theory like Yang-Mills theory but with gauge group $U(N)$ and the metric does not occur in the Lagrangian. Thus the theory is an example of a topological field theory.

The second gauge/gravity correspondence of topological string theory is between the topological B-model and matrix models. More concretely the topological B-model on local CY threefolds containing a Riemann surface as a submanifold are dual to matrix models in the large N limit where the potential $W(x)$ of the matrix model is determined by the Riemann surface. Matrix models are zero dimensional quantum field theories of random $N \times N$ matrices. The potential gives the distribution function of the eigenvalues of the matrices.

¹ For more details on topological string theory see Section 3.1.

The two topological string theories are additionally connected by *mirror symmetry* [19]. This duality states that the A-model topological string on the CY manifold X is identical to the B-model topological string on the CY manifold Y where X and Y is a special pair of related CY manifolds. The pair X and Y has the property that the Kähler moduli spaces and complex structure moduli spaces of X and Y are exchanged.

ABJM theory and non-perturbative effects of topological string theory

Now we focus on topological string theory on the geometry of local $\mathbb{P}^1 \times \mathbb{P}^1$ which can be used to describe Aharony-Bergman-Jafferis-Maldacena (ABJM) theory. ABJM theory is proposed to be a worldvolume theory of M2-branes. It consists of two $\mathcal{N} = 6$ Chern-Simons matter theories with gauge group $U(N) \times U(N)$ and couplings $(k, -k)$ connected by four bifundamental matter multiplets [20]. For a quiver diagram of this ABJM theory see Figure 1.3.

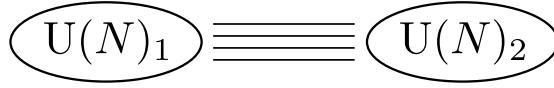


Figure 1.3: The quiver diagram of ABJM theory. The two nodes represent the two gauge groups and the lines between represent the connecting bifundamental matter [21].

In terms of a gauge/gravity correspondence ABJM theory can be interpreted as the three dimensional CFT dual to M-theory on $AdS_4 \times S^7/\mathbb{Z}_k$ where the latter is the large N limit of a stack of N M2-branes on $\mathbb{R}^8/\mathbb{Z}_k$ [21]. Therefore it can be interpreted as a worldvolume theory for a stack of N M2-branes on the geometry $\mathbb{R}^8/\mathbb{Z}_k$. This is reflected by the fact that ABJM theory correctly reproduces the $N^{3/2}$ behaviour of a stack of N M2-branes [22, 23].

To see the connection between topological string theory and ABJM theory one uses localization to reformulate ABJM theory as a matrix model. This matrix model is almost the same as the matrix model for topological string theory on local $\mathbb{P}^1 \times \mathbb{P}^1$ in a special slice of the moduli space. Along this identification one finds that the free energy of topological string theory computes so-called worldsheet instantons which are certain terms in the non-perturbative expansion of the ABJM grand canonical potential. But in [24–26] it was found that these non-perturbative terms are not the complete story. Although a non-perturbative description must hold in the whole plane of coupling constants one finds poles at certain values for the coupling constant. To solve this problem one requires a cancelation of these poles by additional non-perturbative terms. These additional non-perturbative terms in the ABJM grand canonical potential come from M2-brane instantons on the M-theory dual and can be described by *refined topological string theory* [24–26].

Using the connection between ABJM theory and topological string theory one can use these additional M2-brane instanton terms for a non-perturbative completion of topological string theory on local $\mathbb{P}^1 \times \mathbb{P}^1$. This conjecture can be generalized to other local geometries [26]. The geometries in question have a mirror dual B-model geometry which contain a Riemann surface as a submanifold. In [26] the Riemann surface was then used to define a statistical ensemble with a grand canonical potential and a corresponding density matrix.

Apart from the resulting conjecture for a non-perturbative completion of topological string theory the definition of a density matrix makes it possible to describe the system as a non-interacting one dimensional Fermi gas as was done for local $\mathbb{P}^1 \times \mathbb{P}^1$ [27]. This allows a treatment with methods from statistical physics and has the second benefit for the case of local $\mathbb{P}^1 \times \mathbb{P}^1$ that a semiclassical expansion of the quantum gas corresponds to a strong coupling expansion of ABJM theory.

F-theory

A second theory incorporating non-perturbative aspects of string theory is F-theory [28]. This is a non-perturbative formulation of type IIB string theory which is also related to heterotic $E_8 \times E_8$ string theory and M-theory by string dualities.

To see the non-perturbative nature of F-theory one has to look at its connection to type IIB string theory. In general the string coupling constant g_s is dynamically generated. In F-theory one uses the symmetries of the type IIB string theory to introduce an additional torus whose complex structure describes the string coupling constant g_s . Regions of strong coupling $g_s \rightarrow \infty$ can then be described in the geometric picture by singular tori. Thus taking F-theory on a genus-one fibered CY manifold including singularities of the additional torus is a non-perturbative description of type IIB string theory in the string coupling constant g_s .

The non-Abelian gauge group and matter content of the target space effective field theory can also be found from the singularities of the genus-one fiber of the CY manifold. Furthermore the Abelian Mordell-Weil (MW) group of an elliptic fiber leads to the Abelian gauge symmetries. The possibility for complicated gauge groups and the treatment by geometric toolkits makes this theory also a good starting point in string phenomenology for the construction of the standard model of particle physics or grand unified theories.

A common phenomenological problem in grand unified theories are proton decay inducing operators. Usually these operators are forbidden by discrete symmetries. The geometric counterpart of discrete symmetries in F-theory has been studied recently in [29–36]. It is given by the Tate-Shafarevich (TS) group of the genus-one fibered CY manifold. Since the TS group is hard to compute mathematically physical insights might stimulate this topic in the future.

Motivation

In this thesis we want to discuss two examples of non-perturbative aspects of string theory which are connected by the used mathematical methods: Both of the examples depend on elliptic or genus-one curves.

The first example is F-theory. Here we want to construct more explicit examples of compactification spaces to four and six dimensions similar to the ones constructed in [37–39] and find their effective field theories. The goal is a classification of all genus-one fibered compactification spaces whose fibers are constructed as hypersurfaces in the 16 two dimensional toric fano varieties. In this thesis we want to place emphasis on the construction of gauge groups which are physically interesting as for example those in the standard model. Apart from that we want to find more examples of discrete symmetries and especially find an analog to the Shioda map to calculate the discrete charges of matter multiplets.

The second example is based on a recent proposal for a non-perturbative completion of topological string theory [24–26]. This proposal depends on so-called quantum periods. We want to calculate these quantum periods for several examples. Subsequently we want to test the proposed non-perturbative completion. If the non-perturbative completion turns out to be correct this would connect refined and unrefined topological string theory giving the whole theory a very restricting structure. The non-perturbative calculations could then be used in applications of topological string theory as for example the construction of models in Seiberg-Witten gauge theories. Additionally the ansatz of [26] can serve as a starting point for a generalization of the Fermi gas approach to other geometries allowing us to apply the well developed methods from statistical physics.

Outline

This thesis has two major parts. In Chapter 2 we concentrate on F-theory. First we introduce F-theory by its duality to M-theory and as a non-perturbative version of type IIB string theory in Section 2.1. We discuss the calculation of the gauge group and matter content as well as vertical G_4 flux in compactifications to four dimensions. Subsequently we introduce toric geometry as a tool to construct CY manifolds in Section 2.2. Then we discuss two examples for compactifications on CY manifolds constructed from a general base and the fiber being a hypersurface in a two dimensional toric variety in Section 2.3. The examples lead to the gauge group of the standard model and the Pati-Salam model. These two theories are known to be connected via a Higgsing which is reflected on the geometry side by a conifold transition. We find analogous transitions between all genus-one fibered CY manifolds where the fiber is a hypersurface in one of the 16 two dimensional toric fano varieties. After discussing some properties of this network of effective field theories in Section 2.4 we study one of these Higgs transitions which allows the identification of a discrete \mathbb{Z}_3 symmetry in Section 2.5. This chapter is based on the publications [32, 40].

In Chapter 3 we turn to a non-perturbative completion of topological string theory. Therefore we first review the construction of topological string theory by twisting a two dimensional nonlinear sigma model with $\mathcal{N} = (2, 2)$ worldsheet supersymmetry in Section 3.1. We discuss the different possibilities for twisting and the resulting two possible topological string theories called the A-model and the B-model.

Then in Section 3.2 we calculate refined or quantum periods which occur in the non-perturbative completion of topological string theory. In order to do this we first introduce refined topological string theory and the Nekrasov-Shatashvili (NS) limit. Afterwards we introduce quantum geometry as a variant of special geometry which allows the calculation of refined free energies from the refined periods. Subsequently we turn to the calculation of the refined periods. To do this we mainly rely on quantum operators which calculate the corrections to the periods from its zeroth order. We present the calculation for the three examples of local \mathbb{F}_1 , local \mathbb{F}_2 and the resolution of $\mathbb{C}^3/\mathbb{Z}_5$. This section is mainly based on [41].

In Section 3.3 we then introduce the non-perturbative completion of topological string theory proposed in [24–26]. We test this proposal by numerical calculations in the maximally supersymmetric case for the geometry of local \mathbb{F}_2 . This section is based on the upcoming publication [42].

Publications

Parts of this thesis are based on the following publications of the author:

- M.-x. Huang, A. Klemm, J. Reuter and M. Schiereck, *Quantum geometry of del Pezzo surfaces in the Nekrasov-Shatashvili limit*, JHEP **1502** (2015) 031, arXiv:1401.4723 [hep-th].
- D. Klevers, D.K. Mayorga Peña, P.K. Oehlmann, H. Piragua and J. Reuter, *F-Theory on all Toric Hypersurface Fibrations and its Higgs Branches*, JHEP **1501** (2015) 142, arXiv:1408.4808 [hep-th].
- M. Cvetič, D. Klevers, D.K. Mayorga Peña, P.K. Oehlmann and J. Reuter, *Three-Family Particle Physics Models from Global F-theory Compactifications*, arXiv:1503.02068 [hep-th], accepted for publication in JHEP.

In this chapter we want to study the occurrence of elliptic curves in F-theory. First we will introduce briefly F-theory in Section 2.1. We will see that it can be interpreted as a non-perturbative version of type IIB string theory, its connection to M-theory, the calculation of the gauge groups and matter content as well as fluxes in F-theory. In Section 2.2 we will introduce toric geometry as a tool to construct CY manifolds. Then in Section 2.3 we will use two of the 16 polytopes introduced in Section 2.2 to construct two global compactifications to 6D and 4D which lead to the standard model and Pati-Salam gauge group. We will derive the gauge groups, matter content, Yukawa couplings and the possible G_4 fluxes. In Section 2.4 we will find a connection between the two theories via a Higgsing which has a geometric interpretation in terms of a conifold transition. This connection extends to a complete network between the theories constructed from the 16 two dimensional toric polytopes. In Section 2.5 we will then use this network structure to construct a compactification with a discrete \mathbb{Z}_3 gauge symmetry.

The results of this chapter are published in [32] and [40].

2.1 F-theory: Geometry and physics

So far there is no microscopic description of F-theory known yet. Nevertheless F-theory is defined via its dualities to other string theories. In particular the heterotic/F-theory duality, the type IIB/F-theory duality and the M-theory/F-theory duality. In the following we will describe the basic concepts of the latter two dualities in subsections 2.1.1 and 2.1.2. Afterwards we will discuss non-Abelian gauge groups and the properties of genus-one curves which define the Abelian part of the gauge group in subsections 2.1.3 and 2.1.4 respectively. This discussion will be followed by the description of matter in F-theory in Subsection 2.1.5 and of the derivation of fluxes which are necessary to account for the chirality in 4D in Subsection 2.1.6.

This section is mainly based on [43–45]. See these papers for further details and references.

2.1.1 Type IIB/F-theory duality

The string coupling constant in type IIB string theory is given by the dilaton field ϕ as $g_s = e^\phi$. It can be combined with the real axion C_0 to the complex axio-dilaton field

$$\tau = C_0 + \frac{i}{g_s}. \quad (2.1)$$

Introducing a D7-brane in the geometry is sourced by the Ramond-Ramond (R-R) 8-form field C_8 which is dual to the axion C_0 [44]. Together with the field strength tensors $F_1 = dC_0$ and $F_9 = \star F_1$ the Poisson equation for C_8 in the presence of a D7-brane at the position z_0 in the plane perpendicular to the brane

is given by [44]

$$d \star F_9 = \delta(z - z_0). \quad (2.2)$$

Integrating the Poisson equation in the plane perpendicular to the brane we find [44]

$$1 = \int_{\mathbb{C}} d \star F_9 = \oint_{z_0} \star F_9 = \oint_{z_0} dC_0. \quad (2.3)$$

This can be solved by

$$C_0(z) = \tilde{C}_0 + \frac{1}{2\pi i} \ln(z - z_0), \quad (2.4)$$

where \tilde{C}_0 denotes the regular part of $C_0(z)$. By using the definition of the axio-dilaton field τ (2.1) we then find

$$\tau(z) = \tau_0 + \frac{1}{2\pi i} \ln(z - z_0). \quad (2.5)$$

This means that at the position of a D7-brane the complex structure τ diverges and equivalently $g_s \rightarrow 0$. In contrast to that we can rewrite the solution (2.5) to find [44]

$$\frac{1}{g_s} = e^{-\phi} = -\frac{1}{2\pi} \ln \left| \frac{z - z_0}{\lambda} \right|. \quad (2.6)$$

Here we see that $g_s \rightarrow \infty$ when $z - z_0 = \lambda$. Generally g_s is thus strongly varying and not necessarily small. In the region $|z - z_0| \ll \lambda$ the coupling constant remains small and the backreaction of the branes on the geometry are negligible. Only in this limit a perturbative treatment of type IIB string theory is possible. In general the existence of D7-branes however leads to regions in the geometry where the coupling constant is not small and thus non-perturbative effects need to be taken into account.

By encircling a D7-brane (2.5) in the directions perpendicular to the brane $z \rightarrow e^{2\pi i} z$ we observe that the axio-dilaton is shifted by the monodromy

$$\tau \rightarrow \tau + 1. \quad (2.7)$$

This does not pose a problem since the type IIB supergravity action in the Einstein frame [43, 44] is manifestly invariant under $SL(2, \mathbb{R})$ transformations

$$\tau \rightarrow \frac{a\tau + b}{c\tau + d}, \quad \begin{pmatrix} C_2 \\ B_2 \end{pmatrix} \rightarrow \begin{pmatrix} a & b \\ c & d \end{pmatrix} \begin{pmatrix} C_2 \\ B_2 \end{pmatrix}, \quad \text{with } ad - bc = 1, \quad (2.8)$$

where we had to introduce a $SL(2, \mathbb{R})$ doublet where C_2 is the R-R 2-form field and B_2 is the Neveu-Schwarz-Neveu-Schwarz (NS-NS) 2-form field. In the full type IIB string theory this invariance is reduced to $SL(2, \mathbb{Z})$ [44].

Taking the $SL(2, \mathbb{Z})$ invariance seriously we have to give a physical meaning to the $SL(2, \mathbb{Z})$ doublet $\begin{pmatrix} C_2 \\ B_2 \end{pmatrix}$ [44]. In perturbative type IIB string theory the fundamental string is electrically charged under the B_2 field. Due to the mixing of B_2 and C_2 fields under $SL(2, \mathbb{Z})$ transformations we need another string charged electrically under the C_2 field. These strings are D1-strings [44]. Thus after including D7-branes we have to combine fundamental strings and D1-strings into general $\begin{pmatrix} p \\ q \end{pmatrix}$ -strings.

Analogous to the interpretation of D7-branes as hypersurfaces where fundamental strings can end

this leads to the definition of $[p, q]$ -7-branes. Already D1-strings enter in IIB string theory only as non-perturbative objects. Thus also $\binom{p}{q}$ -strings and $[p, q]$ -7-branes are non-perturbative objects [44].

To define F-theory we use the $SL(2, \mathbb{Z})$ invariance of type IIB string theory as in (2.8) to interpret the axio dilaton as the complex structure parameter of an additional torus. Since the volume modulus of the torus has no interpretation in type IIB string theory we define F-theory on a genus-one fibered manifold $X : C \rightarrow \mathcal{B}$ in the limit of vanishing fiber volume $V(C) \rightarrow 0$ to be equal to type IIB on the base of the fibration \mathcal{B} . This effectively geometrizes the dynamics of the axio-dilaton and includes the full backreaction of D7-branes on the geometry of spacetime [44]. For a better understanding of the necessary limit $V(C) \rightarrow 0$ we now have a look at the duality between M-theory and F-theory.

2.1.2 M/F-theory duality

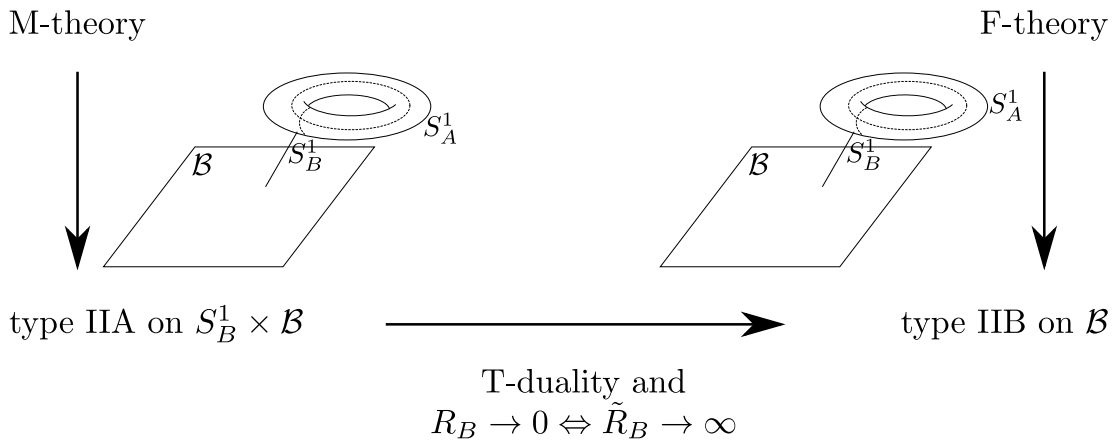


Figure 2.1: Chain of dualities in the M/F-theory duality. M-theory compactified on a genus-one fibered CY manifold $X : C \rightarrow \mathcal{B}$ is equal to type IIA on the base of the fibration and one of the circles in the genus-one fiber $S_B^1 \times \mathcal{B}$. Here we interpreted the other circle S_A^1 in the genus-one fiber as the M-theory circle in the reduction to type IIA. Then we use T-duality on the left over circle S_B^1 together with the limit $R_B \rightarrow 0 \Leftrightarrow \tilde{R}_B \rightarrow \infty$ to obtain type IIB compactified on \mathcal{B} . This is given by F-theory on the original manifold X .

To approach F-theory via the M/F-theory duality we consider eleven-dimensional supergravity compactified on $\mathbb{R}^{1,8} \times T^2$. Here T^2 denotes the torus $T^2 = S_A^1 \times S_B^1$ with complex structure parameter τ . The two circles S_A^1 and S_B^1 of the torus have radii R_A and R_B .

Now we identify the circle S_A^1 with the M-theory circle in the reduction of M-theory to type IIA string theory. Here the ten dimensional coupling constant in type IIA string theory is $g_{IIA} \sim \frac{R_A}{l_s}$ [44]. Thus in the limit $R_A \rightarrow 0$ we recover weakly coupled type IIA on $\mathbb{R}^{1,8} \times S_B^1$.

As a next step in the chain of arguments we use T-duality along the other circle S_B^1 to obtain type IIB string theory on $\mathbb{R}^{1,8} \times \tilde{S}_B^1$. Here the dual circle \tilde{S}_B^1 has the radius $\tilde{R}_B = \frac{l_s^2}{R_B}$. Taking $R_B \rightarrow 0$ leads to the uncompactification limit and we get ten-dimensional type IIB [44]. In the duality transformation from type IIA to type IIB we find for the coupling constant $g_{IIB} \sim g_{IIA} \frac{l_s}{R_B} = \frac{R_A}{R_B}$. For rectangular initial tori this can directly be identified with the imaginary part of the complex structure $g_{IIB} \sim \frac{1}{\text{Im}(\tau)}$. This can be generalized to non-rectangular tori [44]. In a more general discussion one can also trace back the type IIB axion C_0 to the real part of the complex structure of the torus in M-theory [44].

In the duality chain performed above we had to take the two limits $R_A \rightarrow 0$ and $R_B \rightarrow 0$. This is equivalent to the fact that the volume of the torus $V(T^2) \rightarrow 0$ which we already mentioned in Subsection

2.1.1. The vanishing volume of the torus also explains why we could only identify a physical field transforming as the complex structure τ and not as the volume of a torus in type IIB string theory [44].

The duality used above connected M-theory compactified to nine dimensions on a torus and F-theory compactified to ten dimension on the same torus. This can also be generalized and extended to lower dimensions. Then M-theory in $11 - 2n$ dimensions on a genus-one fibered CY n -fold X is dual to F-theory in $12 - 2n$ dimensions compactified on X , see Figure 2.1. From the M-theory picture it is then clear that we thus need to compactify F-theory on a CY fourfold to obtain an $\mathcal{N} = 1$ supergravity theory in four dimensions.

The above duality chain does not need the manifold $\mathbb{R}^{1,8} \times T^2$ to be a direct product. The more general case is given by a general fibration of the torus over the base manifold.

2.1.3 Non-Abelian gauge groups and Cartan divisors

Gauge groups in type IIB string theory are represented by the existence of multiple D7-branes in the geometry. As discussed in Subsection 2.1.1 the presence of D7-branes corresponds to a divergence of the complex structure τ in (2.5) of the additional torus of the genus-one fibration. Divergence of the complex structure of a torus means that the torus itself is singular and for example pinches. If we consider the genus-one curve to be in Weierstrass form

$$p_W = y^2 - x^3 - fxz^4 - gz^6 \quad (2.9)$$

the singularity corresponds to the fact that $p_W = 0 = dp_W$ where d denotes the total derivative. Here $dp_W = 0$ is equivalent to the degeneration of the tangent space which leads to a splitting of the curve. These conditions are exactly fulfilled when the discriminant $\Delta = 4f^3 + 27g^2$ vanishes at one of its irreducible components

$$\mathcal{S}_{G_I}^b := \{\Delta_I = 0\}, \quad I = 1, \dots, N \quad (2.10)$$

which are generally of codimension one in \mathcal{B} . Here f and g can be read off from the Weierstrass form of the CY X or its Jacobian $J(X)$.

The singular geometries need to be resolved without destroying the CY condition. This can be achieved by blowing up the fiber in the singular points over the divisors $\mathcal{S}_{G_I}^b$ and thus replacing it with a tree of \mathbb{P}^1 's which we call $c_{-\alpha_i}^{G_I}$ for $i = 1, \dots, \text{rk}(G_I)$ [32, 43, 44]. In the process of blowing up $h^{1,1}(X)$ increases by $\text{rk}(G_I)$ so that we have in total [32]

$$h^{(1,1)}(X) = h^{(1,1)}(B) + 1 + \text{rk}(G_X). \quad (2.11)$$

The different possible resolutions or equivalently the different types of degenerations have been classified for the case of $K3$ [46]. The classification can be seen in Table 2.1. A more refined classification for higher dimensional CY manifolds was worked out later on in [47] and includes also non-simply laced Lie algebras where monodromies around the brane have to be taken into account.

Next we define the Cartan divisors $D_i^{G_I}$ as the fibration of the rational curves $c_{-\alpha_i}^{G_I}$ over the base loci of the 7-branes $\mathcal{S}_{G_I}^b \subset \mathcal{B}$

$$D_i^{G_I} : c_{-\alpha_i}^{G_I} \rightarrow \mathcal{S}_{G_I}^b. \quad (2.12)$$

singularity type	gauge group	ord(f)	ord(g)	ord(Δ)
none	none	≥ 0	≥ 0	0
A_{n-1}	$SU(n)$	0	0	n
none	none	≥ 1	1	2
A_1	$SU(2)$	1	≥ 2	3
A_2	$SU(3)$	≥ 2	2	4
D_{n+4}	$SO(2n+8)$	2	3	$n+6$
D_4	$SO(8)$	≥ 2	≥ 3	6
E_6	E_6	≥ 3	4	8
E_7	E_7	3	≥ 5	9
E_8	E_8	≥ 4	5	10

Table 2.1: Classification of different singularities due to Kodaira [45, 46].

Then the Cartan divisors intersect the curves $c_{-\alpha_i}^{G_I}$ as

$$D_i^{G_I} \cdot c_{-\alpha_j}^{G_J} = -C_{ij}^{G_I} \delta_{IJ}, \quad (2.13)$$

with the Cartan matrix $C_{ij}^{G_I}$ of G_I . Here the rational curves $c_{-\alpha_i}^{G_I}$ correspond to the simple roots of the gauge group G_I . For a more physical discussion of non-Abelian gauge groups and the corresponding particle spectrum see Subsection 2.1.5.

2.1.4 Elliptic fibrations and Abelian gauge groups

As we have seen in subsections 2.1.1 and 2.1.2 we need to consider genus-one fibered CY manifolds $\pi : X \rightarrow \mathcal{B}$. The general fibers are smooth algebraic genus-one curves C . A general algebraic curve C is defined over a field K which does not necessarily be algebraically closed. As an example consider $K = \mathbb{Q}$: The coefficients in the defining equation of the algebraic curve are then in \mathbb{Q} but the points on the algebraic curve do not have to be in \mathbb{Q} . This leads to the two following qualitatively inequivalent situations.

Curves with points

If the curve C has one or more points with coordinates in the field K it is called an elliptic curve denoted by \mathcal{E} . In analogy to the example given above these points are called rational points [48, 49]. The rational points on \mathcal{E} form an Abelian group under the addition law on the elliptic curve described in Appendix A.1. This is the MW group of rational points. For the addition law one has to choose one of the rational points as zero point P_0 . Then the MW group is generated by the difference of a set of additional rational points P_m , $m = 1, \dots, r$ and the zero point: $P_m - P_0$. The P_m are a ‘‘basis’’ of the MW group.

The MW group of rational points is finitely generated due to the MW theorem [48, 50, 51]. It splits into a free part and a torsion subgroup $\mathbb{Z}^r \times \text{Tors}$. For $K = \mathbb{Q}$ the torsion subgroup was fully classified by Mazur [48, 52, 53].

In the case of elliptic fibrations X K is the field of meromorphic functions on the base \mathcal{B} . Every rational point on the generic elliptic curve \mathcal{E} is enhanced to a rational section of the fibration X . Thus the zero point P_0 becomes the zero section $\hat{s}_0 : \mathcal{B} \rightarrow X$ and the additional rational points P_m , $m = 1, \dots, r$ become the additional rational sections $\hat{s}_m : \mathcal{B} \rightarrow X$, $m = 1, \dots, r$. Defining the addition law for rational sections on the fibration as fiberwise addition on the elliptic curve \mathcal{E} we see that also the MW group of

rational points is enhanced to the MW group of rational sections of the fibration X . The classification of the torsion subgroup of the MW group due to Mazur does not hold for K being the field of meromorphic functions. Counterexamples can be seen in [54].

The free part of the Abelian MW group of rational sections gives the Abelian gauge symmetries in F-theory [55] and the torsion part of the MW group of rational sections leads to non-simply connected non-Abelian gauge symmetries [54, 56].

To define the divisors which support the Abelian gauge fields in F-theory we define the divisor classes of the zero section \hat{s}_0 and the additional rational sections \hat{s}_m to be S_0 and S_m respectively [32]. They have intersection number one with the fiber f

$$S_0 \cdot f = S_m \cdot f = 1. \quad (2.14)$$

These divisors have to be orthogonalized especially with respect to the non-Abelian gauge groups in order to have uncharged gauge groups [37, 57–59]. This leads to the Shioda map

$$\sigma(\hat{s}_m) := S_m - S_0 - [K_B^{-1}] - \pi(S_m \cdot S_0) + \sum_{I=1}^N (S_m \cdot c_{-\alpha_i}^{G_I}) (C_{G_I}^{-1})^{ij} D_j^{G_I}. \quad (2.15)$$

Here $[K_B^{-1}]$ is the anticanonical bundle of the base \mathcal{B} , $\pi(\cdot)$ denotes the projection of a divisor in X to a divisor in the base \mathcal{B} , $C_{G_I}^{-1}$ is the inverse of the Cartan matrix and $D_j^{G_I}$ denote the Cartan divisors as discussed in Subsection 2.1.3. The U(1) charge of a rational curve c in the fiber and the associated hypermultiplet is then given by the intersection with the Shioda map $c \cdot \sigma(\hat{s}_m)$.

For the calculation of anomalies one needs the Néron-Tate height pairing of two rational sections to calculate the anomaly coefficient matrix $b_{mn} = -\pi(\sigma(\hat{s}_m) \cdot \sigma(\hat{s}_n))$. By using the Shioda map (2.15) it is given by [37, 57]

$$\begin{aligned} \pi(\sigma(\hat{s}_m) \cdot \sigma(\hat{s}_n)) &= \pi(S_m \cdot S_n) + [K_B] - \pi(S_m \cdot S_0) - \pi(S_n \cdot S_0) \\ &\quad + \sum_{I=1}^N (C_{G_I}^{-1})^{ij} (S_m \cdot c_{-\alpha_i}^{G_I}) (S_n \cdot c_{-\alpha_j}^{G_I}) \mathcal{S}_{G_I}^b, \end{aligned} \quad (2.16)$$

where again $(C_{G_I}^{-1})^{ij}$ denotes the inverse Cartan matrix. In the derivation of (2.16) and in explicit evaluations in the examples in Section 2.3 we use [57]

$$\pi(S_P^2 + [K_B^{-1}] \cdot S_P) = \pi(S_m^2 + [K_B^{-1}] \cdot S_m) = 0. \quad (2.17)$$

Additionally $\pi(S_m \cdot S_n)$ is given by the homology class of the base locus where the two sections \hat{s}_m and \hat{s}_n agree.

Using the *Nagell* algorithm (see Appendix A.2) an elliptic curve can always be mapped birationally to Weierstrass form

$$y^2 = x^3 + fxz^4 + gz^6 \quad (2.18)$$

in $\mathbb{P}^{(2,3,1)}$. Here the coordinates (x, y, z) are sections in the bundles $(\mathcal{L}^2 \oplus \mathcal{L}^3 \oplus \mathcal{O}_B)$ over the base. \mathcal{O}_B is the trivial bundle on \mathcal{B} and \mathcal{L} is fixed via the CY condition of X and adjunction to be $\mathcal{L} = K_B^{-1}$, with the anticanonical bundle of the base K_B^{-1} . For homogeneity of (2.18) f and g then have to be sections of K_B^{-4} and K_B^{-6} , respectively [32, 44, 45].

Under the birational map the zero section is mapped to the canonical zero section of the Weierstrass

form $[x : y : z] = [\lambda^2 : \lambda^3 : 0]$ and the other rational sections are given by $[x_m : y_m : z_m]$.

Curves without points

If the curve C does not have a point in K it is merely a genus-one curve. A fibration $\pi : X \rightarrow \mathcal{B}$ with general fiber C is then a fibration without a section. Since the Nagell algorithm requires a rational section to be applicable there is no birational map of the given fibration to Weierstrass form.

Nevertheless one can construct an associated *Jacobian* curve $J(C)$ which has a rational point and is thus elliptic. The Jacobian of a curve $J(C)$ is defined to be the complex torus \mathbb{C}/Λ where Λ is the period lattice of the curve C [60]. The trivial line bundle gives a distinguished point on the Jacobian curve and thus it is an elliptic curve. One can then define the Jacobian fibration $\pi : J(X) \rightarrow \mathcal{B}$ to be the fibration with generic fiber $J(C)$. The original fibration $\pi : X \rightarrow \mathcal{B}$ and the Jacobian fibration $\pi : J(X) \rightarrow \mathcal{B}$ have the same discriminant and τ . Since the F-theory compactifications do only depend on the τ function and the discriminant of the genus-one curve we can use the Jacobian fibration to derive the effective field theory [29]. Mathematically the Jacobians for the cubic in \mathbb{P}^2 , the biquadric in $\mathbb{P}^1 \times \mathbb{P}^1$, and the quartic in $\mathbb{P}^2(1, 1, 2)$ have been derived in [61]. The example of a cubic in \mathbb{P}^2 and a quartic in $\mathbb{P}^2(1, 1, 2)$ has also been considered in [29–31, 33–36] in the context of F-theory.

Although genus-one fibrations do not have rational sections they have n -sections which we denote by $\hat{s}^{(n)}$. Locally n -sections map a point in the base to n points in the fiber

$$S^{(n)} \cdot f = n. \quad (2.19)$$

But globally only the set of n points gives a well-defined divisor since the individual points are interchanged by monodromies [32].

Fibrations without rational sections have a non-trivial TS group III. The TS group is the set of all fibrations with the same Jacobian fibration equipped with a map. This map is induced by the Jacobian action on the elements of the set and promotes the set of fibrations to a group. Here the Jacobian action is crucial since in [36] it was found that two of the elements of $\text{III}(X_{F_1})$ are the same geometries but with different Jacobian actions. Physically the TS group gives the discrete part of the gauge group. The n -sections are deeply connected to the discrete symmetry. In Section 2.5.2 [32] we propose in analogy to the Shioda map (2.15) a “discrete Shioda map” which calculates the charges under the discrete symmetry.

2.1.5 Matter and singularities in F-theory

In this section we want to discuss the derivation of the particle spectrum of the $\mathcal{N} = 1$ effective supergravity (SUGRA) resulting from a compactification of F-theory on a genus-one fibered CY manifold X [32, 43–45].

Codimension one

Codimension one singularities of the discriminant Δ indicate the existence of D7-branes and thus lead to the non-Abelian gauge group as discussed in Subsection 2.1.3. Apart from that codimension one singularities lead in six dimensions to matter in the adjoint representation. To understand this we consider a degenerate codimension one locus $\mathcal{S}_{G_I}^b$ with gauge group G_I . Above this locus the genus-one fiber splits into rational curves $c_{-\alpha_i}^{G_I}$ which represent the positive roots α_i of G_I as discussed in Subsection 2.1.3. The curves $c_{-\alpha_i}^{G_I}$ can be wrapped by M2-branes. Quantization of their moduli space leads to

one Bogomol'nyi-Prasad-Sommerfield (BPS) state in a charged vector multiplet and $2g_I$ BPS states in charged half-hyper multiplets with charge $-\alpha_i$. Here g_I denotes the genus of the curve $\mathcal{S}_{G_I}^b$ in the base \mathcal{B} . The M2-brane can wrap the cycle $c_{-\alpha_i}^{G_I}$ as well in the other direction which leads to another vector multiplet and $2g_I$ half-hyper multiplets with charge α_i [32, 44].

In the F-theory limit of vanishing fiber volume the BPS states become massless and the above representations sort in representations of the gauge group. The vector multiplets for every root α_i of the gauge group combine with additional vector multiplets from the M-theory three form C_3 reduced along the cycles dual to the Cartan divisors $D_I^{G_i}$ into a massless vector multiplet in the adjoint representation $\mathbf{adj}(G_I)$ of G_I . This gives rise to the gauge bosons in the effective theory [55, 62].

The $2g_I$ half-hyper multiplets with charge $-\alpha$ and α combine with $g_I \text{rk}(G_I)$ neutral hyper multiplets from complex structure moduli on X into g_I hyper multiplets in the adjoint $\mathbf{adj}(G_I)$ of G_I . Their number can be calculated via the Euler number to be [32]

$$g_I = 1 + \mathcal{S}_{G_I}^b \frac{\mathcal{S}_{G_I}^b - [K_B^{-1}]}{2}. \quad (2.20)$$

Codimension two

A singularity enhancement at the intersection point of two codimension one discriminant loci $\mathcal{S}_{G_1}^b$ and $\mathcal{S}_{G_2}^b$ in codimension two corresponds to intersecting stacks of D7-branes in the dual type IIB picture. Analogous to the intersecting D-brane models this leads to matter multiplets. The enhancement can be understood as follows [44]: Along an enhanced locus in codimension two the fiber degenerates further to an associated gauge group G_A and thus the resolved geometry contains more curves. These further curves can as well be wrapped by M2-branes leading to a vector multiplet. Analogous to the case in codimension one the vector multiplets of the curves combine with additional vector multiplets from the reduction of the M-theory three form C_3 . This leads in total to a vector multiplet in the adjoint representation $\mathbf{adj}(G_A)$ of the enhanced group G_A . The corresponding matter representations $\mathbf{R}_{\underline{q}}$ may then be found by the group theoretical decomposition

$$\begin{aligned} G_A &\rightarrow G_1 \times G_2 \\ \mathbf{adj}(G_A) &\rightarrow (\mathbf{adj}(G_1), \mathbf{1}) \oplus (\mathbf{1}, \mathbf{adj}(G_2)) \oplus \sum \mathbf{R}_{\underline{q}}. \end{aligned} \quad (2.21)$$

The additional shrinkable curves corresponding to the enhanced singularity type of the fiber correspond to the weights of the matter representation $\mathbf{R}_{\underline{q}}$ under the total gauge group G_X with U(1) charges $\underline{q} = (q_1, \dots, q_r)$. The Dynkin labels $\lambda_i^{G_I}$ of the representation \mathbf{R} can be computed as the intersection numbers of the curves c with the Cartan divisors [32]

$$\lambda_i^{G_I} = D_i^{G_I} \cdot c. \quad (2.22)$$

Analogously the U(1) charges can be computed as the intersection of the curve c with the Shioda map (2.15) [57, 58]

$$q_m = \sigma(\hat{s}_m) \cdot c = (S_m \cdot c) - (S_0 \cdot c) + \sum_I (S_m \cdot c_{-\alpha_i})(C_{(I)}^{-1})^{ijI} (D_{jI} \cdot c). \quad (2.23)$$

The loci of singularity enhancement for matter charged under two non-Abelian gauge groups are easily obtained as the intersection loci of two non-Abelian gauge groups $\mathcal{S}_{G_1}^b$ and $\mathcal{S}_{G_2}^b$. For matter charged under one non-Abelian gauge group the locus of enhanced singularity can also easily be read

off from the discriminant.

Matter charged only under U(1) symmetries is harder to obtain. Nevertheless the existence of additional rational sections apart from the zero section leads automatically to additional matter. This can be seen as follows: A rational section in Weierstrass form $[x_m : y_m : z_m]$ fulfills by definition the Weierstrass equation. This gives a relation between the functions f and g . Inserting this relation in the Weierstrass equation leads to a factorization at the loci [37, 57]

$$y_{P_m} = fz_{P_m}^4 + x_{P_m}^2 = 0, \quad m = 1, \dots, r. \quad (2.24)$$

Matter at these loci are generally not charged under non-Abelian gauge groups since in general (2.24) does not intersect the codimension one discriminant loci $\mathcal{S}_{G_I}^b$ where the Cartan divisors are supported. Thus the intersections (2.22) lead to trivial Dynkin labels.

In general the complete intersection loci in (2.24) are reducible varieties. Every irreducible component of (2.24) supports different matter multiplets. Therefore we are interested in all *prime ideals* contained in (2.24). The process of the prime ideal decomposition is described in more detail in [39]. We denote prime ideals by $I_{(k)}$ and the corresponding vanishing sets which are the codimension two varieties in \mathcal{B} by $V(I_{(k)})$.

Codimension two loci have a nontrivial multiplicity. This can be visualized most easily in compactifications to 6D where codimension two loci are points. The number of intersection points of two codimension one discriminant loci $\mathcal{S}_{G_1}^b$ and $\mathcal{S}_{G_2}^b$ is generally different from one. Thus in general the multiplicity of a representation \mathbf{R}_q is given by the homology class of the corresponding codimension two locus. If the codimension two locus is a complete intersection the homology class is easily calculated. In the case of more complicated codimension two varieties $V(I_{(k)})$ the homology class can be computed as follows [37]: First one finds a complete intersection which contains the codimension two variety $V(I_{(k)})$. Then one subtracts the homology classes of the other varieties $V(I_{(k')})$ contained in the complete intersection with order $n_{k'}$ from the homology class of the complete intersection. The order $n_{k'}$ can be calculated using the *resultant technique* [37].

Codimension three

In compactifications to 4D two or more matter curves can meet in codimension three. This leads analogous to the case in codimension two to a further singularity enhancement of the discriminant. Physically these loci correspond to Yukawa points [43, 44].

From the technical point of view we find codimension three singularities of three matter curves at $V(I_{(1)})$, $V(I_{(2)})$ and $V(I_{(3)})$ by testing that the variety $V(I_{(1)}) \cap V(I_{(2)}) \cap V(I_{(3)})$ has a codimension three component in the ring of sections s_i on \mathcal{B} .

2.1.6 Vertical fluxes and compactifications to 4D

Four dimensions are generally non-chiral which means that in order to obtain a chiral spectrum we have to introduce chirality by hand. Therefore we will define chiralities in this subsection via the G_4 flux. Additionally we explain the calculation of vertical G_4 flux in F-theory via comparison to the dual M-theory. For recent works on horizontal G_4 fluxes in F-theory see [63–66]. We will restrict to CY manifolds given as toric hypersurfaces or complete intersection fibrations. The exposition in this section follows [40].

The construction of G_4 flux on a genus-one fibered CY manifold X_4 begins with the computation of the cohomology ring of X_4 . Therefore it is first necessary to choose a basis of divisors $H^{1,1}(X_4)$. This

basis contains the base divisors H_B which we label in the following by α , the zero section \hat{s}_0 which we label by 0, the Cartan divisors $D_i^{G_i}$ which we label by i and the Shioda maps $\sigma(\hat{s}_m)$ corresponding to the $U(1)$ factors which we label by m . Using $H^{1,1}(X_4)$ we can then construct the full cohomology ring of X_4 . To construct the vertical fluxes we need to find $H_V^{2,2}(X_4)$. The elements of $H_V^{2,2}(X_4)$ are products of two elements of $H^{1,1}(X_4)$: $D_A \cdot D_B$. To find the dimension of $H_V^{2,2}(X_4)$ we calculate the inner product matrix $\eta^{(2)}$ of all elements of $H_V^{2,2}(X_4)$. Its rank gives the dimension $h_V^{(2,2)}(X)$ of $H_V^{2,2}(X_4)$

$$h_V^{(2,2)}(X) = \dim(H_V^{2,2}(X_4)) = \text{rk}(\eta^{(2)}) . \quad (2.25)$$

We then choose a basis for $H_V^{2,2}(X_4)$.

G_4 flux in M-theory is a general element of $H_V^{2,2}(X_4)$ where two conditions have to be fulfilled: First it has to fulfill the quantization condition [67]:

$$G_4 + \frac{c_2(X)}{2} \in H^4(X, \mathbb{Z}) . \quad (2.26)$$

The second condition is the cancelation of M2-brane tadpoles. M2-branes lift to D3-branes in type IIB and F-theory. The cancelation requires [68, 69]

$$\frac{\chi(X)}{24} = n_{D3} + \frac{1}{2} \int_X G_4 \wedge G_4 . \quad (2.27)$$

Here n_{D3} denotes the number of D3-branes.

For the definition of G_4 flux in F-theory we compare M-theory compactified on X_4 to 3D and F-theory compactified on $X_4 \times S^1$ to 3D. The comparison leads to further conditions on the G_4 flux in F-theory. They are obtained by comparing the CS terms. In M-theory the CS terms are calculated from the G_4 flux as [70]

$$\Theta_{AB}^M = \int_X G_4 \wedge D_A \wedge D_B . \quad (2.28)$$

Here D_A and D_B denote elements of $H^{(1,1)}(X_4)$. On the F-theory side the CS terms are classically given by circle fluxes or gaugings of axions in the reduction from 4D to 3D [71]. Additionally the CS terms in F-theory get loop corrections by massive fermions in the Kaluza-Klein tower [39]. The full formula for the loop corrected CS terms in F-theory are [39]

$$\Theta_{AB}^F = \Theta_{\text{cl}, AB}^F + \frac{1}{2} \sum_{\underline{q}} n(\underline{q}) q_A q_B \text{sign}(q_A \zeta^A) , \quad (2.29)$$

with the number of 3D fermions $n(\underline{q})$ with charge vector $\underline{q} = (q_0, q_\alpha, q_i, q_m)$. The real parameters ζ^A are the Coulomb branch parameters [39].

The duality between M- and F-theory identifies also the CS terms [39]

$$\Theta_{AB} \equiv \Theta_{AB}^M \stackrel{!}{=} \Theta_{AB}^F . \quad (2.30)$$

The identification imposes additional constraints on the G_4 flux since certain CS terms in F-theory (2.29) are zero. More concretely the additional constraints correspond to the absence of circle fluxes in the circle reduction from 4D to 3D, unbroken non-Abelian gauge symmetries in 4D and the absence of

non-geometric effects [39]

$$\Theta_{0\alpha} = \Theta_{i\alpha} = \Theta_{\alpha\beta} = 0. \quad (2.31)$$

To calculate the chiralities of a multiplet in representation \mathbf{R} in compactifications to 4D we have to integrate the G_4 flux over a corresponding matter surface $C_{\mathbf{R}}^w$ of the multiplet [39]

$$\chi(\mathbf{R}) = n(\mathbf{R}) - n(\bar{\mathbf{R}}) = \int_{C_{\mathbf{R}}^w} G_4. \quad (2.32)$$

Here $n(\mathbf{R})$ is the number of left-chiral Weyl fermions in \mathbf{R} . The matter surface $C_{\mathbf{R}}^w$ is given by the a node in the fiber at codimension two fibered over the codimension two locus in the base \mathcal{B} .

Finally let us comment on the M-theory consistency conditions on the G_4 flux. For a proper treatment one has to expand G_4 and $c_2(X)$ in an integral basis for $H_V^{(2,2)}(X)$. This integral basis can be obtained using mirror symmetry [63, 64, 66]. We apply an indirect workaround to ensure integrality of our base. However the obtained base might not be minimal [40].

Having defined the CS terms (2.28) we observe that the quantization condition of the G_4 flux (2.26) is equivalent to the quantization of the CS terms in the effective field theory [72, 73]. Additionally chiralities are integral by observation. Thus parametrizing the G_4 flux in terms of chiralities we check the quantization condition of the CS terms. Another check is the integrality of the number of D3-branes n_{D3} which is true for smooth CY fourfolds and quantized G_4 flux [67].

2.2 Toric varieties

In this section we want to briefly introduce toric geometry. We use toric geometry throughout this thesis as a tool to construct simple CY manifolds as examples for string compactifications. Some further reviews and references on this subject include [19, 74–76].

A complex d dimensional toric variety is encoded by a d dimensional toric polytope F^1 in a lattice $N = \mathbb{Z}^d$. To construct the corresponding toric variety we assign a coordinate $x_k \in \mathbb{C}$ to each integral point v_k , $k = 1, \dots, m + d$ in the toric polytope except the origin. The integral points are in general linear dependent and fulfill the relations

$$\sum_{k=1}^{m+d} \ell_k^{(a)} v_k = 0, \quad a = 1, \dots, m. \quad (2.33)$$

Using the coefficients $\ell_k^{(a)}$ the toric variety \mathbb{P}_F associated to the toric polytope F is given by \mathbb{C}^{m+d} divided by a $(\mathbb{C}^*)^m$ action

$$\mathbb{P}_F = \frac{\mathbb{C}^{m+d} \setminus \text{SR}}{(\mathbb{C}^*)^m} = \left\{ x_k \sim \prod_{a=1}^m \lambda_a^{\ell_k^{(a)}} x_k \mid \underline{x} \notin \text{SR}, \lambda_a \in \mathbb{C}^* \right\}. \quad (2.34)$$

Here we excluded the points $\underline{x} := (x_1, \dots, x_{m+d})$ in the Stanley-Reisner (SR) ideal of coordinates which are not allowed to vanish at the same time in order to obtain a smooth manifold. The $(\mathbb{C}^*)^m$ action acts by rescaling the coordinates by m factors λ_a making toric varieties generalizations of weighted projective spaces [75].

¹ We use F instead of the commonly used Δ to denote a toric polytope in order to avoid confusion with the discriminant of an elliptic curve, see [32].

The toric variety \mathbb{P}_F can also be interpreted as the groundstate values of the fields in a 2d gauged linear sigma model with $\mathcal{N} = (2, 2)$ [76–78]. Here the coordinates x_i correspond to the vacuum expectation values (vevs) of the bosonic part of chiral superfields which transform under the Abelian gauge group $U(1)^m$ as

$$x_i \rightarrow e^{i\ell_i^{(a)} \epsilon_a} x_i, \quad (2.35)$$

where the $\ell_i^{(a)}$ are the charges of the fields and $\epsilon_a \in \mathbb{R}$. The vevs fall into equivalence classes under the gauge group [78]. Since the theory is supersymmetric the vacuum field configuration has to fulfill the two dimensional D-term constraint

$$D^{(a)} = \sum_{i=1}^{m+d} \ell_i^{(a)} |x_i|^2 = r^{(a)}, \quad a = 1, \dots, m. \quad (2.36)$$

Field theoretically $r^{(a)}$ are the real parts of the Fayet-Iliopoulos (FI) parameters whereas geometrically they can be interpreted as the Kähler parameters. The SR ideal can be understood in this picture as vacuum field configurations where the dimensionality of the gauge group drops [78]. For a consistent theory they have to be excluded.

In this picture the CY condition $c_1(\mathbb{P}_F) = 0$ for the toric geometry (2.34) translates to the cancelation of the chiral $U(1)_A$ anomaly [77]. This holds if and only if

$$\sum_{i=1}^{m+d} \ell_i^{(a)} = 0, \quad a = 1, \dots, m. \quad (2.37)$$

One way to construct toric CY manifolds is by taking the d dimensional toric polytope to lie in a hypersurface of a $d+1$ dimensional lattice. Here the zero point becomes an additional point with negative charge such that condition (2.37) is fulfilled. These CY manifolds are called *local CY* manifolds and are often used in topological string theory on the A-model side, see Chapter 3. Due to (2.36) we see that negative entries in $\ell_i^{(a)}$ which are necessary to fulfill (2.37) lead to noncompact directions. We thus see that local CY manifolds are noncompact. On the level of the toric geometry this is reflected by the fact that the space spanned by all positive linear combinations of the vectors v_i , $k = 1, \dots, m+d$ is not the full space $N \otimes \mathbb{R}$ [75].

Another possibility to construct CY manifolds with the help of toric geometry is by constructing a suitably chosen hypersurface inside the toric variety (2.34). To do this we start by defining a dual polytope F^* to the toric polytope F in the dual lattice $M = \mathbb{Z}^d$ of N as

$$F^* = \{q \in M \otimes \mathbb{R} \mid \langle y, q \rangle \geq -1, \forall y \in F\}. \quad (2.38)$$

Here we used the pairing $\langle \cdot, \cdot \rangle$ between the lattices N and M . The CY hypersurface is then given as the zero loci of a generic section of the anti-canonical line bundle $K_{\mathbb{P}_F}^{-1}$ of the toric variety \mathbb{P}_F . By the *Batyrev construction* this is given by the following polynomial [79]

$$p_F = \sum_{q \in F^* \cap M} a_q \prod_k x_k^{\langle v_k, q \rangle + 1}. \quad (2.39)$$

Here q denotes all integral points in the dual polyhedron F^* , k all integral points of the original polytope F and we sum over all points in the dual polyhedron.

The set of toric divisors on the toric variety \mathbb{P}_F is given by $D_k = \{x_k = 0\}$. To find the full basis of the

toric divisors we additionally have to take some linear equivalences between these divisors into account. The equivalence relations can be read off from the vertices of the toric diagram $v_k^i, k = 1, \dots, m + d$. Namely the divisors fulfill the relations

$$\sum_k^{m+d} v_k^i D_k = 0, \quad i = 1, \dots, d. \quad (2.40)$$

The intersections of these divisors are encoded in the cones of the toric polytope or equivalently in the SR ideal. Apart from toric divisors a toric variety can have additional non-toric divisors. We will encounter this in Subsection 2.5.1.

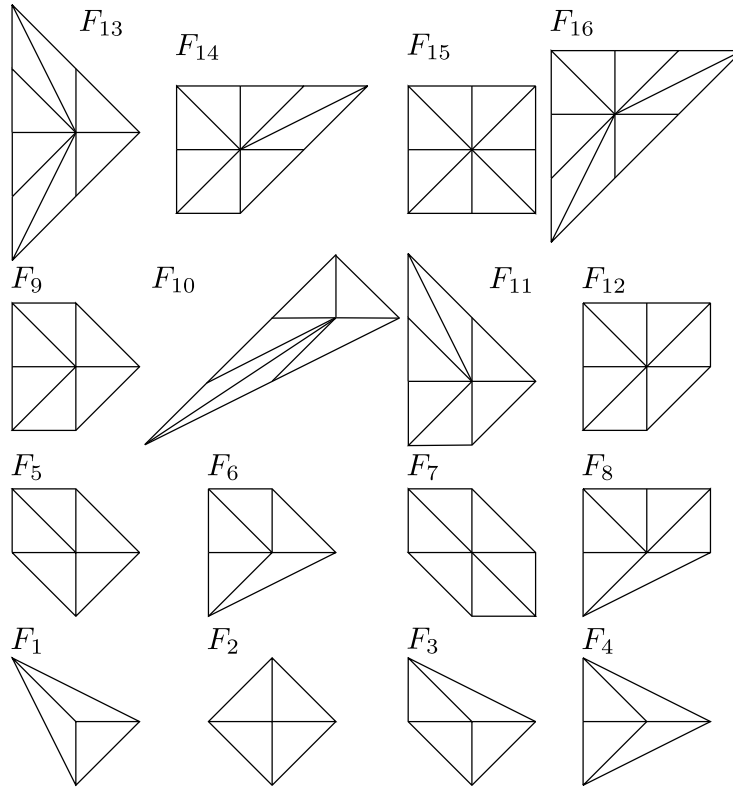


Figure 2.2: The 16 two dimensional reflexive polyhedra [80]. The polyhedron F_i and F_{17-i} are dual for $i = 1, \dots, 6$ and self-dual for $i = 7, \dots, 10$.

Here we focus on two dimensional reflexive toric polytopes which have been classified by [81]. These are the 16 polytopes given in Figure 2.2 [80]. The polyhedron F_1 is associated to \mathbb{P}^2 , F_2 yields $\mathbb{P}_1 \times \mathbb{P}_1$, F_4 gives $\mathbb{P}^2(1, 1, 2)$ and F_{10} is associated to the variety $\mathbb{P}^2(1, 2, 3)$. Among these polytopes there are the generic del Pezzo surfaces \mathbb{P}^2 and $dP_i, i = 1, 2, 3$ as the varieties associated to F_1, F_3, F_5 and F_7 respectively. We can also find the Hirzebruch surfaces $F_i, i = 0, 1, 2$ which are encoded by the polyhedra F_2, F_3 and F_4 respectively. The Hirzebruch surfaces F_n are the nontrivial \mathbb{P}^1 fibrations over $\mathbb{P}^1: \mathbb{P}(\mathcal{O} \oplus \mathcal{O}(n)) \rightarrow \mathbb{P}^1$ [82].

Using the definition for dual polytopes (2.38) we see that the polytopes F_i and F_{17-i} are dual for $i = 1, \dots, 6$ and self-dual for $i = 7, \dots, 10$.

The construction of local CY threefolds to the polyhedra given in Figure 2.2 is done in Chapter 3 for the examples F_3 and F_4 . The hypersurface construction leading to CY onefolds which are tori is

explicitly done in Chapter 2 for the polyhedra F_1 , F_3 , F_{11} and F_{13} .

2.3 Examples: Fibers for the standard model and Pati-Salam

In the following we want to illustrate the general construction from the last section at two explicit examples: The CY manifolds constructed with a general base \mathcal{B} and the fibers being hypersurfaces in the two dimensional toric spaces $\mathbb{P}_{F_{11}}$ and $\mathbb{P}_{F_{13}}$ from Figure 2.2. In each of the two cases we will first give a short description of the fiber geometry including the MW group. Then we will discuss the codimension one, two and three singularities leading to the non-Abelian gauge group, matter content and Yukawa couplings respectively. Subsequently we will construct the G_4 fluxes and discuss the usage of the D3-brane tadpole cancelation condition to obtain a lower bound on the number of families.

This section is based on [32, 40].

2.3.1 Polyhedron F_{11} : $SU(3) \times SU(2) \times U(1)$

Gauge group, matter content and Yukawa couplings

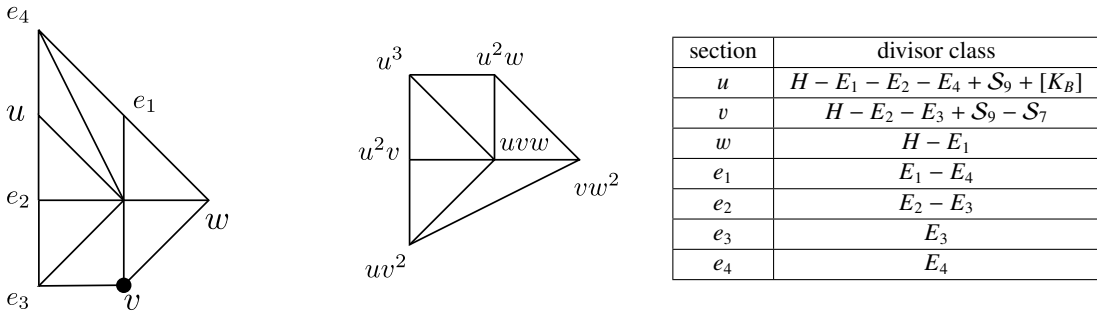


Figure 2.3: The toric polytope of $X_{F_{11}}$ and its dual are given on the left along with a choice of toric coordinates as well as the corresponding Batyrev monomials, respectively. Here we marked the zero section by a dot. On the right we give the divisor classes of the fiber coordinates.

The toric diagram F_{11} of the ambient space of the fiber is depicted in Figure 2.3 together with its dual polyhedron F_6 and the divisor classes of the coordinates. The ambient space can be interpreted as a blow-up of the geometry \mathbb{P}^2 in the blow-up coordinates e_i . On each node in the polyhedron we have written the assigned coordinate and on each node in the dual polyhedron we have given the corresponding monomial from the Batyrev formula (2.39). For ease of notation we have set the blow-up coordinates $e_i = 1$. The zero section is denoted by a dot. Using the monomials from the dual polyhedron the hypersurface equation in the ambient space $\mathbb{P}_{F_{11}}$ is given by

$$p_{F_{11}} = s_1 e_1^2 e_2^2 e_3 e_4^3 u^3 + s_2 e_1 e_2^2 e_3^2 e_4^2 u^2 v + s_3 e_2^2 e_3^2 u w^2 + s_5 e_1^2 e_2 e_3^3 u^2 w + s_6 e_1 e_2 e_3 e_4 u v w + s_9 e_1 v w^2. \quad (2.41)$$

In the full fibration the coefficients s_i are sections on the base \mathcal{B} and thus become line bundles with the divisor classes

section	divisor class	section	divisor class
s_1	$3[K_B^{-1}] - \mathcal{S}_7 - \mathcal{S}_9$	s_6	$[K_B^{-1}]$
s_2	$2[K_B^{-1}] - \mathcal{S}_9$	s_7	\mathcal{S}_7
s_3	$[K_B^{-1}] + \mathcal{S}_7 - \mathcal{S}_9$	s_8	$[K_B^{-1}] + \mathcal{S}_9 - \mathcal{S}_7$
s_4	$2\mathcal{S}_7 - \mathcal{S}_9$	s_9	\mathcal{S}_9
s_5	$2[K_B^{-1}] - \mathcal{S}_7$	s_{10}	$2\mathcal{S}_9 - \mathcal{S}_7$

(2.42)

Here \mathcal{S}_7 and \mathcal{S}_9 parametrize different possibilities of fibering the elliptic curve over the base. Since all sections s_i need to be effective this leads to constraints on the possible ways of fibering.

From the toric diagram in Figure 2.3 we can also read off the SR ideal of $\mathbb{P}_{F_{11}}$ by taking all non-neighboring nodes:

$$SR_{F_{11}} = \{ue_1, uw, uv, ue_3, e_4w, e_4v, e_4e_3, e_4e_2, e_1v, e_1e_3, e_1e_2, we_3, we_2, ve_2\}. \quad (2.43)$$

The set of rational sections of the elliptic fibration $X_{F_{11}}$ contains three toric rational sections. Two of these are linear independent [83] leading to a MW group of rank one. Explicitly we find the following rational sections

$$\begin{aligned} \hat{s}_0 &= X_{F_{11}} \cap \{v = 0\} : [1 : 0 : s_1 : 1 : 1 : -s_5 : 1], \\ X_{F_{11}} \cap \{e_3 = 0\} &: [1 : s_5 : 1 : 1 : -s_9 : 0 : 1], \\ \hat{s}_1 &= X_{F_{11}} \cap \{e_4 = 0\} : [s_9 : 1 : 1 : -s_3 : 1 : 1 : 0]. \end{aligned} \quad (2.44)$$

We choose \hat{s}_0 as the zero section (depicted by a dot in Figure 2.3) and \hat{s}_1 as the generator of the MW group.

Using Nagell's algorithm (see Appendix A.2 for a detailed discussion) we can derive the functions f and g of the Weierstrass form. From the functions f and g we calculate the discriminant $\Delta = 4f^3 + 27g^2$. We find the following results for $f_{F_{11}}$, $g_{F_{11}}$ and $\Delta_{F_{11}}$

$$f_{F_{11}} \propto (24s_3s_9(-s_5s_6 + 2s_1s_9) - (s_6^2 - 4s_2s_9)^2), \quad (2.45)$$

$$\begin{aligned} g_{F_{11}} \propto & (s_6^6 + 36s_3s_5s_6^3s_9 - 12s_2s_6^4s_9 - 144s_2s_3s_5s_6s_9^2 + 24(2s_2^2 - 3s_1s_3)s_6^2s_9^2 \\ & + 8s_9^2(27s_3^2s_5^2 - 8s_2^3s_9 + 36s_1s_2s_3s_9)), \end{aligned} \quad (2.46)$$

$$\begin{aligned} \Delta_{F_{11}} \propto & s_3^2s_9^3(s_3s_5^3s_6^3 - s_2s_5^2s_6^4 + s_1s_5s_6^5 + 27s_3^2s_5^4s_9 - 36s_2s_3s_5^3s_6s_9 + 8s_2^2s_5^2s_6^2s_9 + 30s_1s_3s_5^2s_6^2s_9 \\ & - 8s_1s_2s_5s_6^3s_9 - s_1^2s_6^4s_9 - 16s_2^3s_5^2s_9^2 + 72s_1s_2s_3s_5^2s_9^2 + 16s_1s_2^2s_5s_6s_9^2 - 96s_1^2s_3s_5s_6s_9^2 \\ & + 8s_1^2s_2s_6^2s_9^2 - 16s_1^2s_2^2s_9^3 + 64s_1^3s_3s_9^3). \end{aligned} \quad (2.47)$$

From the discriminant in (2.47) we can directly see two codimension one singularities: Over the divisor $\mathcal{S}_{SU(2)}^b = \{s_3 = 0\} \cap \mathcal{B}$ we find an I_2 singularity and over the divisor $\mathcal{S}_{SU(3)}^b = \{s_9 = 0\} \cap \mathcal{B}$ we find an I_3 singularity. Along these divisors the fiber splits in the following way underlining the corresponding singularity types

$$\begin{aligned} SU(2) : & \quad p_{F_{11}}|_{s_3=0} = e_1 \cdot q_3, \\ SU(3) : & \quad p_{F_{11}}|_{s_9=0} = e_2u \cdot q_2. \end{aligned} \quad (2.48)$$

Here q_3 and q_2 denote cubic and quadric polynomials in $[u, v, w]$ which remain after the factorization. The factorization of the fibers is depicted in Figure 2.4. There we also depict the intersection of the rational sections with the divisors which can be read off from the degree of the divisor polynomial in the neighboring coordinates after plugging in the section.

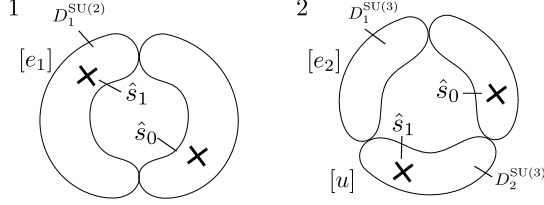


Figure 2.4: Codimension one fibers of $X_{F_{11}}$. The crosses denote the intersections with the two sections.

From the factorization depicted in Figure 2.4 we can read off the following Cartan divisors

$$D_1^{\text{SU}(2)} = [e_1], \quad D_1^{\text{SU}(3)} = [e_2], \quad D_2^{\text{SU}(3)} = [u]. \quad (2.49)$$

Having found the non-Abelian part of the gauge group and the rank of the MW group we can write down the total gauge group. It is given by

$$G_{F_{11}} = \text{SU}(3) \times \text{SU}(2) \times \text{U}(1). \quad (2.50)$$

The set of physically motivated divisors setting up a basis for $H^{1,1}(X_{F_{11}})$ is then given by the Cartan divisors, the base divisors, the zero section and the Shioda map

$$\sigma(\hat{s}_1) = S_1 - S_0 + [K_B] + \frac{1}{2}D_1^{\text{SU}(2)} + \frac{1}{3}\left(D_1^{\text{SU}(3)} + 2D_2^{\text{SU}(3)}\right). \quad (2.51)$$

Here we have used that the zero section does not intersect the section \hat{s}_1 in the base and the intersection numbers of the section \hat{s}_1 with the codimension one fibers in Figure 2.4 implying

$$\begin{aligned} \pi(S_1 \cdot S_0) &= 0, \\ S_1 \cdot C_{-\alpha_1}^{\text{SU}(2)} &= 1, \quad S_1 \cdot C_{-\alpha_1}^{\text{SU}(3)} = 0, \quad S_1 \cdot C_{-\alpha_2}^{\text{SU}(3)} = 1. \end{aligned} \quad (2.52)$$

To later on check for anomaly cancellation the height pairing (2.16) is necessary. For $X_{F_{11}}$ it is given by

$$b_{11} = \frac{3}{2}[K_B^{-1}] - \frac{1}{2}\mathcal{S}_7 - \frac{1}{6}\mathcal{S}_9, \quad (2.53)$$

where we used (2.52) as well as the universal intersection relation (2.17).

After having calculated the gauge group we now turn to the charged matter content by calculating the codimension two singularities of the discriminant $\Delta_{F_{11}}$. The singular loci of the non-Abelian matter representations follow directly from the discriminant after confining to the gauge group divisor. In contrast to that we use a prime ideal decomposition of the codimension two ideal (2.24) to determine the locus of the Abelian matter multiplets. We find the singularity enhancements given in Table 2.2. There we give the representation of the gauge group, the multiplicities which are calculated from the homology classes of the divisors, and the ideal of the singularity. Additionally we depict the splitting of the fiber. In the last two columns we give the adjoint representations for completeness. Using the given matter representations and multiplicities we checked that all 6D anomalies are canceled. For more details on

this see [32, 45].

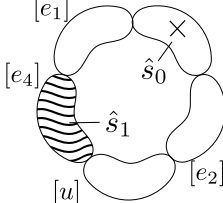
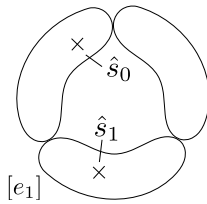
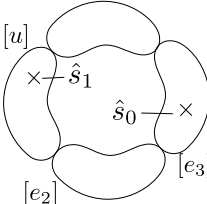
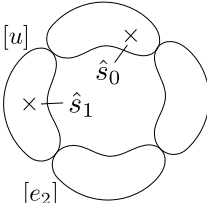
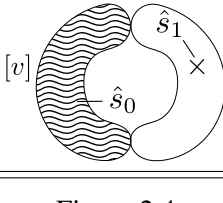
Representation	Multiplicity	Splitting	Locus
$(\mathbf{3}, \mathbf{2})_{-1/6}$	$\mathcal{S}_9([K_B^{-1}] + \mathcal{S}_7 - \mathcal{S}_9)$		$V(I_{(1)}) := \{s_3 = s_9 = 0\}$
$(\mathbf{1}, \mathbf{2})_{1/2}$	$([K_B^{-1}] + \mathcal{S}_7 - \mathcal{S}_9)$ $(6[K_B^{-1}] - 2\mathcal{S}_7 - \mathcal{S}_9)$		$V(I_{(2)}) := \{s_3 = 0$ $s_2 s_5^2 + s_1(s_1 s_9 - s_5 s_6) = 0\}$
$(\mathbf{3}, \mathbf{1})_{-2/3}$	$\mathcal{S}_9(2[K_B^{-1}] - \mathcal{S}_7)$		$V(I_{(3)}) := \{s_5 = s_9 = 0\}$
$(\mathbf{3}, \mathbf{1})_{1/3}$	$\mathcal{S}_9(5[K_B^{-1}] - \mathcal{S}_7 - \mathcal{S}_9)$		$V(I_{(4)}) := \{s_9 = 0$ $s_3 s_5^2 + s_6(s_1 s_6 - s_2 s_5) = 0\}$
$(\mathbf{1}, \mathbf{1})_{-1}$	$(2[K_B^{-1}] - \mathcal{S}_7)$ $(3[K_B^{-1}] - \mathcal{S}_7 - \mathcal{S}_9)$		$V(I_{(5)}) := \{s_1 = s_5 = 0\}$
$(\mathbf{8}, \mathbf{1})_0$	$1 + \mathcal{S}_9 \frac{\mathcal{S}_9 - [K_B^{-1}]}{2}$	Figure 2.4	$s_9 = 0$
$(\mathbf{1}, \mathbf{3})_0$	$1 + \frac{\mathcal{S}_7 - \mathcal{S}_9}{2}$ $\times ([K_B^{-1}] + \mathcal{S}_7 - \mathcal{S}_9)$	Figure 2.4	$s_3 = 0$

Table 2.2: Codimension two singular loci of $X_{F_{11}}$, corresponding fiber degenerations and charged matter representations under $SU(3) \times SU(2) \times U(1)$. The multiplicities of the matter representations are calculated from the homology classes of the divisors. The adjoint matter is included for completeness.

In codimension three we find all field theoretically allowed Yukawa couplings of the charged matter. The Yukawa points and the corresponding loci are given in Table 2.3.

Yukawa	Locus
$(\mathbf{3}, \mathbf{2})_{-1/6} \cdot (\mathbf{3}, \mathbf{1})_{-2/3} \cdot (\mathbf{1}, \mathbf{2})_{1/2}$	$s_3 = s_5 = s_9 = 0$
$(\mathbf{3}, \mathbf{2})_{-1/6} \cdot (\mathbf{3}, \mathbf{1})_{1/3} \cdot (\mathbf{1}, \mathbf{2})_{1/2}$	$s_3 = s_9 = 0 = s_1 s_6 - s_2 s_5$
$(\mathbf{3}, \mathbf{1})_{-2/3} \cdot (\mathbf{3}, \mathbf{1})_{1/3} \cdot (\mathbf{1}, \mathbf{1})_{-1}$	$s_1 = s_5 = s_9 = 0$
$(\mathbf{3}, \mathbf{2})_{-1/6} \cdot (\mathbf{3}, \mathbf{2})_{-1/6} \cdot (\mathbf{3}, \mathbf{1})_{1/3}$	$s_3 = s_9 = s_6 = 0$
$(\mathbf{1}, \mathbf{2})_{1/2} \cdot (\mathbf{1}, \mathbf{2})_{1/2} \cdot (\mathbf{1}, \mathbf{1})_{-1}$	$s_1 = s_5 = s_3 = 0$
$(\mathbf{3}, \mathbf{1})_{1/3} \cdot (\mathbf{3}, \mathbf{1})_{1/3} \cdot (\mathbf{3}, \mathbf{1})_{-2/3}$	$s_5 = s_6 = s_9$

 Table 2.3: Codimension three singular loci and respective Yukawa couplings for $X_{F_{11}}$.

Flux construction

To construct the vertical fluxes we first have to choose a base and then find a basis for the vertical cohomology class $H_V^{2,2}(X_{F_{11}})$. As a base of the fibration we choose in the following discussion $\mathcal{B} = \mathbb{P}^3$. \mathbb{P}^3 has only one independent divisor class H_B . This allows the following choice of basis for $H^{1,1}(X_{F_{11}})$

$$H^{1,1}(X_{F_{11}}) = \langle H_B, \tilde{S}_0, D_1^{\text{SU}(2)}, D_1^{\text{SU}(3)}, D_2^{\text{SU}(3)}, \sigma(\hat{s}_1) \rangle, \quad (2.54)$$

where D_i are the Cartan divisors, $\sigma(\hat{s}_1)$ is the Shioda map of the first section (2.51) and \tilde{S}_0 is the shifted zero section. Here we have to use the shifted zero section [84]

$$\tilde{S}_0 = S_0 + \frac{1}{2}[K_B^{-1}] \quad (2.55)$$

in order to take care of the Kaluza-Klein states which stem from the non-holomorphic zero section. For the flux discussion we also have to use the shifted zero section instead of the unshifted one in the definition of the Shioda map (2.51).

For the base $\mathcal{B} = \mathbb{P}^3$ the divisors $\mathcal{S}_7, \mathcal{S}_9, [K_B^{-1}]$ and c_2 take the form

$$\mathcal{S}_7 = n_7 H_B, \quad \mathcal{S}_9 = n_9 H_B, \quad [K_B^{-1}] = c_1 = 4H_B, \quad c_2 = 6H_B. \quad (2.56)$$

Here n_7 and n_9 are integer coefficients and c_1 and c_2 are the first and second Chern class of the base $\mathcal{B} = \mathbb{P}^3$ respectively. Demanding effectiveness of the divisors in (2.42) then leads to the allowed region for (n_7, n_9) depicted in Figure 2.5.

The SR ideal of the full fibration is obtained as the SR ideal of the fiber (2.43) extended by the base ideal which is given by $SR_{\mathcal{B}} = x_0 x_1 x_2 x_3$. Using this ideal we can calculate the full vertical cohomology ring. As additional input we need the following intersection numbers of the ambient space which follow from the toric intersections in the ambient space of the fiber $\mathbb{P}_{F_{11}}$

$$H_B^3 S_0^2 = -1, \quad H_B^3 S_1^2 = -1. \quad (2.57)$$

By calculating the rank of the matrix $\eta^{(2,2)}$ of intersection numbers of all elements of $H_V^{2,2}(X_{F_{11}})$ (the elements which are constructed as the product of two elements of $H^{1,1}(X_{F_{11}})$) we can obtain the dimension of $H_V^{2,2}(X_{F_{11}})$

$$\dim H_V^{2,2}(X_{F_{11}}) = 7. \quad (2.58)$$

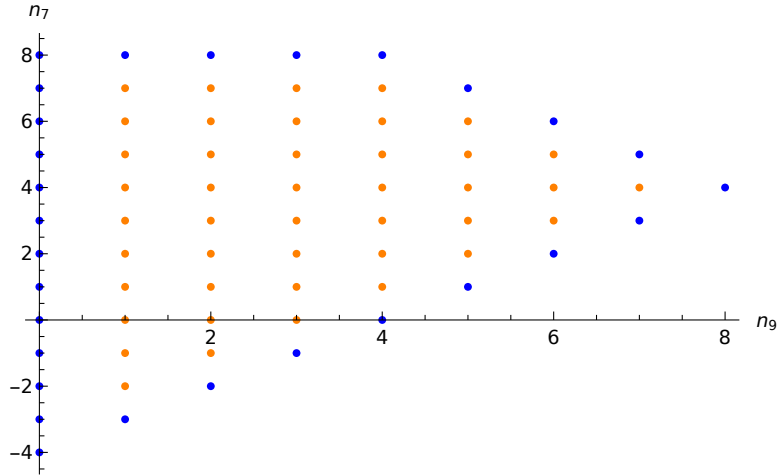


Figure 2.5: Possible values for (n_7, n_9) for the elliptically fibered CY fourfold $X_{F_{11}}$ with base $\mathcal{B} = \mathbb{P}^3$. The yellow dots denote bulk parts of the allowed region where all matter multiplets given in Table 2.2 are present. The blue dots denote the boundaries of the allowed region where generally not all matter multiplets from Table 2.2 are present. Thus the family solution (2.64) is not possible and diverges.

As a basis for $H_V^{2,2}(X_{F_{11}})$ we can then choose

$$H_V^{2,2}(X_{F_{11}}) = \langle (H_B)^2, H_B \tilde{S}_0, D_1^{\text{SU}(2)} H_B, D_1^{\text{SU}(3)} H_B, D_2^{\text{SU}(3)} H_B, H_B \sigma(\hat{s}_1), \tilde{S}_0^2 \rangle. \quad (2.59)$$

The G_4 flux is given as a general element of $H_V^{2,2}(X_{F_{11}})$. Additionally we have to impose the conditions (2.30) on this general element due to the comparison of M- and F-theory CS terms. This leads to five constraints leaving us with the following two parameter G_4 flux on $X_{F_{11}}$

$$G_4 = a_6 H_B \sigma(\hat{s}_1) - a_7 \left[\tilde{S}_0^2 + H_B^2 (-92 + 20n_7 - n_7^2 + 8n_9 - n_7 n_9) \right]. \quad (2.60)$$

Here the parameters a_6 and a_7 are discrete flux parameters. Their quantization is covered by the quantization condition for the G_4 flux (2.26). Since for a direct treatment of the quantization condition one needs an integral basis for $H_V^{(2,2)}(X_{F_{11}})$ we will not cover that here. Instead we reformulate the flux in terms of the chiralities which are necessarily integral.

To calculate the chiralities we have to integrate the G_4 flux over the matter surfaces C^w (2.32). This corresponds to calculating the intersection numbers of the matter surfaces and the G_4 flux. To do this we need the homology classes of the matter surfaces. The matter surfaces are given by one node w (one \mathbb{P}^1 in the fiber) fibered over the baselocus of the matter. As the corresponding node we choose the node which is not intersected by the zero section. Then the homology classes of the toric loci in Table 2.2 are easily computed as the product of the homology classes of the respective polynomials

$$\begin{aligned} C_{(3,2)_{1/6}}^w &= \mathcal{S}_9 \cdot ([K_B^{-1}] + \mathcal{S}_7 - \mathcal{S}_9) \cdot E_4, \\ C_{(\bar{3},1)_{-2/3}}^w &= -\mathcal{S}_9 \cdot (2[K_B^{-1}] - \mathcal{S}_7) \cdot (2H - E_2 - E_3 - \mathcal{S}_7 + \mathcal{S}_9 + [K_B^{-1}]), \\ C_{(1,1)_1}^w &= -(2[K_B^{-1}] - \mathcal{S}_7) \cdot (3[K_B^{-1}] - \mathcal{S}_7 - \mathcal{S}_9) \cdot (2H - E_1 - E_4 + \mathcal{S}_9). \end{aligned} \quad (2.61)$$

The other two matter loci in Table 2.2 are not toric loci. Therefore the matter surfaces are reducible and one needs to inspect the primary decomposition. The homology classes are calculated by taking a com-

plete intersection which contains the matter surface and subtracting the other irreducible components with the multiplicities obtained via the resultant. The homology classes are then

$$\begin{aligned}
 [C_{(1,2)_{-1/2}}^w] &= -\left((D_1^{\text{SU}(2)} + D_1^{\text{SU}(3)} + 2D_2^{\text{SU}(3)} + 4[K_B^{-1}] + 3S_1 - 2S_7) \cdot (6[K_B^{-1}] - 2S_7 - S_9) \right. \\
 &\quad \left. - 2(2[K_B^{-1}] - S_7) \cdot (3[K_B^{-1}] - S_7)\right) \cdot ([K_B^{-1}] + S_7 - S_9), \\
 [C_{(\bar{3},1)_{1/3}}^w] &= (2[K_B^{-1}] \cdot (S_7 - 2[K_B^{-1}]) + (D_1^{\text{SU}(2)} + D_2^{\text{SU}(3)} + 2[K_B^{-1}] + 2S_1 - S_7) \\
 &\quad \times (5[K_B^{-1}] - S_7 - S_9)) \cdot S_9.
 \end{aligned} \tag{2.62}$$

Using the matter surfaces obtained in (2.61) and (2.62) we can calculate the 4D chiralities via integrating over the matter surfaces (2.32). We obtain the chiralities

$$\begin{aligned}
 \chi_{(3,2)_{1/6}} &= \frac{1}{6}(4 + n_7 - n_9)n_9a_6, \\
 \chi_{(1,2)_{-1/2}} &= \frac{1}{2}(4 + n_7 - n_9)((-24 + 2n_7 + n_9)a_6 + 4(-8 + n_7)(-12 + n_7 + n_9)a_7), \\
 \chi_{(\bar{3},1)_{-2/3}} &= \frac{1}{3}(-8 + n_7)n_9(2a_6 + 3(-12 + n_7 + n_9)a_7), \\
 \chi_{(\bar{3},1)_{1/3}} &= -\frac{1}{3}n_9((-20 + n_7 + n_9)a_6 + 3(-8 + n_7)(-12 + n_7 + n_9)a_7), \\
 \chi_{(1,1)_1} &= (-8 + n_7)(-12 + n_7 + n_9)(a_6 + (-16 + 2n_7 + n_9)a_7).
 \end{aligned} \tag{2.63}$$

Enforcing the phenomenologically interesting case that all chiralities are equal to a number of families $\chi_i = b$ we can express the flux parameters a_6 and a_7 in terms of the number of families b

$$a_6 = \frac{6b}{(4 + n_7 - n_9)n_9}, \quad a_7 = -\frac{b(-36 + 3n_7 + n_9)}{n_9(-8 + n_7)(4 + n_7 - n_9)(-12 + n_7 + n_9)}. \tag{2.64}$$

This solution physically corresponds to the case of unbroken U(1) hypercharge which can be seen from the fact that $\theta_{m\alpha} = 0$. The parameters a_6 and a_7 get singular at the boundaries of the allowed region. This corresponds to the fact that at these points not all matter multiplets are present and thus the family structure is not complete.

After reparametrizing the G_4 flux in terms of b , n_7 and n_9 we check for D3-brane tadpole cancelation (2.27) at every point (n_7, n_9) which allows a family structure. Therefore we note that the Euler number as well as the second Chern class $c_2(X)$ can be calculated base independently via adjunction [85]. They are given by

$$\begin{aligned}
 c_2(X_{F_{11}}) &= -c_1^2 + c_2 + c_1E_2 - c_1E_3 - 7c_1E_4 - 7E_4^2 + 4c_1H + 2c_1S_7 + 4E_1S_7 + E_2S_7 \\
 &\quad + E_3S_7 + 6E_4S_7 - 4HS_7 - c_1S_9 - 5E_1S_9 - 3E_2S_9 - E_3S_9 + 3HS_9 - 3S_7S_9 + 3S_9^2, \\
 \chi(X_{F_{11}}) &= 3(24c_1^3 + 4c_1c_2 - 16c_1^2S_7 + 8c_1S_7^2 - 18c_1^2S_9 + 3c_1S_7S_9 - 3S_7^2S_9 \\
 &\quad + 6c_1S_9^2 + S_7S_9^2).
 \end{aligned} \tag{2.65}$$

$$\tag{2.66}$$

Here c_1 and c_2 denote the first and second Chern class of the base. The number of D3-branes n_{D3} needs to be integral for a smooth CY fourfold and quantized G_4 flux [67]. Additionally n_{D3} needs to be positive to avoid supersymmetry breaking [65]. As a further indirect check of the quantization condition (2.26) we verify the equivalent quantization that the CS terms are integral [72, 73]. We find the minimal number of allowed families and the corresponding number of n_{D3} D3-branes given in Table 2.4. The minimal allowed number of families is $b = 3$ at the two strata $(n_7, n_9) = (2, 5)$ and $(n_7, n_9) = (5, 6)$.

$n_7 \setminus n_9$	1	2	3	4	5	6	7
7	-	(27; 16)	-	-	-	-	-
6	-	(12; 81)	(21; 42)	-	-	-	-
5	-	-	(12; 57)	(30; 8)	-	(3; 46)	-
4	(42; 4)	-	(30; 32)	-	-	-	-
3	-	(21; 72)	-	-	-	(15; 30)	-
2	(45; 16)	(24; 79)	(21; 66)	(24; 44)	(3; 64)	-	-
1	-	-	-	-	-	-	-
0	-	-	(12; 112)	-	-	-	-
-1	(36; 91)	(33; 74)	-	-	-	-	-
-2	-	-	-	-	-	-	-

Table 2.4: (b, n_{D3}) gives the minimal possible number of families b which allows for a cancelation of the D3-brane tadpole (2.27) with the positive and integral number n_{D3} of D3-branes. Here we additionally impose that the CS terms are integral which is an indirect check of the quantization condition (2.26). The points where there is no number of families fulfilling these constraints are marked by "-".

2.3.2 Polyhedron F_{13} : $SU(4) \times SU(2)^2 / \mathbb{Z}_2$

Gauge group, matter content and Yukawa couplings

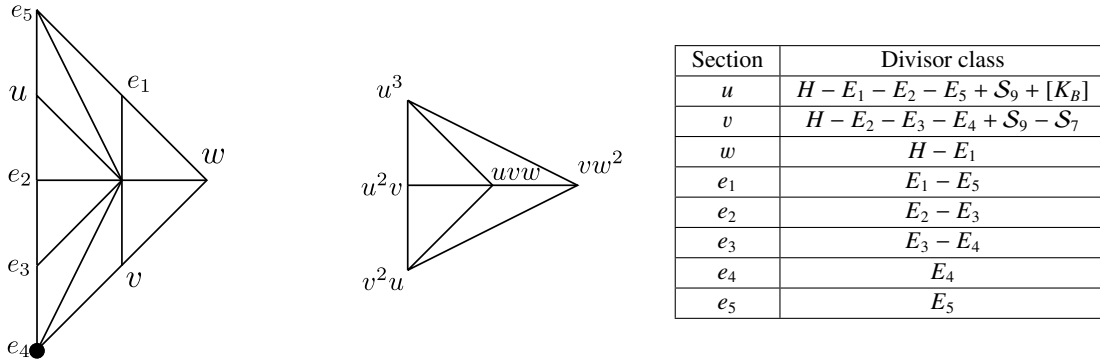


Figure 2.6: The toric polytope of $X_{F_{13}}$ and its dual are given on the left along with a choice of toric coordinates as well as the corresponding Batyrev monomials, respectively. Here we marked the zero section by a dot. On the right we give the divisor classes of the fiber coordinates.

The toric diagram F_{13} of the ambient space of the fiber as well as the corresponding divisor classes of the fiber are given in Figure 2.6. At each node in the toric diagram we give the assigned coordinates. Again the ambient space can be interpreted as a blow-up of the geometry \mathbb{P}^2 in the blow-up coordinates e_i . In the dual polyhedron F_4 we give the monomials corresponding to the nodes. Here all blow-up coordinates have been set to one $e_i = 1$. The elliptic curve is obtained as the following hypersurface in the ambient space $\mathbb{P}_{F_{13}}$ constructed via the Batyrev formula (2.39)

$$p_{F_{13}} = s_1 e_1^2 e_2^2 e_3 e_4^4 u^3 + s_2 e_1 e_2^2 e_3^2 e_4^2 e_5^2 u^2 v + s_3 e_2^2 e_3^3 e_4^4 u v^2 + s_6 e_1 e_2 e_3 e_4 e_5 u v w + s_9 e_1 v w^2. \quad (2.67)$$

As in the case of $X_{F_{11}}$ the coefficients s_i get enhanced to sections on the base \mathcal{B} in the full fibration with the corresponding divisor classes given in (2.42).

From the toric diagram in Figure 2.6 we read off the SR ideal of $\mathbb{P}_{F_{13}}$

$$SR_{F_{13}} = \{ue_1, uw, uv, ue_4, ue_3, e_5w, e_5v, e_5e_4, e_5e_3, e_5e_2, e_1v, e_1e_4, e_1e_3, e_1e_2, we_4, we_3, we_2, ve_3, ve_2, e_4e_2\}. \quad (2.68)$$

$X_{F_{13}}$ has two toric rational sections. However they fulfill a torsional relation [83] leading to a completely torsional MW group. The coordinates of the rational sections as well as our choice for the zero section \hat{s}_0 (depicted by a dot in Figure 2.6) is given by

$$\begin{aligned} \hat{s}_0 &= X_{F_{13}} \cap \{e_4 = 0\} : [1 : s_1 : 1 : 1 : 1 : -s_9 : 0 : 1], \\ \hat{s}_t &= X_{F_{13}} \cap \{e_5 = 0\} : [s_9 : 1 : 1 : -s_3 : 1 : 1 : 1 : 0]. \end{aligned} \quad (2.69)$$

Here \hat{s}_t denotes the torsional section which fulfills $\hat{s}_t + \hat{s}_t = \hat{s}_0$ under the group law of the elliptic curve (see Appendix A.1) [83]. The effect of the torsional part of the MW group is that the gauge group is turned into a non-simply connected gauge group. This reduces the weight lattice of the gauge group and thus should be reflected in the matter content: Fundamental matter should be forbidden [56]. That this is indeed the case can be seen from Table 2.5.

Using again the Nagell algorithm (see Appendix A.2) we derive the Weierstrass form of the hypersurface (2.67). The functions f, g as well as the discriminant $\Delta = 4f^3 + 27g^2$ are given by

$$f_{F_{13}} \propto (-s_6^4 + 8s_2s_6^2s_9 - 16s_2^2s_9^2 + 48s_1s_3s_9^2), \quad (2.70)$$

$$g_{F_{13}} \propto (s_6^2 - 4s_2s_9)(s_6^4 - 8s_2s_6^2s_9 + 16s_2^2s_9^2 - 72s_1s_3s_9^2), \quad (2.71)$$

$$\Delta_{F_{13}} \propto s_1^2s_3^2s_9^4(s_6^4 - 8s_2s_6^2s_9 + 16s_2^2s_9^2 - 64s_1s_3s_9^2). \quad (2.72)$$

Using the Kodaira classification (see Table 2.1) we can directly read off the codimension one singularities. Over the divisors $\mathcal{S}_{\text{SU}(2)_1}^b = \{s_1 = 0\} \cap \mathcal{B}$ and $\mathcal{S}_{\text{SU}(2)_2}^b = \{s_3 = 0\} \cap \mathcal{B}$ we find I_2 singularities and over the divisor $\mathcal{S}_{\text{SU}(4)}^b = \{s_9 = 0\} \cap \mathcal{B}$ we find an I_4 singularity. The singularity type is also supported by the factorization of the hypersurface constraint (2.67) along the divisors

$$\begin{aligned} \text{SU}(2)_1 : \quad p_{F_{13}}|_{s_1=0} &= v \cdot q_2, \\ \text{SU}(2)_2 : \quad p_{F_{13}}|_{s_3=0} &= e_1 \cdot q_3, \\ \text{SU}(4) : \quad p_{F_{13}}|_{s_9=0} &= ue_2e_3 \cdot q_2'. \end{aligned} \quad (2.73)$$

Here q_2, q_2' and q_3 denote the quadric and cubic polynomials in $[u, v, w]$ which remain after the factorization. The factorization of the fiber is depicted in Figure 2.7. There also the intersections of the zero section with the fiber and the definition of the Cartan divisors is shown. From the factorization depicted

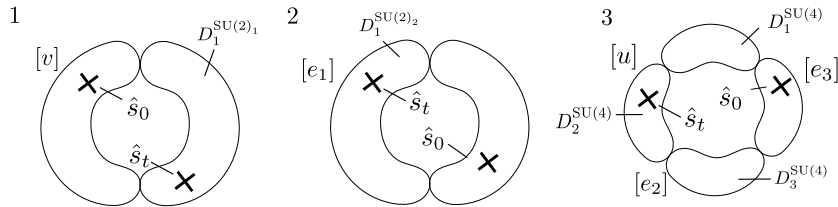


Figure 2.7: Codimension one fibers of $X_{F_{13}}$. The crosses denote the intersections with the zero section.

in Figure 2.7 we can read off the following Cartan divisors

$$\begin{aligned} D_1^{\text{SU}(2)_1} &= [s_1] - [v], & D_1^{\text{SU}(2)_2} &= [e_1], \\ D_1^{\text{SU}(4)} &= [s_9] - [u] - [e_2] - [e_3], & D_2^{\text{SU}(4)} &= [u], & D_3^{\text{SU}(4)} &= [e_2]. \end{aligned} \quad (2.74)$$

The discriminant has another potential codimension one singularity when the polynomial part in (2.72) vanishes. However, as shown in [56], the torsional MW group identifies the two \mathbb{P}^1 's leading to a single singular \mathbb{P}^1 and no additional gauge group.

Then the total gauge group of $X_{F_{13}}$ is given by

$$G_{F_{13}} = (\text{SU}(4) \times \text{SU}(2)^2) / \mathbb{Z}_2. \quad (2.75)$$

Next we proceed with the calculation of the matter content of the theory. We find the four non-Abelian matter representations given in Table 2.5 directly from the discriminant. There we give the representations, the multiplicities which are calculated from the homology classes of the divisors of the loci, the factorization of the fiber and the locus of each singularity. For completeness we also give the three adjoint representations in the table. The fibers of the $(\mathbf{2}, \mathbf{2}, \mathbf{1})$ and the $(\mathbf{1}, \mathbf{1}, \mathbf{6})$ representation are non-split in the sense of [86]. This means that the hypersurface constraint does not fully factorize over the field K but only over a field extension where square roots of the coefficients s_i are allowed. This corresponds to a codimension three monodromy which interchanges the \mathbb{P}^1 's drawn with dashed lines in Table 2.5.

In total we see three bifundamental representations, one antisymmetric representation and no fundamental representation in the spectrum as predicted by the torsional MW group. Using the matter representations and multiplicities given in Table 2.5 we check that all 6D anomalies are canceled [32, 45].

In codimension three we find the Yukawa couplings given in Table 2.6.

Flux construction

For the following part of the flux construction we choose again the base $\mathcal{B} = \mathbb{P}^3$. This leads to divisors $\mathcal{S}_7, \mathcal{S}_9, [K_B^{-1}]$ and c_2 given in (2.56). Then for $X_{F_{13}}$ the allowed region for (n_7, n_9) can be found in Figure 2.8.

Since \mathbb{P}^3 has only the independent divisor class H_B we can choose the following basis for $H^{1,1}(X_{F_{13}})$

$$H^{(1,1)}(X_{F_{13}}) = \langle H_B, \mathcal{S}_0, D_1^{\text{SU}(2)_1}, D_1^{\text{SU}(2)_2}, D_1^{\text{SU}(4)}, D_2^{\text{SU}(4)}, D_3^{\text{SU}(4)} \rangle. \quad (2.76)$$

As before, extending the SR ideal (2.68) by the base part $\mathcal{S}R_{\mathcal{B}} = x_0 x_1 x_2 x_3$ we can calculate the full vertical cohomology ring. Here we need the following intersection numbers of the ambient space which follow from toric intersections in the ambient space of the fiber $\mathbb{P}_{F_{13}}$

$$H_B^3 \mathcal{S}_0^2 = -1, \quad H_B^3 (D_1^{\text{SU}(2)_2})^2 = -2, \quad H_B^3 (D_3^{\text{SU}(4)})^2 = -2. \quad (2.77)$$

Then the dimension of the vertical cohomology $H_V^{2,2}(X_{F_{13}})$ can be calculated as the rank of the matrix of intersection numbers of all elements of $H^{2,2}(X_{F_{13}})$ which are a product of two elements of $H^{1,1}(X_{F_{13}})$

$$\dim H_V^{(2,2)}(X_{F_{13}}) = 8. \quad (2.78)$$

Thus by choosing a set of eight elements of $H_V^{2,2}(X_{F_{13}})$ with an intersection matrix with full rank we find

Representation	Multiplicity	Fiber	Locus
$(2, 2, 1)$	$(3[K_B^{-1}] - \mathcal{S}_7 - \mathcal{S}_9)$ $\times ([K_B^{-1}] + \mathcal{S}_7 - \mathcal{S}_9)$		$V(I_{(1)}) :=$ $\{s_1 = s_3 = 0\}$
$(2, 1, 4)$	$(3[K_B^{-1}] - \mathcal{S}_7 - \mathcal{S}_9)\mathcal{S}_9$		$V(I_{(2)}) :=$ $\{s_1 = s_9 = 0\}$
$(1, 2, 4)$	$([K_B^{-1}] + \mathcal{S}_7 - \mathcal{S}_9)\mathcal{S}_9$		$V(I_{(3)}) :=$ $\{s_3 = s_9 = 0\}$
$(1, 1, 6)$	$\mathcal{S}_9[K_B^{-1}]$		$V(I_{(4)}) :=$ $\{s_6 = s_9 = 0\}$
$(3, 1, 1)$	$1 + \frac{((2[K_B^{-1}] - \mathcal{S}_7 - \mathcal{S}_9))}{2}$ $\times (3[K_B^{-1}] - \mathcal{S}_7 - \mathcal{S}_9)$	Figure 2.7	$s_1 = 0$
$(1, 3, 1)$	$1 + \frac{(\mathcal{S}_7 - \mathcal{S}_9)}{2}$ $\times ([K_B^{-1}] + \mathcal{S}_7 - \mathcal{S}_9)$	Figure 2.7	$s_3 = 0$
$(1, 1, 15)$	$1 + \mathcal{S}_9 \frac{(\mathcal{S}_9 - [K_B^{-1}])}{2}$	Figure 2.7	$s_9 = 0$

Table 2.5: Codimension two singular loci of $X_{F_{13}}$, corresponding fiber degenerations and charged matter representations under $(\text{SU}(4) \times \text{SU}(2)^2)/\mathbb{Z}_2$. The multiplicities of the matter representations are calculated from the homology classes of the divisors. The adjoint matter is included for completeness.

the following basis for $H_V^{2,2}(X_{F_{13}})$

$$H_V^{(2,2)}(X_{F_{13}}) = \langle H_B^2, H_B \mathcal{S}_0, H_B D_1^{\text{SU}(2)_1}, H_B D_1^{\text{SU}(2)_2}, H_B D_1^{\text{SU}(4)}, H_B D_2^{\text{SU}(4)}, H_B D_3^{\text{SU}(4)}, \mathcal{S}_0^2 \rangle. \quad (2.79)$$

Imposing the conditions (2.30) on a general element of $H_V^{(2,2)}(X_{F_{13}})$ leads to seven constraints leaving

Yukawa	Locus
$(\mathbf{2}, \mathbf{2}, \mathbf{1}) \cdot (\mathbf{2}, \mathbf{1}, \mathbf{4}) \cdot (\mathbf{1}, \mathbf{2}, \mathbf{4})$	$s_1 = s_3 = s_9 = 0$
$(\mathbf{1}, \mathbf{1}, \mathbf{6}) \cdot (\mathbf{2}, \mathbf{1}, \mathbf{4}) \cdot (\mathbf{2}, \mathbf{1}, \mathbf{4})$	$s_1 = s_6 = s_9 = 0$
$(\mathbf{1}, \mathbf{1}, \mathbf{6}) \cdot (\mathbf{1}, \mathbf{2}, \mathbf{4}) \cdot (\mathbf{1}, \mathbf{2}, \mathbf{4})$	$s_3 = s_6 = s_9 = 0$

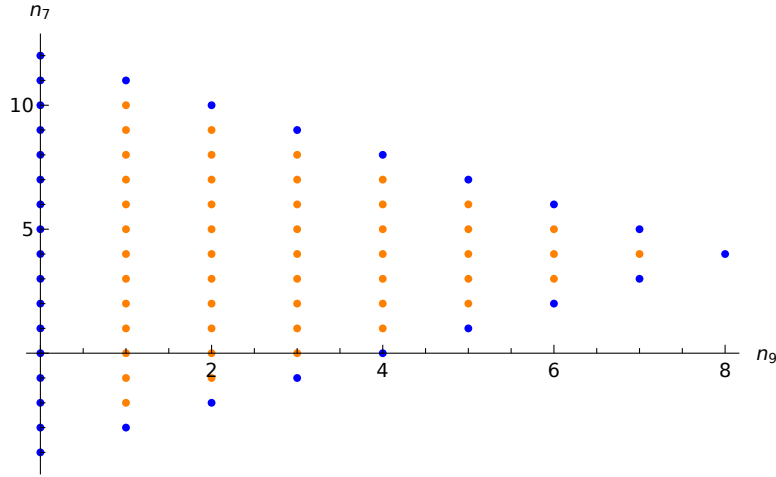
 Table 2.6: Codimension three singular loci and respective Yukawa couplings for $X_{F_{13}}$.


Figure 2.8: Allowed region for (n_7, n_9) for the elliptically fibered CY fourfold $X_{F_{13}}$ with base $\mathcal{B} = \mathbb{P}^3$. The yellow dots denote bulk parts of the allowed region where all matter multiplets given in Table 2.2 are present. The blue dots denote the boundaries of the allowed region where generally not all matter multiplets from Table 2.2 are present. Thus the family solution (2.83) is not possible and thus diverges.

us with the one parameter flux

$$G_4 = -a_8 \left[\hat{s}_0^2 + H_B \left(4\hat{s}_0 + H_B \left(12n_9 - n_7n_9 - n_9^2 \right) - \frac{1}{2}D_1^{\text{SU}(2)_1}n_9 \right. \right. \\ \left. \left. + \left(\frac{3}{4}D_1^{\text{SU}(4)} + \frac{1}{2}D_2^{\text{SU}(4)} + \frac{1}{4}D_3^{\text{SU}(4)} \right) (-12 + n_7 + n_9) \right) \right]. \quad (2.80)$$

Here the parameter a_8 is the only discrete flux parameter. Since we do not have an integral basis for $H_V^{(2,2)}(X_{F_{13}})$ we do not treat the quantization condition (2.26) explicitly. Instead we express the G_4 flux in terms of the integral chiralities.

To calculate the chiralities we first calculate the matter surfaces. The homology classes of the irreducible matter surfaces are calculated as a product of the homology classes of the base loci with the homology classes of the nodes w in the fiber. As nodes in the fiber we take the nodes which are not in the gauge algebra and which are not intersected by the zero section. We obtain

$$C_{(2,1,4)}^w = \mathcal{S}_9(3[K_B^{-1}] - \mathcal{S}_7 - \mathcal{S}_9)(H + [K_B^{-1}]), \\ C_{(1,2,4)}^w = \mathcal{S}_9([K_B^{-1}] + \mathcal{S}_7 - \mathcal{S}_9)E_5. \quad (2.81)$$

Integrating the G_4 flux over the matter surfaces in (2.81) we find the chiralities

$$\chi_{(2,1,4)} = -\chi_{(1,2,4)} = -\frac{1}{4}n_9(-4 - n_7 + n_9)(-12 + n_7 + n_9)a_8. \quad (2.82)$$

The other two matter multiplets $(2, 2, 1)$ and $(1, 1, 6)$ are real representations. Therefore their chiralities (2.32) are zero by definition. Nevertheless there exist fields in this representations but their number is measured by $n(\mathbf{R})$ (see (2.32)). Computationally this is reflected by the fact that they drop out of the anomaly equations and also cannot be computed by field theoretic computations of the CS terms and subsequent comparison to the M-theoretic CS terms like in [39]. Also since these two loci are non-split we cannot calculate the homology classes of the corresponding matter surfaces. Thus we were not able to calculate the multiplicities of these fields.

Now we can express the flux parameters in terms of the chiralities. To do this we set the chirality $\chi_{(2,1,4)} = b$. Then the flux parameter becomes

$$a_8 = \frac{-4b}{n_9(-4 - n_7 + n_9)(-12 + n_7 + n_9)}. \quad (2.83)$$

The flux parameter becomes singular at the boundary of the allowed region. This corresponds field theoretically to the fact that not all gauge groups (2.73) are present. Since the theory must not contain fundamental fields also not all matter multiplets from Table 2.5 are present. The possible values for (n_7, n_9) which allow a family structure are depicted as yellow dots in Figure 2.8.

Next we check for D3-brane tadpole cancelation (2.27) at every point (n_7, n_9) which allows a family structure. Therefor we calculate the following Euler number $\chi(X_{F_{13}})$ and second Chern class $c_2(X)$ via adjunction for a general base [85]

$$c_2(X_{F_{13}}) = -c_1^2 + c_2 - 6c_1E_1 - 6E_1^2 - 2c_1E_3 - 2E_4^2 + 4c_1H + c_1\mathcal{S}_7 + 9E_1\mathcal{S}_7 + E_2\mathcal{S}_7 + E_3\mathcal{S}_7 - E_4\mathcal{S}_7 - E_5\mathcal{S}_7 - 3H\mathcal{S}_7 - 4E_1\mathcal{S}_9 - 2E_2\mathcal{S}_9 + 2H\mathcal{S}_9 - 2\mathcal{S}_7\mathcal{S}_9 + 2\mathcal{S}_9^2, \quad (2.84)$$

$$\chi(X_{F_{13}}) = 12(6c_1^3 + c_1c_2 - 4c_1^2\mathcal{S}_7 + 2c_1\mathcal{S}_7^2 - 6c_1^2\mathcal{S}_9 + 2c_1\mathcal{S}_7\mathcal{S}_9 - \mathcal{S}_7^2\mathcal{S}_9 + 2c_1\mathcal{S}_9^2). \quad (2.85)$$

Here c_1 and c_2 denote the first and second Chern class of the base respectively. For a smooth CY fourfold the number of D3-branes n_{D3} must again be a positive integer [65, 67]. Additionally the G_4 flux needs to be quantized [67]. As before we check the latter indirectly via verifying the equivalent quantization condition of the CS terms [72, 73] by checking integrality of them. This ensures that the basis of $H_V^{(2,2)}(X_{F_{13}})$ is integral but it does not need to be also a minimal basis.

We find the minimal number of allowed families and the corresponding numbers of D3-branes in Table 2.7. The minimal number of families is again $b = 3$.

2.4 The toric Higgs network

One observes that the two examples in the previous section are connected on the field theory side via a Higgs transition. In this section we will first discuss this connection in detail on the basis of the examples. To do this we will discuss the necessary charge identification, possible transformations occurring in the identification and subtleties associated to the allowed regions of possible fibrations.

Afterwards we will generalize the discussion to a larger set of theories and introduce the Higgs network. We then make some interesting observations on the basis of the Higgs network.

In the course of this section we only consider six dimensional theories. In six dimensions a hyper mul-

$n_7 \setminus n_9$	1	2	3	4	5	6	7
10	(13; 204)						
9	—	(11; 140)					
8	(33; 94)	(10; 119)	(9; 90)				
7	—	(9; 100)	(6; 77)	(14; 48)			
6	(15; 108)	(8; 86)	(21; 52)	(12; 46)	(5; 44)		
5	(6; 106)	(35; 44)	—	(30; 16)	—	(3; 44)	
4	(7; 102)	(6; 75)	(15; 50)	(8; 42)	(15; 30)	(6; 41)	(7; 42)
3	(6; 106)	(35; 44)	—	(30; 16)	—	(3; 44)	
2	(15; 108)	(8; 86)	(21; 52)	(12; 46)	(5; 44)		
1	—	(9; 100)	(6; 77)	(14; 48)			
0	(33; 94)	(10; 119)	(9; 90)				
-1	—	(11; 140)					
-2	(13; 204)						

Table 2.7: The entries $(b; n_{D3})$ give the minimal number of families b for which the number of D3-branes n_{D3} is integral and positive for integral CS terms. At the points marked with "—" the number of D3-branes is not a positive integer.

triplet consists of two half-hypers which transform in conjugate representations. Thus after the Higgsing the multiplicities of conjugate half-hypers have to be added.

2.4.1 Higgs connection

The field theoretic Higgsing connecting the two theories discussed in the previous Section 2.3 is a realization of the geometric extremal transition connecting the two CY manifolds $X_{F_{13}}$ and $X_{F_{11}}$. This extremal transition is induced by a blow-up/down in the toric ambient space of the fiber \mathbb{P}_{F_i} and a complex structure deformation of the hypersurface constraint. Both these transformations are needed in order to preserve that the fiber is a genus-one curve.

On the level of the toric diagram the transition corresponds to deleting/adding a node in the polyhedron and adding/deleting a node in the dual polyhedron.

In order to find the node which has to be deleted for a certain Higgsing we define *toric matter*. Toric matter is the matter located at $s_i = s_j = 0$ where s_i and s_j need to be neighboring nodes on the boundary of the dual polyhedron. To make that clearer consider the case of F_{13} depicted in Figure 2.9. From Table 2.5 we see that all multiplets are at loci where $s_i = s_j = 0$. But from the dual polyhedron depicted in Figure 2.9 we find that only two of them are toric. In the case $s_1 = s_3 = 0$ the nodes are not neighboring and in the case $s_6 = s_9 = 0$ the node s_6 is not on the boundary. Thus there are two possible toric Higgsings associated to the multiplets $(\mathbf{2}, \mathbf{1}, \mathbf{4})$ and $(\mathbf{1}, \mathbf{2}, \mathbf{4})$.

To find the node in polyhedron F_{13} which has to be blown-down in order to induce a Higgsing of the $(\mathbf{2}, \mathbf{1}, \mathbf{4})$ multiplet we have to make a blow-up in the dual polyhedron F_4 (see Figure 2.9) at the line connecting the two nodes s_i and s_j of the toric matter. In this case between s_1 and s_9 . The line connecting the nodes s_1 and s_9 is dual to the node e_4 which is deleted (blown-down) in the original polyhedron F_{13} by blowing-up between the two nodes s_1 and s_9 in the dual polyhedron F_4 .

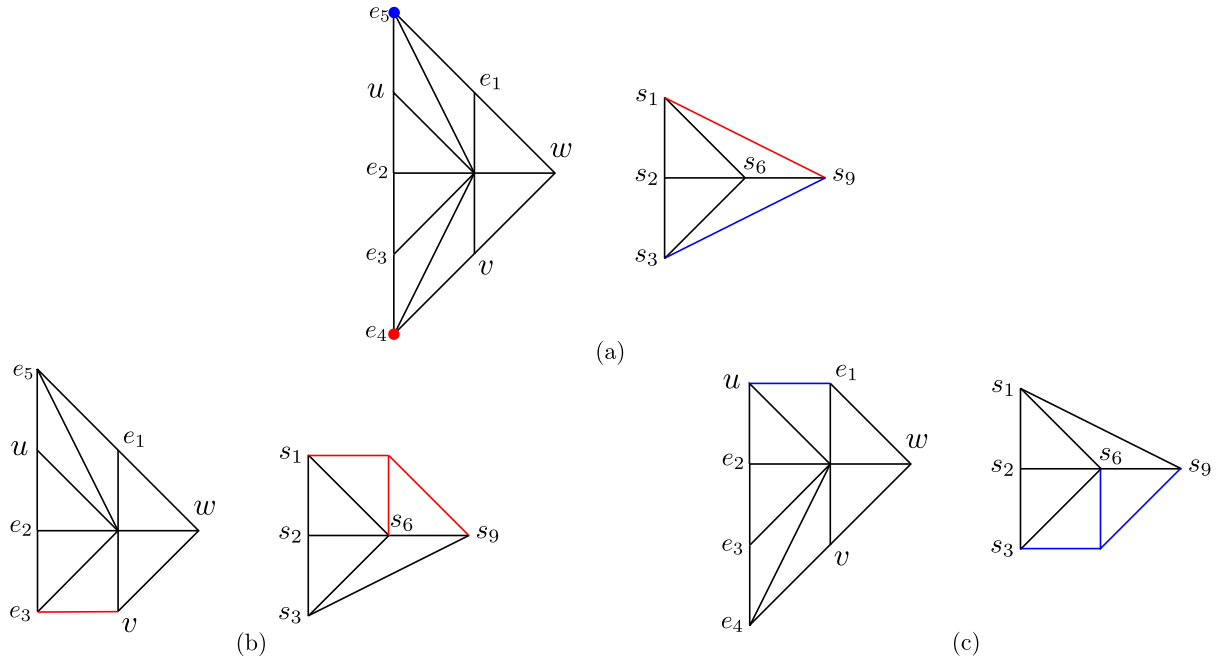


Figure 2.9: (a) Polyhedron F_{13} and its dual polyhedron F_4 . Blue denotes the locus of $(\mathbf{2}, \mathbf{1}, \mathbf{4})$ and red the locus of $(\mathbf{1}, \mathbf{2}, \mathbf{4})$. The transitions to $X_{F_{11}}$ can be triggered by Higgs fields in the representation $(\mathbf{2}, \mathbf{1}, \mathbf{4})$ (b) and $(\mathbf{1}, \mathbf{2}, \mathbf{4})$ (c).

Charge identification

To find a formula for the $U(1)$ charge in the model after the Higgsing we first have to define a torsional Shioda map (2.15) in $X_{F_{13}}$ ²

$$\sigma(\hat{s}_t) = S_t - S_0 - [K_B^{-1}] + \frac{1}{2}D_1^{\text{SU}(2)_1} + \frac{1}{2}D_1^{\text{SU}(2)_2} + \frac{1}{2}(D_1^{\text{SU}(4)} + 2D_2^{\text{SU}(4)} + D_3^{\text{SU}(4)}). \quad (2.86)$$

It can be checked from the intersections of the matter nodes with the torsional section \hat{s}_t depicted in Table 2.5 that all matter multiplets have charge 0 under the Shioda map $\sigma(\hat{s}_t)$. This section can now be expressed in terms of the homology classes of the individual divisors

$$\sigma_{F_{13}}(\hat{s}_t) = [e_5] - [e_4] - [K_B^{-1}] + \frac{1}{2}([s_1] - [v]) + \frac{1}{2}[e_1] + \frac{1}{2}([s_9] - [u] - [e_2] - [e_3]) + 2[u] + [e_2]. \quad (2.87)$$

On the contrary the Shioda map of $X_{F_{11}}$ in terms of the homology classes is given by

$$\sigma_{F_{11}}(\hat{s}_1) = [\tilde{e}_4] - [v] - [K_B^{-1}] + \frac{1}{2}[e_1] + \frac{1}{3}([e_2] + 2[u]). \quad (2.88)$$

Now we consider the Higgsing with the multiplet $(\mathbf{2}, \mathbf{1}, \mathbf{4})$. To do this we have to blow down the node $[e_4]$ in F_{13} as depicted in Figure 2.9. This blow down requires thus $[e_4] = 0$. Then we can express the Shioda map of $X_{F_{11}}$ in terms of the blown down torsional Shioda map and the Cartan divisors of $X_{F_{13}}$.

² This step is not necessary in simpler models without torsion but $U(1)$ symmetries.

This leads to

$$\sigma_{F_{11}}(\hat{s}_1) = \sigma_{F_{13}}(\hat{s}_t) + \frac{1}{2}D_1^{\text{SU}(2)_1} - [s_1] + \frac{1}{6}(-3D_1^{\text{SU}(4)} - 2D_2^{\text{SU}(4)} - D_3^{\text{SU}(4)}). \quad (2.89)$$

The base divisor $[s_1]$ does not contribute to the charges and as we have seen above all multiplets in $X_{F_{13}}$ are uncharged under $\sigma_{F_{13}}(\hat{s}_t)$. After identifying $T_3^{\text{SU}(2)_1} = \frac{1}{2}D_1^{\text{SU}(2)_1}$ and $T_{15}^{\text{SU}(4)} = \frac{1}{6}(3D_1^{\text{SU}(4)} + 2D_2^{\text{SU}(4)} + D_3^{\text{SU}(4)})$ we find the charge formula

$$Q = T_3^{\text{SU}(2)_1} - T_{15}^{\text{SU}(4)}. \quad (2.90)$$

This formula coincides with the field theory expectation³.

To calculate the charges in a Higgsing with the multiplet $(\mathbf{1}, \mathbf{2}, \mathbf{4})$ we have to take two additional effects into account: First the toric diagram needs to be reflected, see Figure 2.9. This effectively amounts to the interchange of $[u]$ and $[e_1]$ with $[e_3]$ and $[v]$ respectively. The second effect we have to deal with is that we need to change the zero section. This leads to a redefinition of one Cartan divisor of each gauge group in $X_{F_{13}}$. Taking all the described effects into account we can express the Shioda map of $X_{F_{11}}$ in terms of the divisors of $X_{F_{13}}$ in the following way

$$\sigma_{F_{11}}(\hat{s}_1) = -\sigma_{F_{13}}(\hat{s}_t) + 2[K_B^{-1}] + \frac{1}{2}[s_1] - \frac{1}{2}[s_3] + \frac{1}{2}D_1^{\text{SU}(2)_2} + \frac{1}{6}(-3D_1^{\text{SU}(4)} - 2D_2^{\text{SU}(4)} - D_3^{\text{SU}(4)}). \quad (2.91)$$

Using the same definitions of the generators of the gauge groups as above we find the following formula for the charges in the effective field theory of $X_{F_{11}}$ after the Higgsing

$$Q = T_{15}^{\text{SU}(4)} - T_3^{\text{SU}(2)_2}. \quad (2.92)$$

$SL(2, \mathbb{Z})$ transformations

Apart from the field theoretic Higgsing obtained by assigning a vev to the $(\mathbf{2}, \mathbf{1}, \mathbf{4})$ multiplet in $X_{F_{13}}$ there is another possible toric Higgsing associated to a vev in the $(\mathbf{1}, \mathbf{2}, \mathbf{4})$ representation. On the level of the toric diagram this corresponds to blowing down the variable e_5 instead of e_4 . Both possible Higgsings lead to theories with the same multiplets but with different multiplicities. In order to match the theory obtained after giving a vev to the $(\mathbf{1}, \mathbf{2}, \mathbf{4})$ representation with the effective field theory of $X_{F_{11}}$ we observe that the toric diagrams do only agree up to mirroring along the e_2 - w axis (see Figure 2.9). In general an $SL(2, \mathbb{Z})$ transformation can occur. The identification has to map the structures onto each other. That means that rational points have to be mapped to rational points and internal points on lines have to be mapped to internal points on lines. Concretely in this case we have to identify the nodes given in Table 2.8.

node in F_{13}	e_4	e_3	e_2	u	e_1	w	v
node in F_{11}	e_4	u	e_2	e_3	v	w	e_1

Table 2.8: The nodes which have to be identified for a proper matching of the theories after the Higgsing with a multiplet in the $(\mathbf{1}, \mathbf{2}, \mathbf{4})$ representation.

³ In [32] this charge formula is given with an overall factor of -1 which is irrelevant in 6D.

In order to identify the points the homology classes need to agree. Thus we get a linear system of equations connecting the homology classes of F_{11} with the homology classes of F_{13} after the Higgsing. Solving this system gives a shift in the bundles \mathcal{S}_7 and \mathcal{S}_9

$$\mathcal{S}_7 \rightarrow 2[K_B^{-1}] - \mathcal{S}_7, \quad \mathcal{S}_9 \rightarrow \mathcal{S}_9, \quad (2.93)$$

and correspondingly in the matter multiplicities.

Allowed region

As discussed in Section 2.3 a specific base fixes the divisor classes \mathcal{S}_7 , \mathcal{S}_9 and $[K_B^{-1}]$. Since we are dealing with CY threefolds in this section we use in the following the base $\mathcal{B} = \mathbb{P}^2$. This gives the following identifications

$$\mathcal{S}_7 = n_7 H_B, \quad \mathcal{S}_9 = n_9 H_B, \quad [K_B^{-1}] = 3H_B. \quad (2.94)$$

The requirement that the sections (2.42) in the hypersurface equation are effective divisors leads to constraints on n_7 and n_9 . Since smaller polyhedra like F_{11} compared to F_{13} have more monomials in the hypersurface equation their values for (n_7, n_9) are more constrained than for larger polytopes. This means that the allowed region of possible values (n_7, n_9) of $X_{F_{11}}$ is contained in the allowed region of $X_{F_{13}}$. Thus there are values for (n_7, n_9) which are allowed in $X_{F_{13}}$ but not allowed in $X_{F_{11}}$. In Figure 2.10 the allowed region of $X_{F_{13}}$ is depicted. The values which are not in the allowed region of $X_{F_{11}}$ are colored blue.

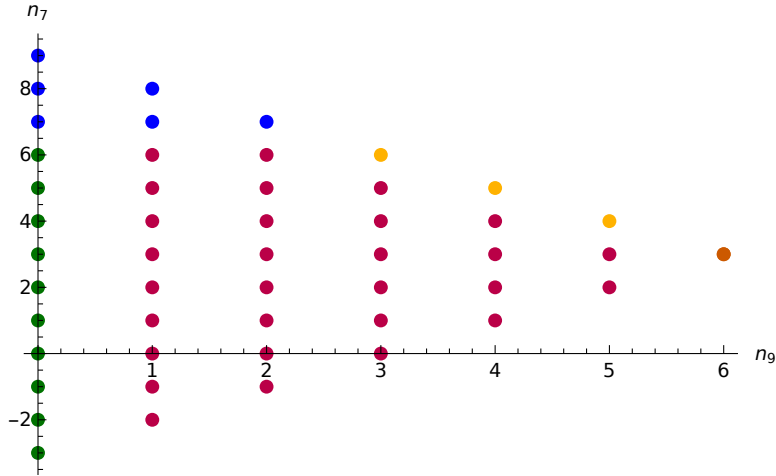


Figure 2.10: Allowed region of $X_{F_{13}}$. The values for (n_7, n_9) which are not in the allowed region of $X_{F_{11}}$ are colored blue. At the green dots the $SU(4)$ is not present. At the yellow dots the $SU(2)_1$ is not present and at the orange dot both $SU(2)$'s are not present.

Hence geometrically a transition at the values for (n_7, n_9) which are not allowed in $X_{F_{11}}$ is not possible. The field theoretic reason for this is as follows: In order to preserve $\mathcal{N} = 1$ supersymmetry and thus be able to connect two SUGRA theories we need a D-flat potential. In [87] it was observed that this requires two Higgs fields in six dimensions.

As an example take the Higgsing $X_{F_{13}} \rightarrow X_{F_{11}}$ by giving a vev to the $(\mathbf{2}, \mathbf{1}, \mathbf{4})$ multiplet. This multiplet

has the multiplicity

$$(3[K_{\mathcal{B}}^{-1}] - \mathcal{S}_7 - \mathcal{S}_9)\mathcal{S}_9 = (9 - n_7 - n_9)n_9. \quad (2.95)$$

Thus outside the allowed region of $X_{F_{11}}$ the multiplicity is smaller than two and a Higgsing is not possible. Nevertheless the Higgsing with the other toric multiplet $(\mathbf{1}, \mathbf{2}, \mathbf{4})$ which requires a redefinition of the bundles as described in Subsection 2.4.1 is possible.

Additionally we see that at some points at the boundary of the allowed region of $X_{F_{11}}$ the multiplicity of the $(\mathbf{2}, \mathbf{1}, \mathbf{4})$ multiplet is also smaller than two. Specifically this happens at the green, yellow and orange dots in Figure 2.10. At the green dots the $SU(4)$ divisor in $X_{F_{13}}$ and the $SU(3)$ divisor in $X_{F_{11}}$ are absent. At the yellow dots the $SU(2)_1$ in $X_{F_{13}}$ is not present and at the orange dots both $SU(2)$'s in $X_{F_{13}}$ and the $SU(2)$ in $X_{F_{11}}$ are not there. In all cases there are no states in the $(\mathbf{2}, \mathbf{1}, \mathbf{4})$ representation. However in all cases the rank of the gauge groups of $X_{F_{11}}$ and $X_{F_{13}}$ agree and an adjoint Higgsing with Higgses in the $(\mathbf{3}, \mathbf{1}, \mathbf{1})$ or the $(\mathbf{1}, \mathbf{1}, \mathbf{15})$ representations is possible.

2.4.2 Higgs network

In Section 2.3 we discussed two examples of elliptically fibered CY manifolds with general base \mathcal{B} and the elliptic fiber being a hypersurface in a two dimensional projective variety associated to polyhedra F_{11} and F_{13} . This discussion can be repeated for all 16 CY manifolds given by a hypersurface in one of the 16 polyhedra in Figure 2.2 fibered over a general base \mathcal{B} [32]. As discussed in Subsection 2.4.1 for the examples $X_{F_{13}}$ and $X_{F_{11}}$ the 16 effective field theories are connected by Higgs transitions. The network of these transitions as well as the gauge groups of the polyhedra are given in Figure 2.11. Since we only consider Higgsings via toric matter this network is called the *toric Higgs network*.

All 16 effective field theories can be obtained by toric Higgsings from the three theories with maximal gauge groups $X_{F_{13}}$, $X_{F_{15}}$ and $X_{F_{16}}$. We note that these three theories with maximal gauge group are also the theories with non-simply connected gauge groups coming from MW torsion [56].

Additionally we make the following observations

- The rank of the total gauge group of each theory is given by the number of points of the toric diagram minus three

$$\text{rk}(G_{F_i}) = \#\text{points in } F_i - 3. \quad (2.96)$$

- The sum of the rank of the gauge group of a polyhedron F_i and the dual polyhedron F_i^* is constant

$$\text{rk}(G_{F_i}) + \text{rk}(G_{F_i^*}) = 6. \quad (2.97)$$

This is a realization of the fact that the sum of the areas of dual polyhedra is constant.

- The set of effective field theories contains theories with discrete symmetries. On the geometry side the discrete symmetries correspond to the TS group of the theory. All discrete symmetries can be obtained via a toric Higgsing from a continuous gauge symmetry. This agrees with general quantum gravity arguments [88]. We will discuss an example of discrete symmetries in the next Section 2.5.
- The network is symmetric under reflection along the horizontal line where the rank of the total gauge group is three. This reflection exchanges polyhedra with their mirror duals. Especially theories with discrete symmetries are mapped to theories with MW torsion leading to the conjecture

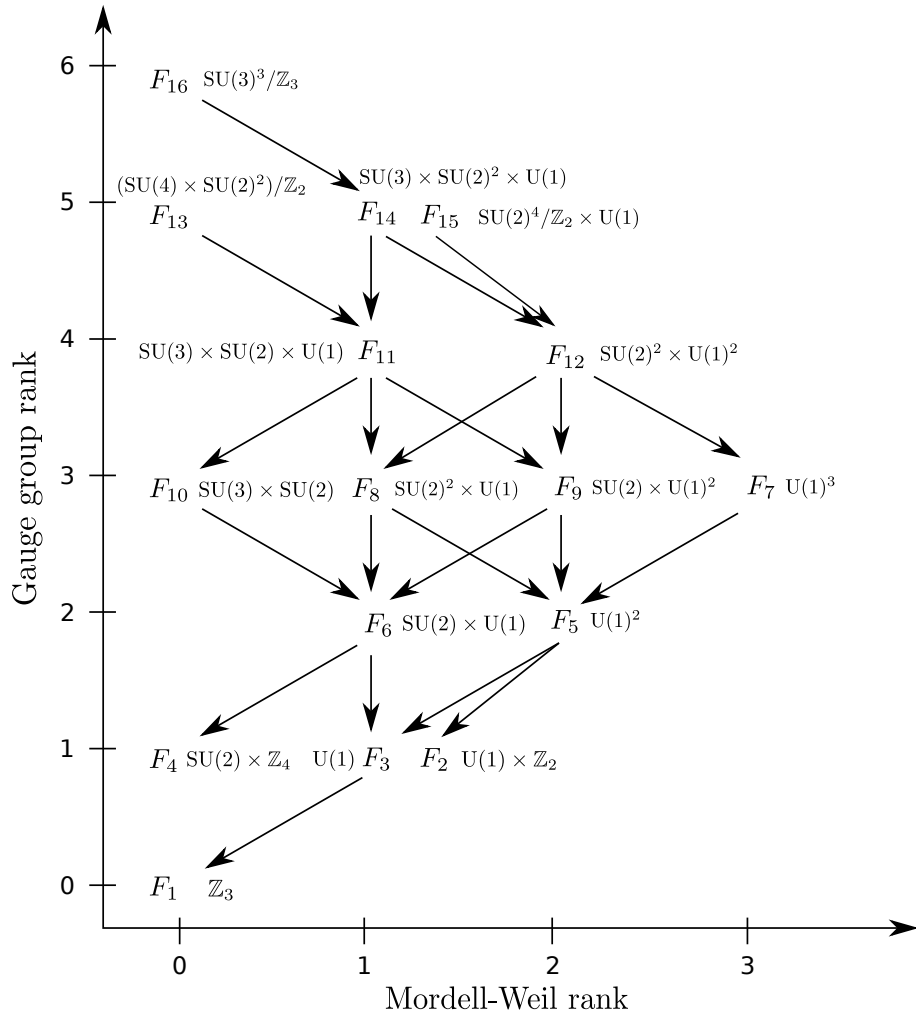


Figure 2.11: The network of Higgsings between all F-theory compactifications on toric hypersurface fibrations X_{F_i} . The axes show the rank of the MW group and the total rank of the gauge group of X_{F_i} . Each CY X_{F_i} is abbreviated by F_i and its corresponding gauge group is shown. The arrows indicate the existence of a toric Higgsing between two CY manifolds.

that MW torsion and the TS group are dual under mirror symmetry in the fiber.⁴ This observation has also been confirmed for another example in [89].

2.5 Genus-one fiber with discrete symmetries

In the last Section 2.4.1 we found a connection between the effective field theories stemming from the 16 polyhedra in Figure 2.2 via Higgs transitions. We also found that the polytopes F_1 , F_2 and F_4 lead to discrete symmetries which are obtained from toric Higgsings of continuous symmetries. The latter agrees as required with general quantum gravity arguments [88]. In the following section we want to concentrate on the example of a \mathbb{Z}_3 discrete symmetry in F-theory compactified on X_{F_1} . Therefore we will first analyze X_{F_3} and find a non-toric rational section which leads to a toric matter multiplet with

⁴ The bare discrete symmetry in X_{F_4} without $SU(2)$ is \mathbb{Z}_2 .

charge three. Higgsing this leads to X_{F_1} . For simplicity we restrict to six dimensions in this section, too.

2.5.1 Polyhedron F_3 : non-toric $U(1)$

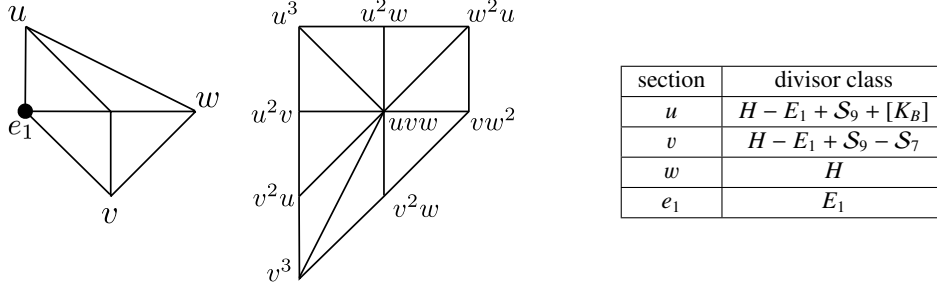


Figure 2.12: The toric diagram of polyhedron F_3 and its dual. The toric zero section is indicated by the dot. In the accompanying table we indicate the divisor classes of the fiber coordinates.

The toric diagram of the fiber ambient space $\mathbb{P}_{F_3} = dP_1$ as well as a choice of projective coordinates is given in Figure 2.12. There we also show the corresponding dual polyhedron and the divisor classes of the projective coordinates. The monomials given at each node in the dual polyhedron are constructed by the Batyrev formula (2.39) where the blow-up coordinate e_1 has been set to one. Collecting the monomials gives the needed hypersurface to construct the elliptically fibered CY X_{F_3} as

$$p_{F_3} = s_1 u^3 e_1^2 + s_2 u^2 v e_1^2 + s_3 u v^2 e_1^2 + s_4 v^3 e_1^2 + s_5 u^2 w e_1 + s_6 u v w e_1 + s_7 v^2 w e_1 + s_8 u w^2 + s_9 v w^2. \quad (2.98)$$

Here the coefficients are sections over the general base \mathcal{B} where the divisor classes are given in (2.42).

The SR ideal can be read off from the toric diagram in Figure 2.12

$$SR_{F_3} = \{uw, we_1\}. \quad (2.99)$$

From (2.98) we can immediately read off one toric rational section [83]

$$\hat{s}_0 = X_{F_3} \cap \{e_1 = 0\} : [s_9 : -s_8 : 1 : 0]. \quad (2.100)$$

Apart from the toric rational section this geometry has a non-toric rational section. To find this we use the fact that if a rational line and a rational cubic have two rational intersection points then their third intersection point is also rational. This statement reduces to the statement that if a cubic rational polynomial has two rational roots then its third root is also rational [48]. By constructing a tangent to the hypersurface (2.98) at the toric rational point we can use this argument to find an additional rational point.

To do this we choose the patch $e_1 = 1$. In this patch the rational point P_0 is at $[u : v : w] = [0 : 0 : 1]$. A general line $a_1 u + a_2 v + a_3 w = 0$ going through P_0 is given by $v = -\frac{a_1}{a_2} u$. We then find the tangent by requiring the first derivative of the hypersurface (2.98) along the line to vanish. This leads to the tangent

$$l_t = s_8 u + s_9 v. \quad (2.101)$$

To find the second intersection point with the hypersurface we go to the patch $u = s_9$ and solve the

hypersurface (2.98) for example for e_1 . We then find the coordinates

$$\hat{s}_1 = X_{F_3} \cap \{l_t = 0\} : [s_9 : -s_8 : s_4 s_8^3 - s_3 s_8^2 s_9 + s_2 s_8 s_9^2 - s_1 s_9^3 : s_7 s_8^2 - s_6 s_8 s_9 + s_5 s_9^2]. \quad (2.102)$$

In principal this argument also works for all other geometries X_{F_i} as well but in the other cases this argument leads to other toric sections (if there are more then one) or the tangent automatically has a triple intersection point with the hypersurface.⁵

Using both sections we find a MW group of rank one. The corresponding Shioda map (2.15) is given by

$$\sigma(\hat{s}_1) = S_1 - S_0 + 3[K_B] + S_7 - 2S_9. \quad (2.103)$$

By using

$$\pi(S_1 \cdot S_0) = [z_1] = 2[K_B^{-1}] + 2S_9 - S_7, \quad (2.104)$$

where z_1 is the base locus where the two sections agree, we can calculate the height pairing (2.16)

$$b_{11} = -2(3[K_B] + S_7 - 2S_9). \quad (2.105)$$

After finding the functions f_{F_3} , g_{F_3} and the birational map to Weierstrass coordinates by using the Nagell algorithm (see Appendix A.2) we find that Δ_{F_3} has no codimension one singularities. Thus the total gauge group is

$$G_{F_3} = U(1). \quad (2.106)$$

To calculate the matter content we have to find the codimension two singular loci of the discriminant. These loci are contained in the ideal (2.24) where we have to use the coordinates of \hat{s}_1 in Weierstrass form. Due to the complexity of the ideal the necessary prime ideal decomposition is not possible at the moment. Therefore we derive the possible splittings and check that they are contained in (2.24).

The first singular locus is found where both sections \hat{s}_0 and \hat{s}_1 are ill-defined since their coordinates are forbidden by the SR ideal (2.99). This happens at the locus $V(I_{(3)}) = \{s_8 = s_9 = 0\}$. At this locus the hypersurface (2.98) splits as follows

$$p_{F_3} \Big|_{s_8=s_9=0} = e_1 (s_1 u^3 e_1 + s_2 u^2 v e_1 + s_3 u v^2 e_1 + s_4 v^3 e_1 + s_5 u^2 w + s_6 u v w + s_7 v^2 w). \quad (2.107)$$

The zero-section \hat{s}_0 wraps the curve where $e_1 = 0$. The locus $V(I_{(3)})$ is the only codimension two locus where such a splitting can occur since it is the only locus where \hat{s}_0 is ill defined. To obtain the behaviour of the other section \hat{s}_1 we recall how we obtained the section \hat{s}_1 : It was obtained as the third intersection point of a tangent of the curve C at the other rational section \hat{s}_0 with the curve C . In the case at hand the curve is singular at the rational point \hat{s}_0 . Since this means that also the first derivatives of the hypersurface constraint (2.98) are zero this implies that every line through this point is a tangent. Geometrically this translates into the fact that the rest of the curve is the other rational point \hat{s}_1 and thus the section \hat{s}_1 wraps the other \mathbb{P}^1 . This argument leads to the intersections and charges given in Table 2.9.

⁵ Nevertheless the same argument works for the complete intersection in $\text{Bl}_1 \mathbb{P}^3$.

Next we consider the locus where only \hat{s}_1 degenerates. Therefore we consider the splitting of the fiber

$$p_{F_3} \rightarrow l_t q_2(e_1 u, e_1 v, w) = (s_8 u + s_9 v) q_2(e_1 u, e_1 v, w). \quad (2.108)$$

To find the corresponding base ideal we calculate the elimination ideal of the ideal of constraints necessary for the factorization given in (2.108). The corresponding ideal $I_{(2)}$ has ten generators and is codimension two in the base. The multiplicity given in Table 2.9 is computed as the homology class of the given complete intersection where the contribution of the ideal $V(I_{(3)})$ has to be subtracted. The corresponding order of subtraction can be calculated by the resultant technique [37, 48].

To calculate the last matter locus we assume the following fiber splitting

$$p_{F_3} \rightarrow (d_1 u + d_2 v + d_3 w) q_2(u, v, w), \quad (2.109)$$

where no section degenerates. Again we calculate the locus via the elimination ideal and check that the resulting locus is codimension two. Under the assumption that there are no more prime ideals of (2.24) we can calculate the multiplicity of this locus by subtracting the homology classes of $V(I_{(2)})$ and $V(I_{(3)})$ from the homology class of (2.24) with the orders obtained by the resultant technique. All results are given in Table 2.9.

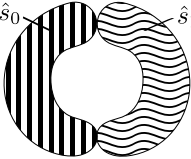
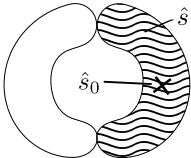
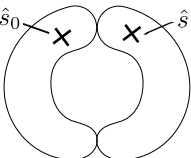
Representation	Multiplicity	Fiber	Locus
$\mathbf{1}_3$	$\mathcal{S}_9([K_B^{-1}] + \mathcal{S}_9 - \mathcal{S}_7)$		$V(I_{(3)}) := \{s_8 = s_9 = 0\}$
$\mathbf{1}_2$	$6[K_B^{-1}]^2 + [K_B^{-1}](4\mathcal{S}_9 - 5\mathcal{S}_7) + \mathcal{S}_7^2 + 2\mathcal{S}_7\mathcal{S}_9 - 2\mathcal{S}_9^2$		$V(I_{(2)}) :=$ $\{s_4 s_8^3 - s_3 s_8^2 s_9 + s_2 s_8 s_9^2 - s_1 s_9^3$ $= s_7 s_8^2 + s_5 s_9^2 - s_6 s_8 s_9 = 0$ with $(s_8, s_9) \neq (0, 0)\}$
$\mathbf{1}_1$	$12[K_B^{-1}]^2 + [K_B^{-1}](8\mathcal{S}_7 - \mathcal{S}_9) - 4\mathcal{S}_7^2 + \mathcal{S}_7\mathcal{S}_9 - \mathcal{S}_9^2$		$V(I_{(1)}) := \{(2.24)\} \setminus (V(I_{(2)}) \cup V(I_{(3)}))$

Table 2.9: Charged matter representations under U(1) and codimension two fibers of X_{F_3} .

For completeness we also compute the codimension three singular loci leading to the Yukawa couplings in Table 2.10.

Yukawa	Locus
$\mathbf{1}_1 \cdot \mathbf{1}_1 \cdot \overline{\mathbf{1}}_2$	$V(I_{(1)}) \cap V(I_{(2)})$
$\mathbf{1}_1 \cdot \mathbf{1}_2 \cdot \overline{\mathbf{1}}_3$	$V(I_{(1)}) \cap V(I_{(2)}) \cap V(I_{(3)})$

Table 2.10: Codimension three loci and corresponding Yukawa couplings for X_{F_3} .

Flux construction

After having calculated the 6D effective field theory let us proceed to calculate the fluxes in compactifications to 4D and the corresponding chiralities. With the base $\mathcal{B} = \mathbb{P}^3$ we again find $\mathcal{S}_7, \mathcal{S}_9, [K_{\mathcal{B}}^{-1}]$ and c_2 given as in (2.56). This leads for the CY X_{F_3} to the allowed region of values for (n_7, n_9) depicted in Figure 2.13.

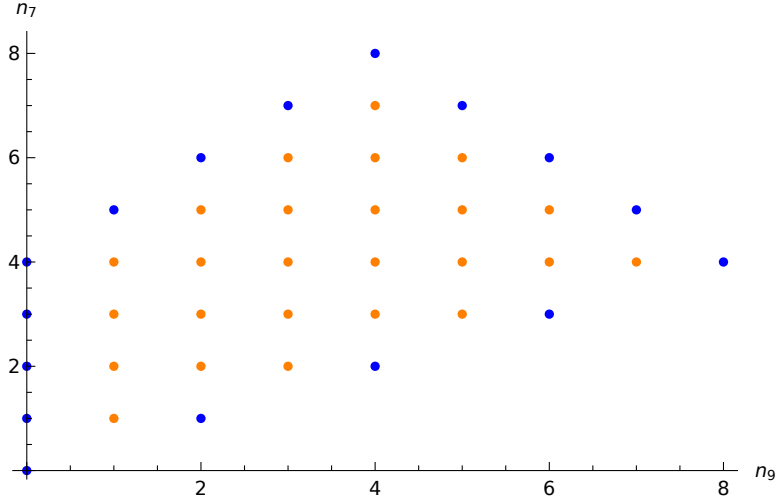


Figure 2.13: Allowed region for (n_7, n_9) for the elliptically fibered CY fourfold X_{F_3} with base \mathbb{P}^3 . The blue dots denote the boundary of the allowed region and the orange dots denote the bulk part where all matter given in Table 2.9 is present.

From the independent divisor classes of X_{F_3} we choose the following basis for $H^{1,1}(X_{F_3})$

$$H^{1,1}(X_{F_3}) = \langle H_B, \tilde{S}_0, \sigma(\hat{s}_1) \rangle, \quad (2.110)$$

where we again chose the shifted zero section as in Section 2.3.1. The full SR ideal of the CY X_{F_3} is then given by the fiber part and the base part $SR_{\mathcal{B}} = x_0 x_1 x_2 x_3$. With the additional intersection number

$$H_B^3 S_0^2 = -1, \quad H_B^3 S_0 S_1 = 1, \quad (2.111)$$

obtained from the fiber part and (2.102) we can calculate the full vertical cohomology ring. We then find for the dimension of the vertical cohomology $H_V^{2,2}(X_{F_3})$

$$\dim H_V^{2,2}(X_{F_3}) = 4, \quad (2.112)$$

by calculating the rank of the intersection matrix $\eta^{(2,2)}$. As a basis for the vertical cohomology we choose

$$H_V^{2,2}(X_{F_3}) = \langle (H_B)^2, H_B \tilde{S}_0, H_B \sigma(\hat{s}_1), \tilde{S}_0^2 \rangle. \quad (2.113)$$

Imposing the conditions (2.30) from the comparison of M- and F-theory CS terms on a general element of $H_V^{2,2}(X_{F_3})$ we find two restrictions leading to the flux

$$G_4 = H_B \tilde{S}_0 a_2 - H_B \sigma(\hat{s}_1) a_2 + \tilde{S}_0^2 a_4 + H_B^2 \left(-(2 + n_7 - 2n_9) a_2 - (4 - 4n_9 + n_7 n_9 - n_9^2) a_4 \right). \quad (2.114)$$

Due to the quantization condition (2.26) we know that the flux parameters must be discrete. But since we do not have an integral basis we cannot use this explicitly. Instead we parametrize the flux parameters a_2 and a_4 in terms of the integral chiralities.

The chiralities can be computed either via the integral of the G_4 flux over the matter surfaces C^ω (2.32) or via comparison of the loop corrected CS terms (2.29) with the M-theory CS terms. In the case at hand we found the following matter surface

$$C_3^\omega = -S_9([K_B^{-1}] + S_9 - S_7)E_1. \quad (2.115)$$

The other matter surfaces have complicated ideals of which we were not able to calculate the homology classes. Thus we calculate the chiralities via the CS terms

$$\begin{aligned} \chi_3 &= (-4 + n_7 - n_9)n_9(-3a_2 + (n_7 - 2n_9)a_4), \\ \chi_2 &= 2\left(-96 + n_7^2 + 260n_9 + 67n_9^2 - n_7(4 + 67n_9)\right)a_2 \\ &\quad + 3n_9\left(-32 + 15n_7^2 + 112n_9 + 30n_9^2 - n_7(52 + 45n_9)\right)a_4, \\ \chi_1 &= -\left(192 + 4n_7^2 + 1892n_9 + 457n_9^2 - n_7(64 + 457n_9)\right)a_2 \\ &\quad - 3n_9\left(32 + 51n_7^2 + 416n_9 + 102n_9^2 - n_7(212 + 153n_9)\right)a_4. \end{aligned} \quad (2.116)$$

These chiralities do not allow for a family structure. Nevertheless we can express the flux parameters a_2 and a_4 for example in terms of the chiralities χ_3 and χ_2

$$a_2 = -\frac{45\chi_3 n_7 - 90\chi_3 n_9 + 24\chi_3 - \chi_2 n_7 + 2\chi_2 n_9}{(n_7 - 2n_9 + 8)(2n_7 - n_9)(n_7 + n_9 - 12)}, \quad (2.117)$$

$$a_4 = \frac{2\chi_3 n_7^2 - 134\chi_3 n_7 n_9 - 8\chi_3 n_9^2 + 134\chi_3 n_9^2 + 520\chi_3 n_9 - 192\chi_3 + 3\chi_2 n_7 n_9 - 3\chi_2 n_9^2 - 12\chi_2 n_9}{n_9(n_7 - 2n_9 + 8)(n_7 - n_9 - 4)(2n_7 - n_9)(n_7 + n_9 - 12)}. \quad (2.118)$$

Here the occurring singularity which is not the boundary of the allowed region of X_{F_3} is a coordinate singularity which can be checked by choosing another parametrization.

To check for D3-brane tadpole cancelation (2.27) we calculate the second Chern class and the Euler number of X_{F_3}

$$\chi(X_{F_3}) = 6\left(12c_1^3 + 2c_1c_2 - 8c_1^2\mathcal{S}_7 + 5c_1\mathcal{S}_7^2 + \mathcal{S}_7^3 - 8c_1^2\mathcal{S}_9 - 2\mathcal{S}_7^2\mathcal{S}_9 + 4c_1\mathcal{S}_9^2\right), \quad (2.119)$$

where c_1 and c_2 are the first and second Chern class of the base \mathcal{B} . As before we check that the chiralities in Table 2.11 lead to integral positive numbers of D3-branes as required for smooth CY fourfolds. Additionally we checked integrality of the CS terms which implies that the flux quantization condition (2.26) is fulfilled but not necessarily minimal.

2.5.2 Higgsing to X_{F_1} with \mathbb{Z}_3

All points in the charge lattice are occupied as required by general quantum gravity arguments [90]. Therefore the matter located at $V(I_{(3)})$ is clearly of non-minimal charge⁶. Thus field-theoretically it is clear that a Higgsing with the toric matter with charge $q = 3$ leads to a discrete \mathbb{Z}_3 symmetry.

⁶ In the more general case of two U(1) symmetries the minimality of a charge is not as easy to see. There one has to consider the unit cell spanned by two charge vectors. If the number of occupied points of the charge lattice in this unit cell is equal to one, the two vectors are of minimal charge.

$n_7 \setminus n_9$	1	2	3	4	5	6	7
1	$\begin{pmatrix} 2 & 7 \\ -404 & 148 \end{pmatrix}$	-					
2	$\begin{pmatrix} 3 & 22 \\ -545 & 135 \end{pmatrix}$	$\begin{pmatrix} 8 & 24 \\ -1800 & 12 \end{pmatrix}$	$\begin{pmatrix} 15 & 522 \\ -2637 & 27 \end{pmatrix}$	-			
3	$\begin{pmatrix} 1 & 69 \\ -129 & 127 \end{pmatrix}$	$\begin{pmatrix} 3 & 161 \\ -391 & 100 \end{pmatrix}$	$\begin{pmatrix} 6 & 87 \\ -1344 & 26 \end{pmatrix}$	$\begin{pmatrix} 10 & 351 \\ -1884 & 6 \end{pmatrix}$	$\begin{pmatrix} 15 & 617 \\ -2491 & 40 \end{pmatrix}$	-	
4	$\begin{pmatrix} 1 & 22 \\ -155 & 136 \end{pmatrix}$	$\begin{pmatrix} 1 & 34 \\ -155 & 108 \end{pmatrix}$	$\begin{pmatrix} 3 & 24 \\ -645 & 82 \end{pmatrix}$	$\begin{pmatrix} 1 & 38 \\ -163 & 76 \end{pmatrix}$	$\begin{pmatrix} 5 & 176 \\ -1075 & 2 \end{pmatrix}$	-	$\begin{pmatrix} 7 & 290 \\ -973 & 4 \end{pmatrix}$
5	-	$\begin{pmatrix} 1 & 69 \\ -129 & 127 \end{pmatrix}$	$\begin{pmatrix} 3 & 161 \\ -391 & 100 \end{pmatrix}$	$\begin{pmatrix} 6 & 87 \\ -1344 & 26 \end{pmatrix}$	$\begin{pmatrix} 10 & 351 \\ -1884 & 6 \end{pmatrix}$	$\begin{pmatrix} 15 & 617 \\ -2491 & 40 \end{pmatrix}$	-
6		-	$\begin{pmatrix} 3 & 22 \\ -545 & 135 \end{pmatrix}$	$\begin{pmatrix} 8 & 24 \\ -1800 & 12 \end{pmatrix}$	$\begin{pmatrix} 15 & 522 \\ -2637 & 27 \end{pmatrix}$	-	
7			-	$\begin{pmatrix} 2 & 7 \\ -404 & 148 \end{pmatrix}$	-		

Table 2.11: The entries $\begin{pmatrix} \chi_3 & \chi_2 \\ \chi_1 & n_{D3} \end{pmatrix}$ give chiralities χ_1, χ_2 and χ_3 for which the number of D3-branes n_{D3} is integer and positive while the CS terms are also integral. The fluxes were parametrized by the chiralities χ_2 and χ_3 . At the allowed points for (n_7, n_9) marked as "-" the flux coefficients a_2 and a_4 diverge for the chosen parametrization.

Geometrically we find that a Higgsing with the matter located at $V(I_{(3)})$ corresponds to a transition to X_{F_1} . In the following we want to discuss the geometry of X_{F_1} and how the discrete symmetry is reflected there.

The toric diagram of the fiber ambient space is given in Figure 2.14. There we also give a coordinate assignment, the dual polyhedron F_{16} along with the monomials corresponding to the nodes via the Batyrev formula (2.39) as well as the divisor classes of the coordinates.

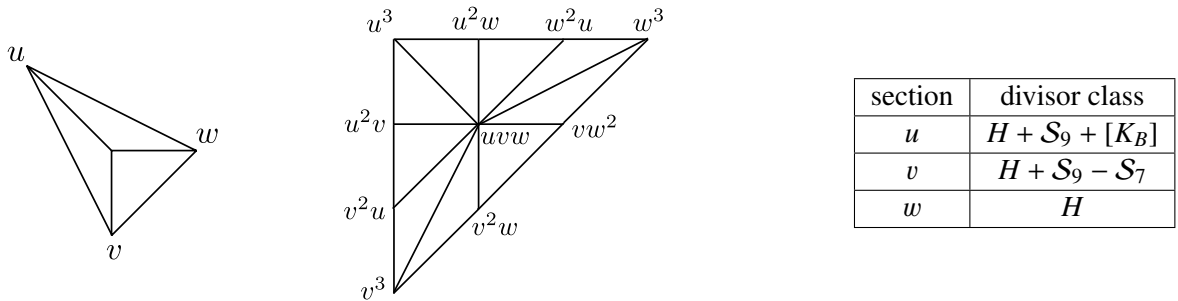


Figure 2.14: The toric diagram of polyhedron F_1 and its dual F_{16} with coordinate assignment and the monomials corresponding to the nodes via the Batyrev formula (2.39) respectively. By brevity of notation we set $e_i = 1$ in the Batyrev monomials. In the accompanying table we indicate the divisor classes of the fiber coordinates.

Collecting the monomials from the dual polyhedron we find the following hypersurface which leads to a genus-one fiber

$$p_{F_1} = s_1 u^3 + s_2 u^2 v + s_3 u v^2 + s_4 v^3 + s_5 u^2 w + s_6 u v w + s_7 v^2 w + s_8 u w^2 + s_9 v w^2 + s_{10} w^3. \quad (2.120)$$

This is the most general cubic in \mathbb{P}^2 . In the fibration the coefficients s_i are sections over the base in the line bundles given in (2.42). From the toric diagram in Figure 2.14 we can also read off the SR ideal

$$SR = \{uvw\}. \quad (2.121)$$

From the hypersurface equation (2.120) we can see that this geometry does not have any toric rational

sections. We also could not find any non-toric rational section leading us to the conclusion that the rank of the MW group of X_{F_1} is zero.

Since this geometry does not have a rational section it is not an elliptic fibration but only a genus-one fibration (see Subsection 2.1.4). Using the Jacobian for a cubic in \mathbb{P}^2 from [61] we can calculate f_{F_1} , g_{F_1} and Δ_{F_1} . There are no codimension one singular loci of the discriminant Δ_{F_1} . We therefore find a trivial continuous gauge group as expected from the Higgsing of the effective field theory of X_{F_3} .

The discrete part of the gauge group is geometrically reflected by the TS group $\text{III}(X_{F_1})$ (see Subsection 2.1.4). To find the TS group one observes that although the F-theory compactifications on X_{F_1} and $\text{Jac}(X_{F_1})$ to 6D are identical the M-theory compactifications to 5D are not: The Kaluza-Klein towers in a circle compactification from the 6D F-theory compactification are different and only one of the compactifications has a discrete \mathbb{Z}_3 symmetry also in 5D [36]. The additional degree of freedom to differentiate the M-theory vacua is generated by flux along the additional S^1 (a discrete Wilson line). To find the elements of the TS group the authors of [36] explicitly construct three different curves in X_{F_3} ⁷ which lead to three different possible Higgs fields in 5D M-theory. Higgsing the M-theory compactification with the three different fields then lead to three inequivalent 5D M-theory vacua. Along with their respective Jacobian actions this gives the TS group \mathbb{Z}_3 [36]. Thus we find the total gauge group

$$G_{F_1} = \mathbb{Z}_3. \quad (2.122)$$

Although the geometry X_{F_1} does not have any rational sections it has a three-section

$$\hat{s}^{(3)} = X_{F_1} \cap \{u = 0\} : s_4 v^3 + s_7 v^2 w + s_9 v w^2 + s_{10} w^3 = 0. \quad (2.123)$$

This three-section marks three points in the fiber. The individual points are not well-defined since they get exchanged by monodromies around branch cuts. Since an n -section comes from $n + 1$ rational sections by a chain of Higgsings [36] (in the present case it comes from the three $U(1)$'s in X_{F_7}) the three-section reflects the \mathbb{Z}_3 symmetry coming from the TS group. They are necessary in the calculation of the discrete charges. Therefore we define analogously to the Shioda map for $U(1)$ symmetries the following divisor class by imposing the same three conditions as on page 21 in [58] on (2.123)

$$\sigma_{\mathbb{Z}_3}(\hat{s}^{(3)}) = S^{(3)} + [K_B] + \frac{4}{3}S_9 - \frac{2}{3}S_7. \quad (2.124)$$

To find the codimension two discriminant loci leading to the matter representations we observe that there is only one possible factorization of a smooth cubic: Namely into a line and a conic

$$p_{F_1} \stackrel{!}{=} s_1(u + \alpha_1 v + \alpha_2 w)(u^2 + \beta_1 v^2 + \beta_2 w^2 + \beta_3 uv + \beta_4 vw + \beta_5 uw). \quad (2.125)$$

Here α_i and β_j are unknown coefficients. Comparing the coefficients on both sides we find an ideal of constraints. As before in Section 2.5.1 we calculate the elimination ideal to eliminate the coefficients α_i and β_j . We find an ideal $I_{(1)}$ with 50 generators which has codimension two in the ring of sections $K[s_i]$. The corresponding multiplicity of this locus can in principal be found as in the sections above. Due to a lack of computing power this was not possible in this case and the given multiplicity in Table 2.12 was found by the Higgsing of X_{F_3} .

To calculate the discrete charge given in Table 2.12 we calculate the intersection numbers one and two of the three-section (2.123) with the fiber components. Naive application of the 'discrete Shioda map' (2.124) leads to two different charges $q = 1$ and $q = 2$ and thus not to a well-defined charge. But since in

⁷ They actually only find two different curves in X_{F_3} . To find the third curve they have to consider a different resolution of the singular fiber coming from an unhiggsing of X_{F_1} .

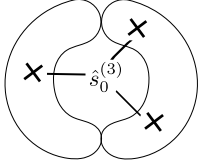
Representation	Multiplicity	Fiber	Locus
$\mathbf{1}_1$	$3(6[K_B^{-1}]^2 - S_7^2 + S_7 S_9 - S_9^2 + [K_B^{-1}](S_7 + S_9))$		$V(I_{(1)})$

Table 2.12: Charged matter representation under \mathbb{Z}_3 and corresponding codimension two fiber of X_{F_1} . The given multiplicity is obtained field theoretically by the Higgsing from X_{F_3} .

six dimensions a hyper multiplet consists of two half-hypermultiplets transforming in conjugate representations the hyper multiplet with charge $q = 1$ also contains a half-hyper with charge $q = -1$. Due to the discrete \mathbb{Z}_3 symmetry this is equivalent to a half-hyper with charge $q = 2$. Thus the two charges are indeed in the same hyper multiplet and the \mathbb{Z}_3 charge is well-defined.

For completeness we give the field theoretic expectation for the Yukawa coupling and codimension three singular locus in Table 2.13. Due to the size of the ideal $I_{(1)}$ we could not check geometrically for its existence.

Yukawa	Locus
$\mathbf{1}_1 \cdot \mathbf{1}_1 \cdot \mathbf{1}_1$	$V(I_1) \cap V(I_1) \cap V(I_1)$

Table 2.13: Codimension three locus and corresponding Yukawa coupling for X_{F_1} .

Topological string theory

In the last chapter we studied the application of elliptic curves to F-theory as an example for a non-perturbative type IIB string theory. Now we turn to another example of the occurrence of elliptic curves in non-perturbative string theories: the topological string on local geometries. In this example it was found that the refined topological string gives a non-perturbative completion of the unrefined topological string [24–26].

We will first introduce topological string theory in Section 3.1. Then in Section 3.2 we will discuss the calculation of refined periods of the studied geometry in the refined topological string. This is needed for the discussion of the conjectured non-perturbative completion of the topological string in Section 3.3.

3.1 Topological string construction

In the following section we want to give a short introduction to the concepts of topological string theory used in this thesis. To do this we will first introduce topological field theories in Subsection 3.1.1. There we will also discuss two examples constructed by twisting a $\mathcal{N} = (2, 2)$ sigma model. In Subsection 3.1.2 we will couple the field theories to gravity to obtain the topological string A- and B-model.

There are several existing reviews on the topic of topological string theory [18, 19, 91–95]. We will follow mainly the discussion in [93].

3.1.1 Topological field theories

Topological field theories are field theories which do not depend on the metric of the underlying manifold \mathcal{M} . This means that all physical observables which are the correlation functions of physical operators do not depend on the metric [93]

$$\langle \mathcal{O}_1(x_1) \dots \mathcal{O}_n(x_n) \rangle_b. \quad (3.1)$$

Here the path integral involved in $\langle \cdot \rangle_b$ might depend on background properties as for example the manifold \mathcal{M} or the coupling constants. If the theory is a topological field theory these quantities do not depend on the metric of \mathcal{M} but only on its topological data.

We can distinguish two different kinds of topological field theories [93]

1. In *Schwarz-type* topological field theories the exponential of the action e^{iS} and the measure do not depend on the metric from the beginning. A famous example of this kind is CS theory where the action is metric independent and the measure does not have any quantum anomalies. This leads to the knot invariants as observables.

2. In *Cohomological field theories* on the other hand the action might be metric dependent. The dependency on the metric drops out in the process of calculating the physical observables. In the following we want to study this case in more detail.

Cohomological field theories

To become metric independent cohomological field theories need four requirements [93]

1. The theory needs to have a nilpotent symmetry operator Q

$$Q^2 = 0. \quad (3.2)$$

2. The physical operators O_i of the theory are defined to be Q closed

$$\{Q, O_i\} = 0. \quad (3.3)$$

3. The Q symmetry must not be spontaneously broken which means that the vacuum is annihilated by the symmetry generator

$$O_i \sim O_i + \{Q, \Lambda\} \Leftrightarrow Q|0\rangle = 0. \quad (3.4)$$

4. The energy-momentum tensor needs to be Q exact

$$T_{\alpha\beta} = \frac{\delta S}{\delta h^{\alpha\beta}} = \{Q, G_{\alpha\beta}\}. \quad (3.5)$$

The first two requirements (3.2) and (3.3) are for example fulfilled in the case of BRST symmetries which occur in gauge theories after fixing the gauge [93, 96].

To see that theories with these properties are topological field theories we observe [93]

$$\begin{aligned} \frac{\delta}{\delta h^{\alpha\beta}} \langle O_{i_1} \dots O_{i_n} \rangle &= i \int \mathcal{D}\phi O_{i_1} \dots O_{i_n} \frac{\delta S}{\delta h^{\alpha\beta}} e^{iS[\phi]} \\ &= i \langle O_{i_1} \dots O_{i_n} \{Q, G_{\alpha\beta}\} \rangle \\ &= 0. \end{aligned} \quad (3.6)$$

Here we have used that the operators O_i do not explicitly depend on the metric and that the operator Q in the anticommutator in the second line can be moved to the left or right by use of (3.3) which then yields zero by (3.4).

A topological field theory for topological strings

In view of topological string theory we are particularly interested in two dimensional nonlinear sigma models on the worldsheet Σ_g into the target space X . An example of a cohomological field theory can be obtained by “twisting” $\mathcal{N} = (2, 2)$ supersymmetric field theories in two dimensions. The action of such a theory is given by [93, 97]

$$S_D = \int_{\Sigma_g} d^2z \left(\frac{1}{2} g_{ij} \partial_z \phi^i \partial_{\bar{z}} \phi^j + \frac{i}{2} g_{ij} \psi_-^i D_z \psi_-^j + \frac{i}{2} g_{ij} \psi_+^i D_{\bar{z}} \psi_+^j + \frac{1}{4} R_{ijkl} \psi_+^i \psi_+^j \psi_-^k \psi_-^l \right). \quad (3.7)$$

Here $(\phi, \psi_+, \psi_-, F)$ are the components of the chiral superfield Φ in the $\mathcal{N} = (2, 2)$ theory. Additionally we have introduced

$$\begin{aligned}\Gamma_{jk}^i &= g^{i\bar{l}} g_{\bar{l}j,k} \\ D_{\bar{z}} \psi_+^i &= \frac{\partial}{\partial \bar{z}} \psi_+^i + \frac{\partial \phi^j}{\partial \bar{z}} \Gamma_{jk}^i \psi_+^k,\end{aligned}\tag{3.8}$$

and the Riemann tensor R_{ijkl} of the target space X . The derivative D_z is defined analogous. The metric g_{ij} is the Kähler metric of X . Due to the $\mathcal{N} = (2, 2)$ supersymmetry X is a Kähler manifold [93].

Next we define the following SUSY generators of the theory [93]

$$\begin{aligned}Q_{\pm} &= \frac{\partial}{\partial \theta^{\pm}} + i\bar{\theta}^{\pm} \partial_{\pm}, & \bar{Q}_{\pm} &= -\frac{\partial}{\partial \bar{\theta}^{\pm}} - i\theta^{\pm} \partial_{\pm}, \\ D_{\pm} &= \frac{\partial}{\partial \theta^{\pm}} - i\bar{\theta}^{\pm} \partial_{\pm}, & \bar{D}_{\pm} &= -\frac{\partial}{\partial \bar{\theta}^{\pm}} + i\theta^{\pm} \partial_{\pm}.\end{aligned}\tag{3.9}$$

Here we use the notation $\partial_+ = \partial_z$ and $\partial_- = \partial_{\bar{z}}$. Using that the complex conjugate of θ^+ is $\bar{\theta}^-$ and that of θ^- is $\bar{\theta}^+$ [93] we find that complex conjugation also maps \bar{Q}_- to Q_+ and so on. The nonvanishing anticommutators between these operators can then be calculated to be [93]

$$\{Q_{\pm}, \bar{Q}_{\pm}\} = P \pm H, \quad \{D_{\pm}, \bar{D}_{\pm}\} = -P \mp H,\tag{3.10}$$

where we used the Hamiltonian $H = -i(\partial_+ - \partial_-)$ and the momentum operator $P = -i(\partial_+ + \partial_-)$.

The generator of the Lorentz group $SO(2) = U(1)$ in two dimension with $\mathcal{N} = (2, 2)$ supersymmetry is [93]

$$M = 2z\partial_+ - 2\bar{z}\partial_- + \theta^+ \frac{d}{d\theta^+} - \theta^- \frac{d}{d\theta^-} + \bar{\theta}^+ \frac{d}{d\bar{\theta}^+} - \bar{\theta}^- \frac{d}{d\bar{\theta}^-}.\tag{3.11}$$

Using (3.11) and the definition of the SUSY generators (3.9) we can calculate the commutators of the Lorentz generator with the Hamiltonian, the momentum operator as well as the SUSY generators [93]

$$\begin{aligned}[M, H] &= -2P, & [M, P] &= -2H, & [M, Q_{\pm}] &= \mp Q_{\pm} \\ [M, \bar{Q}_{\pm}] &= \mp \bar{Q}_{\pm}, & [M, D_{\pm}] &= \mp D_{\pm}, & [M, \bar{D}_{\pm}] &= \mp \bar{D}_{\pm}.\end{aligned}\tag{3.12}$$

There are two additional $U(1)$ symmetries¹ which respect the chirality of the superfield and become important later on. The corresponding generators of these R-symmetries are [93]

$$\begin{aligned}F_V &= -\theta^+ \frac{d}{d\theta^+} - \theta^- \frac{d}{d\theta^-} + \bar{\theta}^+ \frac{d}{d\bar{\theta}^+} + \bar{\theta}^- \frac{d}{d\bar{\theta}^-}, \\ F_A &= -\theta^+ \frac{d}{d\theta^+} + \theta^- \frac{d}{d\theta^-} + \bar{\theta}^+ \frac{d}{d\bar{\theta}^+} - \bar{\theta}^- \frac{d}{d\bar{\theta}^-}.\end{aligned}\tag{3.13}$$

These rotations have vanishing commutators with the Hamiltonian and momentum operator as well as

¹ Only in the case of vanishing first Chern class and thus CY target manifolds F_A is a symmetry of the theory. In order for F_V to be a symmetry one has to demand for vanishing R charges of the fields. For more details see [93].

the Lorentz generator. The nonvanishing commutators are [93]

$$\begin{aligned} [F_V, Q_{\pm}] &= Q_{\pm}, & [F_V, \bar{Q}_{\pm}] &= -\bar{Q}_{\pm}, \\ [F_A, Q_{\pm}] &= \pm Q_{\pm}, & [F_A, \bar{Q}_{\pm}] &= \mp \bar{Q}_{\pm}. \end{aligned} \quad (3.14)$$

Using (3.10) we can construct two independent possible exact representations of the Hamiltonian and the momentum [93]

$$\begin{aligned} \{\bar{Q}_+ + Q_-, Q_+ - \bar{Q}_-\} &= 2H, & \{\bar{Q}_+ + Q_-, Q_+ + \bar{Q}_-\} &= 2P \quad \text{and} \\ \{\bar{Q}_+ + \bar{Q}_-, Q_+ - Q_-\} &= 2H, & \{\bar{Q}_+ + \bar{Q}_-, Q_+ + Q_-\} &= 2P. \end{aligned} \quad (3.15)$$

Defining the following two new operators Q_A and Q_B

$$Q_A = \bar{Q}_+ + Q_-, \quad Q_B = \bar{Q}_+ + \bar{Q}_- \quad (3.16)$$

we see that since both P and H are $Q_{A/B}$ exact this leads in most examples also to a $Q_{A/B}$ exact Lagrangian [93]. We will come back to this point after discussing the twisting procedure. A Q exact Lagrangian $L = \{Q, V\}$ on the other hand ensures the fourth requirement (3.5) for a cohomological field theory that the energy-momentum tensor has to be Q exact.

Nevertheless this is not yet a topological field theory since the worldsheet Σ_g is up to now just flat space \mathbb{C} or a flat torus T^2 . To obtain a topological theory we have to relax this condition and define the theory also on manifolds with curved metric. At the level of the action (3.7) this is easily done by replacing the derivatives ∂_z and $\partial_{\bar{z}}$ by their covariant counterpart D_z and $D_{\bar{z}}$ defined in (3.8). But to maintain supersymmetry on curved manifolds we have to work harder.

Twisting field theories

The problem in defining the theory on arbitrarily curved manifolds is the need of a globally covariantly constant spinor ϵ^+ due to the supersymmetry variation [93]

$$\delta\Phi^i = \epsilon^+ Q_+ \Phi^i. \quad (3.17)$$

Since spinors parallel transported around a closed path only agree up to a general rotation this is not possible for generally curved backgrounds. On the other hand it is possible to find globally covariantly constant scalars. Thus to define the theory on arbitrary manifolds we have to change the definition of scalars and spinors. In order to do this we introduce the new operators [93]

$$M_A = M - F_V \quad \text{or} \quad M_B = M - F_A \quad (3.18)$$

and define them as the Lorentz generators of new Lorentz groups. Here we have twisted the Lorentz group with the R-symmetries given in (3.13). This is possible since the operators M , F_V and F_A have the same kind of commutation relations with the supersymmetry generators (3.9) and vanishing commutation relations among themselves. Then the theory on a general manifold is given by replacing the ordinary derivatives with covariant derivatives with respect to one of the new Lorentz groups.

As a result we find the following commutation relations with the supersymmetry generators

$$\begin{aligned}
 [M_A, Q_+] &= -2Q_+ & [M_B, Q_+] &= -2Q_+ \\
 [M_A, Q_-] &= 0 & [M_B, Q_-] &= 2Q_- \\
 [M_A, \bar{Q}_+] &= 0 & [M_B, \bar{Q}_+] &= 0 \\
 [M_A, \bar{Q}_-] &= 2\bar{Q}_- & [M_B, \bar{Q}_-] &= 0.
 \end{aligned} \tag{3.19}$$

We can see that for the Lorentz generator M_A the operator Q_A has vanishing commutator and is thus a scalar and for M_B the operator Q_B . This allows the definition on arbitrarily curved manifolds and hence leads to two topological field theories.

3.1.2 Coupling to gravity: Topological string theory

To obtain topological string theory from the two topological field theories constructed in Subsection 3.1.1 we need to couple the field theories to gravity on the worldsheet. To do this we have to first formulate the action for general metrics and introduce the corresponding Einstein-Hilbert term. After the twisting this can be done. See [16] for more details.

As a second step we have to do a path integral over all metrics. Naively we could think that this path integral is trivial since the observables of the topological field theory do not depend on the metric. Nevertheless this is not the case since there might be quantum anomalies and metrics which cannot be continuously reached [93].

Using the same conformal formulation for the two dimensional metric $h_{\alpha\beta}$ as in usual string theory [5] we arrive at the usual quantum Virasoro algebra for the modes of the energy-momentum tensor $T_{zz} = T(z) = \sum L_m z^{-m-2}$ and the modes of the additional U(1) current $J(z) = F_V + F_A = \sum J_m z^{-m-1}$ [93]

$$\begin{aligned}
 [L_m, L_n] &= (m-n)L_{m+n} + \frac{c}{12}m(m^2-1)\delta_{m+n}, \\
 [L_m, J_n] &= -nJ_{m+n}, \quad [J_m, J_n] = \frac{c}{3}m\delta_{m+n}.
 \end{aligned} \tag{3.20}$$

Here we have used the theory before twisting as a starting point. We see the conformal anomaly which is proportional to the central charge c . In string theory this conformal anomaly is canceled by choosing the right dimensionality. This is not necessary in topological string theory since it cancels automatically if we perform the twists (3.18). The twists mix the modes of the energy-momentum tensor with the modes of the additional U(1) current as [93]

$$\tilde{L}_m = L_m - \frac{1}{2}(m+1)J_m. \tag{3.21}$$

Using (3.20) to calculate the commutation relations for the shifted generators (3.21) we find that the central charge drops out and there is no conformal anomaly left. Thus we can locally use the same gauge fixing $h_{\alpha\beta} = \eta_{\alpha\beta}$ as in string theory.

In the global case such a gauge fixing is not always possible everywhere (for more details see [93]). Instead we are left with a remaining moduli space which we have to integrate over in the path integral. The first order deformations of this complex structure moduli space are given by

$$dz \mapsto dz + \epsilon \mu_i^{\bar{z}}(z) d\bar{z}. \tag{3.22}$$

To find a path integral measure from the generators of the first order deformations $\mu_i(z, \bar{z})$ and $\bar{\mu}_i(z, \bar{z})$

leading to nontrivial correlation functions we have to contract them like in bosonic string theory with the ghosts which are in this case the Q partners G of the energy-momentum tensor T [93]. We then find the following possible amplitudes with no insertions [98]

$$F_g = \int_{\mathcal{M}_g} \left\langle \prod_{i=1}^{3g-3} \left(dm^i d\bar{m}^i \int_{\Sigma_g} G_{zz}(\mu_i)_{\bar{z}} \int_{\Sigma_g} G_{\bar{z}\bar{z}}(\bar{\mu}_i)_{\bar{z}} \right) \right\rangle, \quad g \geq 2, \quad (3.23)$$

where m^i are the $3(g-1)$ complex structure moduli we have to integrate over. Besides we find the n point functions for a genus g worldsheet [98]

$$C_{i_1 \dots i_n}^g = \int_{\mathcal{M}_g} \left\langle \prod_{r=1}^n \int_{\Sigma_g} O_{i_r} \prod_{i=1}^{3g-3} \left(dm^i d\bar{m}^i \int_{\Sigma_g} G_{zz}(\mu_i)_{\bar{z}} \int_{\Sigma_g} G_{\bar{z}\bar{z}}(\bar{\mu}_i)_{\bar{z}} \right) \right\rangle. \quad (3.24)$$

Here a genus zero worldsheet requires at least $n = 3$ insertions and a genus-one worldsheet at least $n = 1$ insertion to fix the remaining continuous symmetries of the worldsheet.

For a CY threefold as target space geometry the free energy is even nonzero for all genera which makes this dimension also special in topological string theory (see [93] for more details). The free energies F_g can then be combined to the generating function

$$F(t) = \sum_{g=0}^{\infty} g_s^{2g-2} F_g(t), \quad (3.25)$$

where g_s is the coupling constant of the topological string.

We have now constructed two possible topological string theories stemming from the two possible twists of the operator algebra. These theories are called the A-model and the B-model. In the following we want to have a closer look at these theories.

A-model

Let us first discuss the A-model topological string. After the A twist given in (3.18) the action of the field theory can be written as [93]

$$S = -it \int_{\Sigma_g} d^2z \{Q_A, V\} + 2t \int_{\Sigma_g} d^2z g_{i\bar{j}} \left(\partial_z \phi^i \partial_{\bar{z}} \bar{\phi}^{\bar{j}} - \partial_{\bar{z}} \phi^i \partial_z \bar{\phi}^{\bar{j}} \right). \quad (3.26)$$

Here t is the coupling constant of the theory and the Q_A exact term is given by

$$V = g_{i\bar{j}} \left(\psi_z^i \partial_{\bar{z}} \bar{\phi}^{\bar{j}} + \partial_z \phi^i \bar{\psi}_{\bar{z}}^{\bar{j}} \right). \quad (3.27)$$

For the fields we used the notation that $\psi_z^i = \psi_+^i$ and $\bar{\psi}_{\bar{z}}^{\bar{i}} = \bar{\psi}_-^{\bar{i}}$ in terms of the notation of (3.7). The second part in (3.26) which is not Q_A exact can be reformulated as a pullback of the target space Kähler

form $\omega = 2ig_{i\bar{j}}dz^i \wedge d\bar{z}^{\bar{j}}$ [93]

$$\begin{aligned} 2t \int_{\Sigma_g} d^2z g_{i\bar{j}} (\partial_z \phi^i \partial_{\bar{z}} \bar{\phi}^{\bar{j}} - \partial_{\bar{z}} \phi^i \partial_z \bar{\phi}^{\bar{j}}) &= t \int_{\Sigma_g} \phi^*(\omega) \\ &= t \int_{\phi(\Sigma_g)} \omega \\ &= t\omega\beta, \end{aligned} \quad (3.28)$$

where $\beta \in H_2(X, \mathbb{Z})$ is the homology class of $\phi(\Sigma_g)$. Since this term does not depend anymore on the fields or the metric it can be factored out of the path integral and just contributes a prefactor. The rest of the action is \mathcal{Q}_A exact which leads up to the prefactor to a \mathcal{Q}_A exact energy-momentum tensor and thus a topological theory.

Apart from that we notice that the left over path integral after factoring out the prefactors $e^{-t\omega\beta}$ is also independent of t . This can be seen by taking the derivative with respect to t which leads to the expectation value of $\frac{dS'}{dt}$ which is also \mathcal{Q}_A exact. Thus this expectation value vanishes and the path integral is independent of t . As usually in localization the integral can then be evaluated at any value for t especially $t \rightarrow \infty$. This then allows a classical treatment with the \mathcal{Q}_A exact part of the action (3.26). With (3.27) we then see from the classical equations of motion that [93]

$$\partial_{\bar{z}} \phi^i = \partial_z \bar{\phi}^{\bar{i}} = 0. \quad (3.29)$$

This means that the partition function localizes up to prefactors onto holomorphic maps $\phi : \Sigma_g \rightarrow X$ to the target space. For the genus g free energy (3.23) we find up to classical terms

$$F_g(t) = \sum_{\beta \in H_2(X, \mathbb{Z})} N_{g,\beta} q^\beta, \quad q_i = e^{-t_i}. \quad (3.30)$$

Here t_i are the complexified Kähler parameters and $N_{g,\beta}$ are the Gromov-Witten (GW) invariants which count the number of holomorphic curves of genus g and homology class β .

Furthermore we observe that the non \mathcal{Q}_A exact part of the action (3.28) does not depend on the complex structure of the target space manifold X . As discussed above for the example of a t dependency the observables do not depend on quantities which only show up in V (3.27). Hence we find that the free energy does not depend on the complex structure moduli but only on the Kähler moduli.

B-model

In the case of the B-model we find for the action after the B twist in (3.18) [93]

$$S = -it \int_{\Sigma_g} d^2z \{Q_B, V\} - t \int_{\Sigma_g} d^2z \left(i\theta_i (D_{\bar{z}} \rho_z^i - D_z \rho_{\bar{z}}^i) + \frac{1}{2} R_{i\bar{j}k}{}^l \rho_z^i \rho_{\bar{z}}^k \eta^{\bar{j}} \theta_l \right). \quad (3.31)$$

Here D_z denotes the covariant derivative of the target space X , R_{ijkl} is the target space Riemann tensor and we used the following notation for the fields in terms of the notation of (3.7)

$$\begin{aligned} \bar{\eta}^{\bar{j}} &= \bar{\psi}_+^{\bar{j}} + \bar{\psi}_-^{\bar{j}}, & \theta_i &= g_{i\bar{j}} (\bar{\psi}_+^{\bar{j}} - \bar{\psi}_-^{\bar{j}}), \\ \rho_z^i &= \psi_+^i, & \rho_{\bar{z}}^i &= \psi_-^i. \end{aligned} \quad (3.32)$$

The \mathcal{Q}_B exact part of the action (3.31) is given by

$$V = g_{i\bar{j}} \left(\rho_z^i \partial_{\bar{z}} \bar{\phi}^j + \rho_{\bar{z}}^{\bar{i}} \partial_z \phi^{\bar{j}} \right). \quad (3.33)$$

Note that the non \mathcal{Q}_B exact part of the action (3.31) is antisymmetric in z and \bar{z} . This allows us to rewrite it as a (1, 1) form which is independent of the metric after integrating over a Riemann surface. Thus we again see that the energy-momentum tensor is \mathcal{Q}_B exact and the theory is topological [93].

To use again localization techniques on the path integral it must be independent of the coupling constant t . In the case of the A-model this was achieved by factoring out the non \mathcal{Q}_A exact part of the action and using localization on the left over path integral. In the case of the B-model we cannot factor the non \mathcal{Q}_B exact part out since it still depends on the fields. Nevertheless we observe that only the non \mathcal{Q}_B exact part depends on the field θ_i and that it does so only linear. Hence we can absorb the coupling constant t in the definition of the field θ and make the non \mathcal{Q}_B exact part t independent [93].

After this we can again apply localization and evaluate the path integral for $t \rightarrow \infty$. The classical equations of motion of the t dependent part of the action are obtained using (3.33) [93]

$$\partial_z \phi^i = \partial_{\bar{z}} \phi^i = \partial_z \bar{\phi}^{\bar{i}} = \partial_{\bar{z}} \bar{\phi}^{\bar{i}} = 0. \quad (3.34)$$

Hence we see that the path integral localizes to constant maps $\phi : \Sigma_g \rightarrow X$. The corresponding moduli space we still have to integrate over is just the target space manifold itself $\mathcal{M} = X$. This makes the evaluation of B-model correlation functions much easier than the evaluation of A-model correlation functions where we still have to integrate over a more complicated moduli space.

Since the operator \mathcal{Q}_B acts differently on the complex conjugated fields ϕ^i and $\bar{\phi}^{\bar{i}}$ the theory explicitly depends on the choice of complex structure of the target space X . Additionally it can be shown that the theory does not depend on the Kähler parameters [93]. So in total we see that the dependence of the B-model on the moduli is opposite to the one of the A-model which only depends on the Kähler moduli.

Mirror symmetry reflects this by identifying the Kähler moduli space of a CY X with the complex structure moduli space of a mirror CY Y . The observables calculated on the A-model topological string with target space CY X are the same as the observables calculated on the B-model side on the CY Y .

3.2 Quantum mirror curves

In this section we want to find a way to derive the refined periods of local geometries in the NS limit which we will call *quantum periods*. Using the quantum periods we can apply special geometry to derive the free energies in the NS limit. These free energies can be checked against other calculations of the refined free energies for example by using the extended holomorphic anomaly equations [99–102] or the refined topological vertex [103].

In Subsection 3.2.1 we first review the construction of refinement. Then in Subsection 3.2.2 we discuss the derivation of special geometry in the case of quantum periods which then allows to calculate the free energies in the NS limit instead of only the prepotential in the unrefined case. In the subsections 3.2.3, 3.2.4 and 3.2.5 we then discuss the examples of local \mathbb{F}_1 , local \mathbb{F}_2 and the resolution of the orbifold $\mathbb{C}^3/\mathbb{Z}_5$. This section is mainly based on [41].

In the following discussion we only use non-compact local geometries which are constructed as the anti-canonical line bundle over a variety \mathcal{B}

$$\mathcal{O}(-K_{\mathcal{B}}) \rightarrow \mathcal{B}. \quad (3.35)$$

Via the adjunction formula this defines a non-compact² CY d -fold for a $d - 1$ dimensional variety \mathcal{B} (see Section 2.2). To find CY threefolds we take two dimensional base varieties. A simple class of two dimensional varieties is given by two dimensional reflexive toric varieties. The reflexive two dimensional varieties are given by the toric diagrams in Figure 2.2. As examples of this type we take for \mathcal{B} the Hirzebruch surfaces \mathbb{F}_1 and \mathbb{F}_2 . Hirzebruch surfaces \mathbb{F}_n are nontrivial fibrations of \mathbb{P}^1 over \mathbb{P}^1 : $\mathbb{P}(\mathcal{O}(1) \oplus \mathcal{O}(n)) \rightarrow \mathbb{P}^1$ [82]. The last example in Subsection 3.2.5 is not of this type since it is not reflexive. Nevertheless it is a toric geometry leading to a toric variety as described in Section 2.2 but this time with a spectral curve of genus two.

To use mirror symmetry to simplify the calculations by going to the B-model side we consider the mirror dual geometry. This is given by the following hypersurface in \mathbb{C}^4

$$uv = H(e^p, e^x; z_I), \quad (3.36)$$

where $u, v, p, x \in \mathbb{C}$ and z_I denote the complex structure moduli. The geometry contains a Riemann surface as a submanifold. Here the function $H(e^p, e^x; z_I)$ describes the Riemann surface which is defined via $H(e^p, e^x; z_I) = 0$. u and v denote non-compact line bundle directions.

3.2.1 Refinement and Nekrasov-Shatashvili limit

In Section 3.1 we discussed the construction of the unrefined topological string. Since in the following we will consider the refined topological string let us briefly introduce the relevant changes.

In [104] it was found that the topological A-model on the CY X is dual to M-theory on the space

$$X \times TN \times S^1. \quad (3.37)$$

Here TN denotes a Taub-NUT space with coordinates z_1 and z_2 . The last \times is not a direct product but is actually a nontrivial fibration: The TN is fibered over the S^1 such that the coordinates z_1 and z_2 are twisted when going around the circle

$$z_1 \rightarrow e^{i\epsilon_1} z_1 \quad \text{and} \quad z_2 \rightarrow e^{i\epsilon_2} z_2. \quad (3.38)$$

This introduces two parameters ϵ_1 and ϵ_2 . To preserve supersymmetry one requires in the unrefined topological string $\epsilon_1 = -\epsilon_2$. In the case of non-compact CY manifolds one has an additional $U(1)_R$ symmetry acting on X which allows to relax this condition [105]. The refined topological string is then defined to be dual to the M-theory geometry with general ϵ_1 and ϵ_2 . Physically one can interpret both ϵ_i as couplings to $SU(2)$ spins. Here we directly see that the two parameters ϵ_1 and ϵ_2 are in general both necessary since M-theory compactified on X leaves a five dimensional uncompactified space which has the little group $SO(4) = SU(2) \times SU(2)$ [105]. The free energy is then generalized to

$$F(\epsilon_1, \epsilon_2, t) = \log(Z) = \sum_{n,g=0}^{\infty} (\epsilon_1 + \epsilon_2)^{2n} (\epsilon_1 \epsilon_2)^{g-1} F^{(n,g)}(t). \quad (3.39)$$

Taking the limit $\epsilon_1 = -\epsilon_2 = ig_s$ which leaves us with the $F^{0,g}$ we then arrive at the free energy of the topological string (3.25).

² The resulting manifold is non-compact due to the non-compact line bundle direction.

Nekrasov-Shatashvili limit

Another particularly simple limit is reached when one of the expansion parameters ϵ_i is equal to zero. This NS limit was introduced in [106]. To calculate the free energy in this limit one defines the twisted superpotential [41]

$$\mathcal{W}(\hbar) = \lim_{\epsilon_2 \rightarrow 0} \epsilon_1 \epsilon_2 F. \quad (3.40)$$

The twisted superpotential can be expanded in the non-vanishing $\epsilon_i = \hbar$ as

$$\mathcal{W}(\hbar) = \sum_{n=0} \hbar^{2n} \mathcal{W}^{(n)}. \quad (3.41)$$

Here the coefficients can be identified with the coefficients in the refined free energy (3.39)

$$\mathcal{W}^{(i)} = F^{(i,0)}. \quad (3.42)$$

The free energy is a generating function for the instanton numbers n_{g_R, g_L}^β . In terms of these numbers the refined free energy is given by [25]

$$F(\epsilon_1, \epsilon_2, t) = \sum_{g_L, g_R \geq 0} \sum_{k \geq 1} \sum_{\beta \in H_2(M, \mathbb{Z})} \frac{1}{k} n_{g_L, g_R}^\beta \frac{\left(q_L^{\frac{k}{2}} - q_L^{-\frac{k}{2}}\right)^{2g_L} \left(q_R^{\frac{k}{2}} - q_R^{-\frac{k}{2}}\right)^{2g_R}}{q_1^{\frac{k}{2}} - q_1^{-\frac{k}{2}} q_2^{\frac{k}{2}} - q_2^{-\frac{k}{2}}} e^{-k\beta t}. \quad (3.43)$$

Here we used $q_{1,2} = e^{\epsilon_{1,2}}$ and $q_{L,R} = e^{\frac{\epsilon_1 \mp \epsilon_2}{2}}$. This simplifies in the NS limit to

$$\mathcal{W}(\hbar, t) = \hbar \sum_{g=0, k=1}^{\infty} \sum_{\beta \in H_2(M, \mathbb{Z})} \frac{\hat{n}_g^\beta (q^{\frac{k}{4}} - q^{-\frac{k}{4}})^{2g}}{k^2 2 \sinh\left(\frac{k\hbar}{2}\right)} e^{-k\beta t} \quad (3.44)$$

where $q = e^{\hbar}$ and we defined

$$\hat{n}_g^\beta = \sum_{g_L + g_R = g} n_{g_L, g_R}^\beta. \quad (3.45)$$

3.2.2 Quantum geometry

Cycles and periods

To discuss special geometry and quantum special geometry it is necessary to introduce the periods of the holomorphic three-form Ω of a CY threefold X . This subsection follows the discussion in [41]. First we choose a basis of three cycles A^I and B_J of $H_3(X, \mathbb{Z})$ with $I, J = 0 \dots h^{2,1}(X)$. We choose the basis of cycles with the intersection numbers

$$A^I \cap B_J = -B_J \cap A^I = \delta_J^I, \quad A^I \cap A^J = B_I \cap B_J = 0. \quad (3.46)$$

Next we choose a dual basis of three forms α_I and β^J in $H^3(X, \mathbb{Z})$ with $I, J = 0, \dots, h^{2,1}(X)$. The dual basis is chosen such that

$$\int_{A^I} \alpha_I = \delta_I^J, \quad \int_{B_I} \beta^J = -\delta_I^J, \quad (3.47)$$

while the other combinations vanish. Then the cohomology basis satisfies

$$\int_X \alpha_I \wedge \beta^J = \delta_I^J, \quad \int_X \beta^J \wedge \alpha_I = -\delta_I^J, \quad \int_X \alpha_I \wedge \alpha_J = 0 \quad \text{and} \quad \int_X \beta^I \wedge \beta^J = 0. \quad (3.48)$$

Now it is possible to expand the holomorphic three form Ω in the cohomology basis

$$\Omega = X^I \alpha_I - \mathcal{F}_I \beta^I. \quad (3.49)$$

Here the expansion coefficients X^I and \mathcal{F}_I are the periods of the holomorphic three form and given by

$$X^I = \int_{A^I} \Omega, \quad \mathcal{F}_I = \int_{B_I} \Omega. \quad (3.50)$$

Due to the scaling freedom of the holomorphic differential the X^I are elements of $\mathbb{P}^{h^{2,1}(X)+1}$ and are locally homogeneous coordinates of the complex structure moduli space \mathcal{M} of the CY X . Using the scaling relation we can define the affine coordinates

$$t^a = \frac{X^a}{X^0}, \quad a = 1, \dots, h^{2,1}(X). \quad (3.51)$$

In the following we have a closer look at B-model geometries which are described as the following hypersurface in \mathbb{C}^4

$$uv = H(e^x, e^p; z_I). \quad (3.52)$$

Here $H(e^x, e^p; z_I) = 0$ defines a Riemann surface. In this special case the holomorphic three form Ω factorizes as

$$\Omega = \frac{du}{u} \wedge dx \wedge dp. \quad (3.53)$$

As an additional simplification the three cycles A^I and B_J on X descend to one cycles on the Riemann surface Σ and also the periods of the holomorphic three form Ω descend to periods of a meromorphic one form λ on the Riemann surface. Here the one form λ is given by

$$\lambda = p dx. \quad (3.54)$$

In this case we can focus on the $2g$ one cycles A^i, B_j with $i, j = 1, \dots, g$ of a Riemann surface of genus g . The corresponding periods are defined as

$$x^i = \oint_{A^i} \lambda, \quad p_i = \oint_{B_i} \lambda. \quad (3.55)$$

As discussed above the g periods x^i correspond to moduli of the CY manifold X which we call in the following normalizable. In the case of non-compact CY manifolds there can be additional non-

normalizable moduli which are not actual moduli of the geometry but just undynamical parameters. Physically they can be interpreted via the engineered Seiberg-Witten theory [107]. Here the meromorphic one form λ of Σ corresponds to the Seiberg-Witten differential. Its g periods are related to the $N - 1 = g$ Coulomb parameters of pure $SU(N)$ Seiberg-Witten theory. In Seiberg-Witten theories with matter the meromorphic differential λ has additional poles. The residues around these poles are the *mass parameters* of additional matter fields and correspond to the non-normalizable moduli in non-compact CY manifolds.

Branewavefunctions

Quantum special geometry relies on the insertion of branes into the geometry. Therefore we briefly describe the effects of non-compact brane insertions. Here we follow the description in [41, 105, 108].

In particular we focus on the description of two-branes. These can be viewed as fixing a point $(p_0, x_0) \in \mathbb{C}^2$ in the (p, x) plane. The other coordinates are then fixed by the hypersurface condition of the fibration to fulfill

$$uv = H(p_0, x_0). \quad (3.56)$$

If we restrict the coordinates (p_0, x_0) to lie on the Riemann surface with $H(p_0, x_0) = 0$ the moduli space of the brane is given by the Riemann surface itself. From the worldvolume action on this brane one can see [108] that the coordinates p and x have to be non-commutative and fulfill the commutation relation

$$[\hat{x}, \hat{p}] = g_s. \quad (3.57)$$

Furthermore the insertion of a brane into the geometry changes the periods of the geometry as [108]

$$\oint_{x_0} \lambda = g_s. \quad (3.58)$$

This behaviour can be described by the Kodaira-Spencer field via $\lambda = \partial\phi$ on Σ . Via bosonization we then find the brane insertion operator [108]

$$\psi(x) = e^{\phi(x)/g_s} \quad (3.59)$$

The leading order of the partition function of the brane is given by [108]

$$\Psi_{\text{cl.}}(x) = \exp\left(\frac{1}{g_s} \int^x p(y) dy\right). \quad (3.60)$$

This brane partition function can also be interpreted as a brane wavefunction [108, 109]. In this picture g_s plays the role of \hbar and $p(x)$ is connected to a Wentzel-Kramers-Brillouin (WKB) expansion. The Hamilton operator of such a quantum system could be identified with the equation of the Riemann surface $H(p, x)$ which needs to be quantized in a suitable way.

In the refined case one has two parameters ϵ_1 and ϵ_2 which results in two possible kinds of branes. The Hamiltonians for the corresponding brane wavefunctions can be derived by the analysis of the brane insertion operators into the corresponding matrix model [105, 108]. As a matrix model description of refined topological strings the β ensemble was proposed in [110]³. It is defined by the following partition

³ There is another proposal for a matrix model dual to refined topological string theory proposed in [111]. For more details see Appendix A.4.

function

$$Z = \int d^N \lambda \prod_{i < j} (\lambda_i - \lambda_j)^{-2\epsilon_1/\epsilon_2} e^{-\frac{1}{2\epsilon_2} \sum_i W(\lambda_i)}. \quad (3.61)$$

As in the unrefined topological string $W(x)$ maps under the duality to the Riemann surface of the topological string geometry: $uv = p(x)^2 - (W'(x)^2 + f(x))$ with a deformation to smoothen out possible singularities (introduced by branes) [112]. Here the power of the Vandermonde determinant of the matrix model describing unrefined topological strings is deformed as

$$2 \rightarrow 2\beta = -2\frac{\epsilon_1}{\epsilon_2}. \quad (3.62)$$

In [105] the Schrödinger equation for the brane wave function was derived by considering the expectation value of a brane insertion operator $\psi_i(x) = e^{\frac{\phi(x)}{\epsilon_i}}$ (for the unrefined case see (3.59)) in the above β ensemble. The resulting loop equation⁴ then leads to the following equation

$$\left(-\epsilon_i^2 \frac{\partial^2}{\partial x^2} + W'(x)^2 + f(x) + g_s^2 \sum_{n=0}^g x^n \partial_{(n)} \right) \Psi_i(x) = 0, \quad (3.63)$$

where i denotes whether we consider an ϵ_1 or ϵ_2 brane and $\partial_{(n)}$ denotes a derivative with respect to the coefficients in the potential $W(x) = \sum_{n=0}^{g+2} t_n x^n$ [105]

$$\partial_{(n)} = \sum_{k=n+2}^{g+2} k t_k \frac{\partial}{\partial t_{k-n-2}}. \quad (3.64)$$

The Schrödinger equation (3.63) has a complicated additional derivative term proportional to g_s . This is interpreted in [105] as a multi-time dependence. In general this equation is hard to solve. But in the NS limit we have that $g_s^2 = -\epsilon_1 \epsilon_2 \rightarrow 0$. Thus the multi-time dependence drops out. If we furthermore implement the commutation relation (3.57) in the NS limit by setting

$$\hat{p} = i\hbar \frac{\partial}{\partial x}, \quad (3.65)$$

we obtain the Schrödinger equation

$$\left(\hat{p}^2 + W'(x)^2 + f(x) \right) \Psi(x) = 0. \quad (3.66)$$

Here we chose $\epsilon_1 = \hbar$ and $\epsilon_2 \rightarrow 0$ and dropped the index at $\Psi_1(x)$ to simplify the notation. The other ϵ_2 brane decouples and the corresponding Schrödinger equation becomes algebraic [105]. Interpreting the Schrödinger equation (3.66) in terms of the Riemann surface we see that it is equivalent to

$$H(x, i\hbar \partial_x) \Psi(x) = 0, \quad (3.67)$$

where $H(x, p) = 0$ is the defining equation of the Riemann surface. We can solve (3.67) perturbatively

⁴ A loop equation can be interpreted field theoretically as a Ward identity. For more informations on the derivation of loop equations see [113].

via the WKB method. Therefore we make the ansatz

$$\Psi(x, \hbar) = \exp\left(\frac{1}{\hbar}S(x, \hbar)\right), \quad (3.68)$$

where $S(x, \hbar)$ is a series in \hbar

$$S(x, \hbar) = \sum_{n=0}^{\infty} S_n(x)\hbar^n. \quad (3.69)$$

Plugging this ansatz into the Schrödinger equation (3.67) we can solve recursively for $S_i(x)$. Comparing the result to the classical brane partition function (3.60)⁵ we can identify at leading order

$$S_0(x) = - \int^x p(x')dx'. \quad (3.70)$$

As a next step it was proposed in [105] to interpret the higher order WKB functions $S_i(x)$ as corrections for the differential $\lambda = p(x)dx$ and define the quantum differential

$$\partial S = \partial_x S(x, \hbar)dx \xrightarrow{\hbar \rightarrow 0} -\lambda = -p(x)dx. \quad (3.71)$$

Monodromy and quantum special geometry

To properly interpret the quantum differential proposed in the last subsection we need to look at the monodromy behaviour of the partition function of the brane around the A and B cycles of the Riemann surface. For general A and B cycle

$$\gamma_A = \sum_I l^I A_I, \quad \gamma_B = \sum_I m_I B^I \quad (3.72)$$

we have in general the monodromy [105, 108]

$$\mathcal{M}_{\gamma_A} : Z_{\text{top}}(\vec{a}) \rightarrow \exp\left(\frac{1}{\epsilon_i} \sum_I l^I a_I\right) Z_{\text{top}}(\vec{a}) \quad (3.73)$$

$$\mathcal{M}_{\gamma_B} : Z_{\text{top}}(\vec{a}) \rightarrow Z_{\text{top}}\left(\vec{a} + \frac{g_s^2}{\epsilon_i} \vec{m}\right) \quad (3.74)$$

for ϵ_i branes with a set of flat coordinates \vec{a} on the moduli space. First we have a detailed look at the monodromy around the B cycle. We additionally know that the partition function is given by

$$Z_{\text{top}}(\vec{a}; \epsilon_1, \epsilon_2) = \exp\left(\sum_{g=0}^{\infty} g_s^{2g-2} \mathcal{F}^{(g)}(\vec{a}; \hbar)\right). \quad (3.75)$$

In the NS limit with $\epsilon_1 = \hbar$ and $\epsilon_2 \rightarrow 0$ this becomes

$$Z_{\text{top}}(\vec{a}; \epsilon_1 = \hbar, \epsilon_2 = 0) = \lim_{\epsilon_2 \rightarrow 0} \exp\left(\frac{1}{\hbar \epsilon_2} \mathcal{W}(\vec{a}; \hbar)\right). \quad (3.76)$$

⁵ Which can be interpreted as a wave function, see [108, 109]

Using the explicit form of the partition function (3.76) with the monodromy behaviour (3.74) in the NS limit we find [105, 108]

$$Z_{\text{top}}(\vec{a}) \rightarrow \exp\left(\frac{1}{\hbar} \sum_I m_I \partial_{a_I} \mathcal{W}(\vec{a}; \hbar)\right) Z_{\text{top}}(\vec{a}). \quad (3.77)$$

Here we have neglected higher derivative terms which is possible since in the NS limit $\frac{g_s^2}{\hbar} \rightarrow 0$ and thus the monodromy transformation becomes infinitesimal.

On the other hand the brane partition function is given as the expectation value of the brane insertion operator which is the solution to the Schrödinger equation (3.67) [108]

$$\Psi(x) = \langle e^{-\frac{1}{\hbar} \phi(x)} \rangle = e^{\frac{1}{\hbar} \int^x \partial S}. \quad (3.78)$$

Explicitly going around the B cycle γ_B we then get the monodromy

$$Z_{\text{top}}(\vec{a}) \rightarrow e^{\frac{1}{\hbar} \oint_{\gamma_B} \partial S} Z_{\text{top}}(\vec{a}) = e^{\frac{1}{\hbar} \sum_I m_I \oint_{\gamma_B} \partial S} Z_{\text{top}}(\vec{a}). \quad (3.79)$$

Comparing the two results (3.77) and (3.79) we find the relation [105, 108]

$$a_{D,I}(\hbar) := \oint_{\gamma_{B^I}} \partial S = \partial_{a_I} \mathcal{W}(\vec{a}; \hbar) \quad (3.80)$$

To interpret a_I we need to have a closer look at the monodromy around γ_A . Going around γ_A with the explicit form of the brane partition function in (3.78) we find

$$Z_{\text{top}}(\vec{a}) \rightarrow e^{\frac{1}{\hbar} \oint_{\gamma_A} \partial S} Z_{\text{top}}(\vec{a}) = e^{\frac{1}{\hbar} \sum_I m_I \oint_{\gamma_A} \partial S} Z_{\text{top}}(\vec{a}). \quad (3.81)$$

Comparing this to the general monodromy behaviour in (3.73) we find

$$\oint_{\gamma_{A_I}} \partial S = a_I(\hbar). \quad (3.82)$$

The A and B-periods thus generalize to quantum A and B-periods which fulfill a generalized special geometry relation (3.80). The quantum corrected prepotential is just the free energy in the NS limit $\mathcal{W}(\hbar)$.

Quantum operators

Deriving the periods in practice requires integration of the meromorphic differential λ around the A and B cycles of the geometry. For the A-periods these integrals reduce to residues up to a diverging part in the leading order in \hbar which leads to the logarithmic contribution to the classical period. Nevertheless collecting the contributions to different periods from the in general more than one residue is not an easy task. Additionally the computation of the B-periods is much harder since it involves different patches of the geometry corresponding to different parametrizations [41, 105]. For few examples direct calculations are possible but heavily depend on the symmetries of the respective geometries. In [41, 105] the analysis was done for local \mathbb{P}^2 , local \mathbb{F}_0 and local \mathbb{F}_1 .

To avoid these complications we use an ansatz proposed in [114] and further used in [41, 105, 115]. Using partial integration one can derive *quantum operators* \mathcal{D}_n (for more details see Appendix A.3) which map the zeroth order differential $S_0(x)$ to higher order differentials $S_n(x)$ up to exact forms in

x . The quantum operators are differential operators in the moduli. We found in all examples that they were of second order and only contained derivatives with respect to the normalizable moduli u . For genus-one Riemann surfaces we find the general form

$$\mathcal{D}_i = c_{1,i}(u, \vec{m})\Theta_u + c_{2,i}(u, \vec{m})\Theta_u^2. \quad (3.83)$$

For genus two Riemann surfaces there are more normalizable moduli which leads to the following form

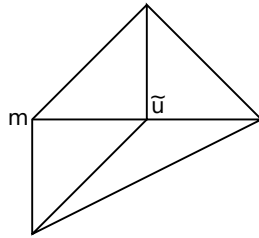
$$\begin{aligned} \mathcal{D}_i = & c_{1,i}(u_1, u_2, \vec{m})\Theta_{u_1} + c_{2,i}(u_1, u_2, \vec{m})\Theta_{u_2} \\ & + c_{3,i}(u_1, u_2, \vec{m})\Theta_{u_1}^2 + c_{4,i}(u_1, u_2, \vec{m})\Theta_{u_1}\Theta_{u_2} + c_{5,i}(u_1, u_2, \vec{m})\Theta_{u_2}^2. \end{aligned} \quad (3.84)$$

Here $\Theta_u = u\partial_u$ and the prefactors $c_i(\vec{u}, \vec{m})$ are rational functions of their arguments. After integration around a closed contour as in the case of the periods the exact forms drop out. Since the quantum operators and the integration commute the quantum operators are exact on the level of the periods. The full quantum periods are then obtained from the classical ones by

$$\Pi(\vec{u}, \vec{m}; \hbar) = \left[1 + \sum_{i=1}^{\infty} \hbar^{2i} \mathcal{D}_{2i} \right] \Pi(\vec{u}, \vec{m}) =: \mathcal{D}^{(2)}(\vec{u}, \vec{m}, \hbar) \Pi(\vec{u}, \vec{m}). \quad (3.85)$$

3.2.3 Example 1: local \mathbb{F}_1

To make the previous discussion more concrete we want to study three examples in the following: the local \mathbb{F}_1 , the local \mathbb{F}_2 and the resolution of the orbifold $\mathbb{C}^3/\mathbb{Z}_5$ geometries. We will calculate the quantum periods $\vec{\Pi}_A(\hbar)$ and $\vec{\Pi}_B(\hbar)$ ⁶. Then we use special geometry to calculate the free energies and the instanton numbers. This section is based on [41].



divisor	ν_i			$l^{(1)} = l^{(f)}$	$l^{(2)} = l^{(b)}$
$x_0 = \tilde{u}$	1	0	0	-2	-1
x_1	1	1	0	1	0
x_2	1	0	1	0	1
$x_3 = m$	1	-1	0	1	-1
x_4	1	-1	-1	0	1

Figure 3.1: Toric diagram of \mathbb{F}_1 and toric data of local \mathbb{F}_1 . The toric diagram of local \mathbb{F}_1 is three dimensional and can be projected to the given two dimensional polytope.

The toric diagram and data of the local \mathbb{F}_1 geometry are given in Figure 3.1. Using the definition

$$z_i = \prod_k x_k^{l_k^{(i)}} \quad (3.86)$$

we can derive the following Batyrev coordinates which are small around the large complex structure point

$$z_1 = \frac{m}{\tilde{u}^2}, \quad z_2 = \frac{1}{m\tilde{u}}. \quad (3.87)$$

⁶ In the case of genus-one geometries there are only one A and one B-period which we call a and a_D respectively.

Here we have already set $x_0 = \tilde{u}$ and $x_3 = m$. Defining $u = \frac{1}{\tilde{u}}$ we can derive the following quantum mirror curve via $\sum_i x_i$

$$H(x, p) = -1 + e^x + mu^2 e^{-x} + e^p + e^{-\hbar/2} \frac{u}{m} e^x e^{-p}. \quad (3.88)$$

Classical periods

To obtain the classical A period a we use [102]

$$\frac{da}{du} = \sqrt{\frac{E_6(\tau)g_2(u, m)}{E_4(\tau)g_3(u, m)}}. \quad (3.89)$$

Here $E_4(\tau)$ and $E_6(\tau)$ are the Eisenstein series and $g_2(u, m)$ and $g_3(u, m)$ are the coefficients in the Weierstrass form of the elliptic curve. Note that we use another normalization of the Weierstrass form than in Section 2. Namely

$$y^2 = 4x^3 - g_2(u, m)x - g_3(u, m). \quad (3.90)$$

The $g_i(u, m)$ may still be rescaled according to $g_i \rightarrow \lambda^i(u, \vec{m})g_i$ but this freedom in $\frac{da}{du}$ can be fixed by matching the leading terms to the expansion of the period integral (3.82).

The parameter τ in (3.89) is the complex structure parameter of the torus and can be computed in terms of u and m by the series expansion of the j -invariant

$$j = 1728 \frac{E_4^3(\tau)}{E_4^3(\tau) - E_6^2(\tau)} = \frac{1}{q} + 744 + 196884q + 21493760q^2 + \mathcal{O}(q^3), \quad (3.91)$$

with $q = \exp(2\pi i\tau)$. After inverting the series (3.91) one uses the expression of j in terms of the discriminant of the elliptic curve

$$j = 1728 \frac{g_2^3(u, m)}{\Delta(u, m)}, \quad (3.92)$$

where $\Delta(u, m) = g_2^3(u, m) - 27g_3^2(u, m)$.

Applying the Nagell algorithm A.2 to the classical mirror curve (3.88) with $\hbar = 0$ we obtain the following Weierstrass parameters

$$\begin{aligned} g_2(u, m) &= 27u^4(1 - 8mu^2 + 24u^3 + 16m^2u^4), \\ g_3(u, m) &= 27u^6(1 - 12mu^2 + 36u^3 + 48m^2u^4 - 144mu^5 + 216u^6 - 64m^3u^6). \end{aligned} \quad (3.93)$$

To find the B-period a_D we use the relation [101]

$$\frac{\partial}{\partial a} a_D(a, \vec{m}) = -\frac{1}{2\pi i} \tau(u, \vec{m}) \quad (3.94)$$

Operator approach

Solving the Schrödinger equation of (3.88) with the WKB ansatz (3.68) in (3.67) we find the following zeroth order solution

$$p(x) = S'_0(x) = \log\left(\frac{1}{2}e^{-x}\left(e^x - e^{2x} - z_1 - \sqrt{(-e^x + e^{2x} + z_1)^2 + 4e^{3x}z_2}\right)\right). \quad (3.95)$$

This can be integrated over the A and B cycles of the geometry to find the classical periods. Solving the Schrödinger equation to higher WKB orders we can use the algorithm in Appendix A.3 to find the following quantum operator

$$\mathcal{D}_2 = \frac{mu^2(4m - 9u)}{6\delta}\Theta_u + \frac{4m - 3u - 16m^2u^2 + 36u^3m}{24\delta}\Theta_u^2. \quad (3.96)$$

Here we defined $\delta = (-8m + 9u)$ and $\theta_u = u\partial_u$. Higher order quantum operators can be found in [41]. Applying the operators on the classical periods obtained via (3.89) and (3.94) we find the following quantum A and B-periods

$$a = \log(u) + mu^2 - 2u^3 - \frac{1}{4}u^3\hbar^2 + O(\hbar^4, u^4), \quad (3.97)$$

$$a_D = -4\log(u)^2 - \log(u)\log(m) - \log(u^8m)\left(mu^2 - 2u^3 - \frac{1}{4}u^3\hbar^2\right) + \frac{u}{m} + u^2\left(\frac{1}{4m^2} - 4m\right) + 10u^3 + \frac{1}{9m^3}u^3 - \frac{1}{24}\hbar^2\left(4 + \frac{u}{m} + u^2\left(\frac{1}{m^2} + 8m\right) + u^3\left(\frac{1}{m^3} - 62\right)\right) + O(\hbar^4, u^4). \quad (3.98)$$

To find the quantum mirror map we use $Q_u = e^a$. Inverting the resulting series $Q_u(u, m)$ leads to

$$u(Q_u) = Q_u - mQ_u^3 + 2Q_u^4 + \frac{1}{4}Q_u^4\hbar^2 + O(\hbar^4, Q_u^5). \quad (3.99)$$

To check the above results we want to calculate the free energies in the NS limit by using special geometry (3.80). To make contact to the usual expansion in the coordinates z_1 and z_2 from the Batyrev construction we invert (3.87). From the resulting expressions for u and m we see that

$$Q_u = Q_1^{1/3}Q_2^{1/3}, \quad m = Q_1^{1/3}Q_2^{-2/3}. \quad (3.100)$$

These relations can also be checked perturbatively against a direct calculation of Q_1 and Q_2 . Note the quantum operators can also be used to calculate the corrections to Q_1 and Q_2 . Integrating the special geometry relation (3.80) and using (3.100) we can calculate the free energies in the NS limit. We then find the instanton numbers in Table 3.1 and 3.2.

Difference equation

The above calculation of the quantum corrected periods by using the quantum operators has the advantage that the quantum operators are exact in the complex structure moduli u and m . This allows the transformation to other points in the moduli space and thus the calculation of quantum corrections for example at the orbifold point as was done in [41] for \mathbb{F}_0 and \mathbb{P}^2 . But this technique has the drawback that it is perturbative in \hbar .

For some calculations an exact solution in \hbar is necessary. Therefore we want to discuss the calcu-

\hbar^0	d_1	0	1	2	3	4
d_2						
0			1			
1		-2	3			
2			5	-6		
3			7	-32	27	
4			9	-110	286	-192

\hbar^2	d_1	0	1	2	3	4
d_2						
0						
1		-1	4			
2			20	-35		
3			56	-368	396	
4			120	-2055	6732	-5392

 Table 3.1: Instanton numbers for local \mathbb{F}_1 at order \hbar^0 and \hbar^2 .

\hbar^4	d_1	0	1	2	3	4
d_2						
0						
1			1			
2			21	-56		
3			126	-1352	1875	
4			462	-12892	55363	-53028

\hbar^6	d_1	0	1	2	3	4
d_2						
0						
1						
2			8	-36		
3			120	-2412	4344	
4			792	-41594	242264	-277430

 Table 3.2: Instanton numbers for local \mathbb{F}_1 at order \hbar^4 and \hbar^6 .

lation of quantum periods using the difference equation. This technique leads to exact results in \hbar but perturbative in the moduli u and m . Additionally this technique has special requirements which are not fulfilled by several models.

We begin by defining the function

$$V(x) = \frac{\Psi(x + \hbar)}{\Psi(x)}. \quad (3.101)$$

Here $\Psi(x)$ is a solution to the Schrödinger equation (3.67). Using the elliptic curve (3.88) as the Hamilton operator we find

$$0 = (-1 + e^x + mu^2 e^{-x}) \Psi(x) + \Psi(x + \hbar) + \frac{u}{m} e^{-\hbar/2} e^x \Psi(x - \hbar). \quad (3.102)$$

This can be massaged such that we find an expression for $V(x)$

$$V(x) = 1 - e^x - mu^2 e^{-x} - \frac{u}{m} e^{-\hbar/2} e^x \frac{1}{V(x - \hbar)}. \quad (3.103)$$

Expanding this around $u = 0$ ⁷ leads to

$$V(x) = 1 - e^x - mu^2 e^{-x} - \frac{u}{m} q^{-1/2} e^x \frac{1}{1 - q^{-1} e^x} + \mathcal{O}(u^3). \quad (3.104)$$

Here we defined $q = e^{\hbar}$.

⁷ This is the special requirement mentioned earlier: Not every geometry leads to a $V(x)$ which can be expanded in u such that the term including $V(x - n\hbar)$ is shifted to higher and higher orders.

Since $V(x)$ includes the wavefunction $\Psi(x)$ we can insert the WKB ansatz such that the quantum differential appears. Unfortunately we cannot extract the differential directly but only the periods. To do this we integrate over $\log(V(x))$ after inserting the WKB ansatz $\Psi(x) = e^{\frac{1}{\hbar} \sum_{i=0}^{\infty} S_i(x) \hbar^i}$ [41]

$$\int \log(V(x)) = \int S'(x) dx + \sum_{n=2}^{\infty} \frac{\hbar^n}{n!} \int S^{(n)}(x) dx. \quad (3.105)$$

The differential λ does not need to be exact. Therefore it is not necessarily possible to find an antiderivative for $S'(x)$. Nevertheless we have for $n \geq 2$ [41]

$$\oint dx S^{(n)}(x) = [S^{(n-1)}]. \quad (3.106)$$

Thus (3.105) simplifies for integration around closed contours

$$\oint \partial S = \oint \log(V(X)). \quad (3.107)$$

Using this we can directly calculate the integral around the A cycle to find

$$a = \log(u) + mu^2 - \left(\sqrt{q} + \frac{1}{\sqrt{q}} \right) u^3 + \frac{3m^2 u^4}{2} + O(u^5). \quad (3.108)$$

The B-period in contrast is much harder to find since we have to change the parametrization of the curve (3.88) to find all contributions. In this case we need the following parts [41]

$$\begin{aligned} \mathcal{A} &: -1 + e^p + e^x + u^2 m e^{-x} - e^{\hbar/2} u^3 e^{-p-x} \\ \mathcal{B} &: -1 + e^p + e^x + u^2 m e^{-p} - e^{\hbar/2} u^3 e^{-p-x} \\ \mathcal{C} &: -1 + e^p + e^x + u^2 m e^{-x} - e^{-\hbar/2} \frac{u}{m} e^{-p+x}. \end{aligned} \quad (3.109)$$

The proper B-period can be found by integrating the different parts and adding them appropriately. The right combination can be found by comparing the zeroth order in \hbar with known results. We find

$$a_D = -\log(u) \log(mu^4) - \log(mu^8) \tilde{a} + \tilde{a}_D, \quad (3.110)$$

with

$$\begin{aligned} \tilde{a}_D &= \frac{\sqrt{q} u \log(q)}{m(q-1)} + \frac{u^2 (q - 4m^3(q+1)^2) \log(q)}{2m^2(q^2-1)} \\ &+ \frac{u^3 (6m^3(2q^4 + 3q^3 + 5q^2 + 3q + 2) + q^2) \log(q)}{3m^3 \sqrt{q}(q^3-1)} + O(u^4). \end{aligned} \quad (3.111)$$

The right combination of the last part is given by

$$\tilde{a}_D = -3I_{\mathcal{A}} - 4I_{\mathcal{B}} - I_{\mathcal{C}} \quad (3.112)$$

where $I_{\mathcal{A}/\mathcal{B}/\mathcal{C}} = \int_0^{\infty} \log(V(x)) dx$ denotes the integration of the curves in the patches $\mathcal{A}/\mathcal{B}/\mathcal{C}$ of (3.109) respectively. Additionally we have to symmetrize in $\hbar \rightarrow -\hbar$ such that the odd terms in \hbar disappear.

This process is necessary because the integration process does not explicitly takes the full curve into account [41].

Finally we can again invert the A-period (3.108) to obtain the mirror map and use this to integrate the B-period (3.110) with respect to a in order to apply the special geometry relation (3.80). To compare with other results we transform again to the usual flat coordinates via (3.100). We find the following free energy which is exact in \hbar

$$\mathcal{W} = \frac{(q+1)Q_1 - \sqrt{q}Q_2}{1-q} + \frac{(q^2+1)Q_1^2 - qQ_2^2}{4(1-q^2)} - \frac{(4q^2+q+4)Q_1Q_2}{3(1-q)\sqrt{q}} + \mathcal{O}(Q_i^3). \quad (3.113)$$

3.2.4 Example 2: local \mathbb{F}_2

Next we discuss the geometry of local \mathbb{F}_2 : $\mathcal{O}(-K_{\mathbb{F}_2}) \rightarrow \mathbb{F}_2$. This section is based on [41]. The projection of the three dimensional toric polyhedron to the plane with the first coordinate equal to one is depicted in Figure 3.2. The 2D toric polyhedron is equal to polyhedron F_4 in Figure 2.2 up to an $SL(2, \mathbb{Z})$ transformation.

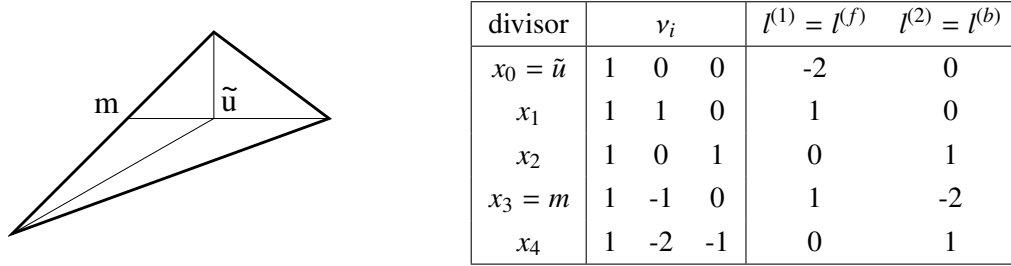


Figure 3.2: Toric diagram of \mathbb{F}_2 and toric data of local \mathbb{F}_2 . The toric diagram of local \mathbb{F}_2 is three dimensional and can be projected to the given two dimensional polytope.

Using (3.86) and the toric data of local \mathbb{F}_2 in Figure 3.2 we find the following Batyrev coordinates

$$z_1 = \frac{m}{\tilde{u}^2}, \quad z_2 = \frac{1}{m^2}. \quad (3.114)$$

Here we have already set $x_0 = \tilde{u}$ and $x_3 = m$. Defining then $u = \frac{1}{\tilde{u}^2}$ we find the quantum mirror curve

$$H = 1 + e^x + e^p + mue^{2x} + \frac{1}{m^2}e^{-p}. \quad (3.115)$$

Applying the Nagell algorithm (see Appendix A.2) on (3.115) we find the Weierstrass coefficients

$$\begin{aligned} g_2(u, m) &= 27u^4 \left((1 - 4mu)^2 - 48u^2 \right), \\ g_3(u, m) &= -27u^6 \left(64m^3u^3 - 48m^2u^2 - 288mu^3 + 12mu + 72u^2 - 1 \right). \end{aligned} \quad (3.116)$$

Using the WKB ansatz (3.68) with the mirror curve (3.115) as Hamilton operator we obtain for the zeroth order of the WKB function

$$S'_0(x) = \log \left(\frac{1}{2} \left(-1 - e^x - e^{2x}mu - \sqrt{(1 + e^x + e^{2x}mu^2)^2 - \frac{4}{m^2}} \right) \right). \quad (3.117)$$

After solving for the higher orders of the WKB function we can integrate by parts using the algorithm in Appendix A.3 to find the quantum operator

$$\mathcal{D}_2 = -\frac{mu}{6}\Theta_u + \frac{1-4mu}{12}\Theta_u^2, \quad (3.118)$$

with the discriminant $\Delta = g_2^3(u, m) - 27g_3^2(u, m) = 16m^2u^2 - 8mu - 64u^2 + 1$ and $\theta_u = u\partial_u$. Higher order operators can be found in the Appendix of [41]. Using (3.89) and (3.94) to calculate the nontrivial classical periods and applying the operator (3.118) we find the quantum periods

$$a = \log(u) + 2mu + u^2(6 + 3m^2 + 2\hbar^2) + u^3(40m + \frac{20}{3}m^3 + 20m\hbar^2) + \mathcal{O}(\hbar^4, u^4), \quad (3.119)$$

$$\begin{aligned} a_D = & -2\log(u)^2 + \log(u)(-8mu - 24u^2 - 12m^2u^2 - 160mu^3 - \frac{80}{3}m^3u^3 - 8\hbar^2u^2 - 80m\hbar^2u^3) \\ & - \frac{\hbar^2}{3} + u(-8m - \frac{2}{3}m\hbar^2) + u^2(-28 - 26m^2 + \hbar^2(-\frac{52}{3} - 2m^2)) \\ & + u^3(-\frac{832}{3}m - \frac{656}{9}m^3 + \hbar^2(-\frac{616}{3}m - \frac{20}{3}m^3)) + \mathcal{O}(\hbar^4, u^4). \end{aligned} \quad (3.120)$$

To proceed we calculate the quantum mirror map by inverting $Q_u = e^a$

$$u(Q_u) = Q_u - 2mQ_u^2 - 6Q_u^3 + 3m^2Q_u^3 + 8mQ_u^4 - 4m^3Q_u^4 + (-2Q_u^3 - 4mQ_u^4)\hbar^2 + \mathcal{O}(\hbar^4, Q_u^5). \quad (3.121)$$

To check this result against other refined calculations we now want to calculate the free energy in the NS limit. Therefor we need to transform back to the usual Batyrev coordinates z_1 and z_2 . This time inverting (3.114) would lead to m being only proportional to Q_2 which would lead to m becoming quantum corrections. This cannot be right. Therefore one can check algebraically the following equation at the level of the classical period [102]

$$\frac{1 + Q_2}{\sqrt{Q_2}} = \frac{1}{\sqrt{z_2}} = m. \quad (3.122)$$

The transformation of Q_u can nevertheless be found by inverting (3.114) to be

$$Q_u = Q_1Q_2^{1/2}. \quad (3.123)$$

Using this after integrating the special geometry relation (3.80) we find the instanton numbers listed in Tables 3.3 and 3.4. Here we see a discrepancy in $n^{0,1} = 1$ for \hbar^0 in comparison to the topological vertex [103, 116]. This discrepancy has also been reported in previous publications and was discussed there [117].

3.2.5 Example 3: $\mathbb{C}^3/\mathbb{Z}_5$

In the following we discuss the resolved $\mathbb{C}^3/\mathbb{Z}_5$ orbifold geometry. The spectral curve of this geometry is of genus two which makes it much more complicated to deal with than the previous examples. The 2D projection of the toric polyhedron as well as the toric data are given in Figure 3.3.

Using (3.86) and the toric data from Figure 3.3 we find the Batyrev coordinates (3.86)

$$z_1 = \frac{x_1x_2x_3}{x_0^3} = \frac{u_2}{u_1^3}, \quad z_2 = \frac{x_0x_4}{x_3^2} = \frac{u_1}{u_2^2}. \quad (3.124)$$

\hbar^0	d_1	0	1	2	3	4
d_2						
0						
1			2	2		
2				4		
3				6	6	
4				8	32	8

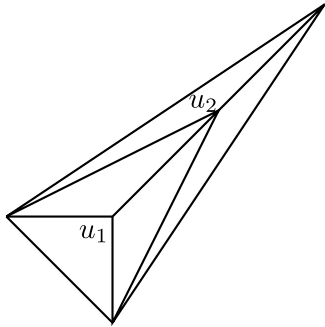
\hbar^2	d_1	0	1	2	3	4
d_2						
0						
1			1	1		
2				10		
3				35	35	
4				84	368	84

Table 3.3: Instanton numbers for local \mathbb{F}_2 at order \hbar^0 and \hbar^2 . Note the difference in $n^{0,1}$ for \hbar^0 compared to topological vertex calculations [103, 116]. This discrepancy has also been found and discussed in [117].

\hbar^4	d_1	0	1	2	3	4
d_2						
0						
1						
2				6		
3				56	56	
4				252	1352	252

\hbar^6	d_1	0	1	2	3	4
d_2						
0						
1						
2				1		
3				36	36	
4				330	2412	330

Table 3.4: Instanton numbers for local \mathbb{F}_2 at order \hbar^4 and \hbar^6 .



divisor	v_i	$l^{(1)}$	$l^{(2)}$
$x_0 = u_1$	1 0 0	-3	1
x_1	1 -1 0	1	0
x_2	1 0 -1	1	0
$x_3 = u_2$	1 1 1	1	-2
x_4	1 2 2	0	1

Figure 3.3: Toric diagram and data of resolved $\mathbb{C}^3/\mathbb{Z}_5$. The toric diagram of the resolution of $\mathbb{C}^3/\mathbb{Z}_5$ is three dimensional and can be projected to the given two dimensional polytope.

From these we can derive the following quantum corrected spectral curve

$$H = 1 + e^x + e^p + z_2 e^{2x} + z_1 e^{-x-p+\hbar/2}. \tag{3.125}$$

Using the WKB ansatz (3.68) with the mirror curve (3.125) we can recursively solve for the WKB functions S'_n . Integration by parts as in Appendix A.3 then leads to the following quantum operator

$$\mathcal{D}_2 = \frac{1}{8}\theta_1^2 + \frac{1}{6}\theta_1\theta_2. \tag{3.126}$$

Here $\theta_i = z_i \partial_{z_i}$.

A genus two curve has two A-periods and two B-periods. Since from the generalizations of (3.89)

and (3.94) for genus two we cannot find the derivatives of the periods we need to find a different way. A standard method is to solve the Picard-Fuchs (PF) equations. In order to do this we calculate the GKZ operators⁸ which are given by [118]

$$D_\alpha = \prod_{i|l_i^{(\alpha)}>0} \partial_{x_i}^{l_i^{(\alpha)}} - \prod_{i|l_i^{(\alpha)}<0} \partial_{x_i}^{l_i^{(\alpha)}} \quad (3.127)$$

for toric geometries. For the resolution of $\mathbb{C}^3/\mathbb{Z}_5$ the GKZ operators are

$$\begin{aligned} D_1 &= \theta_1^3 - 2\theta_1^2\theta_2 - z_1(\theta_2^3 - 9\theta_1\theta_2^2 + 27\theta_1^2\theta_2 - 27\theta_1^3 - 3\theta_2^2 + 18\theta_1\theta_2 - 27\theta_1^2 - 6\theta_1 + 2\theta_2) \\ D_2 &= -3\theta_1\theta_2 + \theta_2^2 - z_2(-\theta_1 + 2\theta_2 + \theta_1^2 - 4\theta_1\theta_2 + 4\theta_2^2), \end{aligned} \quad (3.128)$$

with $\theta_i = z_i\partial_{z_i}$. We can find solutions to the PF operators by using Frobenius method: The periods of local geometries are found as the derivatives of a fundamental period [118]

$$\Pi_{\vec{n}} = \left[\prod_{\alpha} \frac{\partial^{n_\alpha}}{\partial(\rho^\alpha)^{n_\alpha}} \omega_0(\vec{z}, \vec{\rho}) \right]_{\vec{\rho}=0}. \quad (3.129)$$

For $\vec{n} = 0$ we find the trivial period and for $\vec{n} = e_i$ we find the i th A-period. The fundamental period ω_0 is in general given by

$$\omega_0(\vec{z}, \vec{\rho}) = \sum_{\vec{n}} \frac{\prod_{\alpha} z_\alpha^{n_\alpha + \rho_\alpha}}{\prod_i \Gamma(\sum_{\alpha} l_i^{(\alpha)}(n_\alpha + \rho_\alpha) + 1)}. \quad (3.130)$$

Afterwards we can check that these results solve the GKZ equations $D_\alpha \Pi = 0$.

This method does not use the u_i, m_i notation which splits the moduli into dynamical moduli u_i and mere parameters m_i . Thus in general one has to make a coordinate transformation and find a linear combination of the periods which starts with $\log(u_i)$ in order to apply the quantum operators and find the free energies. In the case at hand we find after applying the operator (3.126) the two quantum corrected A-periods

$$\begin{aligned} \Pi_{A_1} &= \log(z_1) - 6z_1 - z_2 + 45z_1^2 - \frac{3z_2^2}{2} - 560z_1^3 - 18z_2z_1^2 - \frac{10z_2^3}{3} \\ &\quad + \hbar^2 \left(-\frac{3}{4}z_1 + \frac{45}{2}z_1^2 - 630z_1^3 - 15z_2z_1^2 \right) + \mathcal{O}(\hbar^4, z_i^4) \end{aligned} \quad (3.131)$$

$$\begin{aligned} \Pi_{A_2} &= \log(z_2) + 2z_1 + 2z_2 - 15z_1^2 + 3z_2^2 + \frac{560z_1^3}{3} + 6z_2z_1^2 + \frac{20z_2^3}{3} \\ &\quad + \hbar^2 \left(210z_1^3 - \frac{15}{2}z_1^2 + 5z_2z_1^2 + \frac{1}{4}z_1 \right) + \mathcal{O}(\hbar^4, z_i^4). \end{aligned} \quad (3.132)$$

⁸ The GKZ operators are not exactly the PF operators. Nevertheless the GKZ operators can be factored into the PF operators on the right and an additional operator on the left. Thus solutions to the PF operators are also solutions to the GKZ system.

Using $q_i = e^{\Pi_{A_i}}$ we can invert the two A-periods to find the mirror maps

$$\begin{aligned} z_1 &= q_1 + 6q_1^2 + 9q_1^3 + q_1q_2 + 10q_1^2q_2 + \frac{3q_1^2\hbar^2}{4} - 9q_1^3\hbar^2 + \frac{5}{4}q_1^2q_2\hbar^2 + \mathcal{O}(\hbar^4, q_i^4) \\ z_2 &= q_2 - 2q_1q_2 + 5q_1^2q_2 - 2q_2^2 + 6q_1q_2^2 + 3q_2^3 - \frac{1}{4}q_1q_2\hbar^2 + 5q_1^2q_2\hbar^2 + \frac{3}{4}q_1q_2^2\hbar^2 + \mathcal{O}(\hbar^4, q_i^4). \end{aligned} \quad (3.133)$$

Plugging the mirror maps into the B-periods

$$\begin{aligned} \Pi_{B_1} &= \log(q_1)^2 + \log(q_1)\log(q_2) + \frac{3\log(q_2)^2}{2} - 15q_1 + \frac{225q_1^2}{4} - \frac{1220q_1^3}{3} - 20q_1q_2 + 100q_1^2q_2 \\ &\quad - 15q_1q_2^2 + \hbar^2 \left(-\frac{35q_1}{8} + \frac{645q_1^2}{8} - \frac{25q_1q_2}{6} - \frac{2945q_1^3}{2} + \frac{325q_1^2q_2}{3} - \frac{35q_1q_2^2}{8} \right) + \mathcal{O}(\hbar^4, q_i^4) \\ \Pi_{B_2} &= \frac{1}{2}\log(q_1)^2 + 3\log(q_1)\log(q_2) + \frac{9}{2}\log(q_2)^2 + 10q_2 - 20q_1q_2 + 50q_1^2q_2 + \frac{5q_2^2}{2} - 30q_1q_2^2 \\ &\quad + \frac{10q_2^3}{9} + \hbar^2 \left(\frac{5q_2}{6} - \frac{25q_1q_2}{6} + \frac{5q_2^2}{6} + \frac{325q_1^2q_2}{6} - \frac{35q_1q_2^2}{4} + \frac{5q_2^3}{6} \right) + \mathcal{O}(\hbar^4, q_i^4) \end{aligned} \quad (3.134)$$

we can integrate the special geometry relation (3.80). This leads to the following instanton part of the free energies in the NS limit

$$\begin{aligned} F^{(0,0)} &= 3q_1 - 2q_2 + \left(-\frac{45q_1^2}{8} + 4q_1q_2 - \frac{q_2^2}{4} \right) + \left(\frac{244q_1^3}{9} - 10q_1^2q_2 + 3q_1q_2^2 - \frac{2q_2^3}{27} \right) + \mathcal{O}(q_i^4) \\ F^{(1,0)} &= \frac{7q_1}{8} - \frac{q_2}{6} + \left(-\frac{129q_1^2}{16} + \frac{5q_1q_2}{6} - \frac{q_2^2}{12} \right) + \left(\frac{589q_1^3}{6} - \frac{65q_1^2q_2}{6} + \frac{7q_1q_2^2}{8} - \frac{q_2^3}{18} \right) + \mathcal{O}(q_i^4) \\ F^{(2,0)} &= \frac{29q_1}{640} + \frac{q_2}{360} + \left(-\frac{207q_1^2}{64} + \frac{67q_1q_2}{1440} + \frac{q_2^2}{180} \right) + \left(\frac{18447q_1^3}{160} - \frac{263q_1^2q_2}{72} + \frac{29q_1q_2^2}{640} + \frac{q_2^3}{120} \right) + \mathcal{O}(q_i^4). \end{aligned} \quad (3.135)$$

Here we could also fix the terms which only depend on one of the q_i since we have two special geometry relations. The free energies can be compared to the ones obtained in [119].

3.3 Non-perturbative completion

In this section we want to present a recent conjecture on a non-perturbative completion of topological string theory. This conjecture was first anticipated for a special slice of the geometry of local $\mathbb{P}^1 \times \mathbb{P}^1$ from ABJM theory [24, 25] and later on refined in [26]. In subsections 3.3.1 and 3.3.2 we will review shortly the conjecture as presented in [26] and introduce the corresponding formalism. Then we will use this formalism in Subsection 3.3.5 to test the conjecture for the example of local \mathbb{F}_2 [42].

3.3.1 Quantum mechanics of spectral curves

In this subsection we introduce the connection of topological strings to quantum mechanics as presented in [26]. This is necessary to motivate and test the non-perturbative completion introduced in [26]. The topological string B-model on geometries mirror dual to non-compact local CY manifolds is based on their spectral curve (see Section 3.2 for more details). The spectral curve of a geometry X has the general

form

$$W_X(e^x, e^p) = \tilde{u}_1 + \sum_i f_i(\{\tilde{u}_l\}, \{m_k\}) e^{a_i x + b_i p} = 0 \quad (3.136)$$

where \tilde{u}_l are the normalizable moduli and m_k the non-normalizable parameters of the geometry. To associate a quantum mechanical system to each non-compact local CY we split the spectral curve into

$$W_X = O_X(x, p) + \tilde{u}_1 = 0. \quad (3.137)$$

The normalizable variable \tilde{u}_1 is then interpreted as the energy of a Hamiltonian $\tilde{u}_1 = -e^E$. With (3.136) this then leads to the Hamiltonian

$$O_X(x, p) = e^{H_X}. \quad (3.138)$$

To quantize the system we quantize the variables x , p and E and demand the canonical quantum mechanical commutation relation to hold

$$[\hat{x}, \hat{p}] = i\hbar. \quad (3.139)$$

The quantum mechanical system defined by this Hamiltonian has a discrete and positive eigenvalue spectrum as was shown in [120] and is thus a well-defined quantum system.

The inverse of the operator $\widehat{O}_X(\hat{x}, \hat{p})$ is then the density matrix of the system

$$\hat{\rho}_X = \widehat{O}_X^{-1}(\hat{x}, \hat{p}) = e^{-\widehat{H}_X}, \quad (3.140)$$

which for the case of topological strings was previously only defined for the geometry of local $\mathbb{P}^1 \times \mathbb{P}^1$ and lead to the Fermi gas formulation of topological strings [27].

From the density matrix one can calculate the *spectral traces*

$$Z_\ell = \text{tr } \hat{\rho}_X^\ell = \text{tr } e^{-\ell \widehat{H}_X} = \sum_{n=0}^{\infty} e^{-\ell E_n}, \quad \ell = 1, 2, \dots \quad (3.141)$$

3.3.2 Connecting topological strings and quantum mechanics: Spectral determinants

In this subsection we want to introduce the conjectured non-perturbative completion of the topological string as introduced in [26].

To better extract the information of the operator $\hat{\rho}_X$ we define the *spectral determinant* as

$$\Xi(\kappa, \hbar) = \det(1 + \kappa \hat{\rho}) = \prod_{n=0}^{\infty} (1 + \kappa e^{-E_n}). \quad (3.142)$$

Physically the above defined spectral determinant coincides with the grand canonical partition function of the Hamiltonian \widehat{H}_X . For more details see [26]. We can then read of the energy levels of this Hamiltonian as the zeros of $\Xi(-e^E, \hbar)$. Following the line of statistical physics we can define the grand canonical potential

$$\mathcal{J}(\mu, \hbar) = \log \Xi(\mu, \hbar). \quad (3.143)$$

Using the definition of the spectral traces (3.141) we can express the spectral determinant in terms of the spectral traces by expanding around $\kappa = e^\mu = 0$ [26]

$$\mathcal{J}(\mu, \hbar) = - \sum_{\ell=1}^{\infty} Z_{\ell} \frac{(-\kappa)^{\ell}}{\ell}. \quad (3.144)$$

From the definition of the grand canonical partition function in statistical mechanics we know that the spectral determinant can also be directly expanded around $\kappa = 0$

$$\Xi(\kappa, \hbar) = 1 + \sum_{N=1}^{\infty} Z(N, \hbar) \kappa^N. \quad (3.145)$$

Here $Z(N, \hbar)$ is the canonical partition function and N is the number of particles in the system with Hamiltonian \hat{H}_X .

By comparing the two expansions (3.144) and (3.145) we can find a relation between the spectral traces Z_{ℓ} and the canonical partition functions $Z(N, \hbar)$ [26]

$$Z(N, \hbar) = \sum_{\{m_{\ell}\}} \prod_{\ell} \frac{(-1)^{(\ell-1)m_{\ell}} Z_{\ell}^{m_{\ell}}}{m_{\ell}! \ell^{m_{\ell}}}. \quad (3.146)$$

Here the sum goes over all sets of integers $\{m_{\ell}\}$ which can satisfy the constraint

$$\sum_{\ell} \ell m_{\ell} = N. \quad (3.147)$$

The main proposal of [26] was now to conjecture the following general form of the spectral determinant for a given toric CY X (in the following we restrict to the description of genus-one spectral curves)

$$\Xi_X(\mu, m_i, \hbar) = e^{J_X(\mu, m_i, \hbar)} \Theta_X(\mu, \hbar). \quad (3.148)$$

Here $J_X(\mu, \hbar)$ denotes the *modified grand potential* and $\Theta_X(\mu, \hbar)$ is the *generalized theta function*. Let us examine these quantities in more detail.

The modified grand potential

The modified grand potential gives up to a canonical transformation the conjecture for a non-perturbative completion of the topological string free energy. As done in [26] the modified grand potential can be split into three parts

$$J_X(\mu, m_i, \hbar) = J^{(p)}(\mu_{\text{eff}}, m_i, \hbar) + J_{M2}(\mu_{\text{eff}}, m_i, \hbar) + J_{\text{WS}}(\mu_{\text{eff}}, m_i, \hbar). \quad (3.149)$$

Here the effective chemical potential μ_{eff} is defined in (3.163). $J^{(p)}(\mu, \hbar)$ gives the perturbative part of the expansion and has a similar form as the perturbative part of the free energy of topological strings [26]

$$J^{(p)}(\mu, m_i, \hbar) = \frac{C(\hbar)}{3} \mu^3 + D(m_i, \hbar) \mu^2 + B(m_i, \hbar) \mu + A(m_i, \hbar). \quad (3.150)$$

The occurring functions $C(\hbar)$ and $B(m_i, \hbar)$ can be inferred from the perturbative part of the quantum

phase space volume [26, 121]

$$\text{vol}_p(E) = 2\pi\hbar \left(C(\hbar)E^2 + B(\hbar) - \frac{\pi^2}{3}C(\hbar) \right) + \mathcal{O}(e^{-E}). \quad (3.151)$$

In general $C(\hbar)$ and $B(\hbar)$ have the form

$$C(\hbar) = \frac{C}{2\pi\hbar}, \quad (3.152)$$

$$B(\hbar) = \frac{B_0}{\hbar} + B_1\hbar. \quad (3.153)$$

Using the general forms for $C(\hbar)$ and $B(\hbar)$ we can find the lowest order contributions in \hbar to the perturbative quantum phase space volume (3.151)

$$\text{vol}_0(E) = CE^2 + 2\pi \left(B_0 - \frac{\pi}{6}C \right) + \mathcal{O}(e^{-E}), \quad (3.154)$$

$$\text{vol}_1(E) = 2\pi B_1 + \mathcal{O}(e^{-E}). \quad (3.155)$$

The function $D(m_i, \hbar)$ does not play a role in our examples. On the other hand the function $A(m_i, \hbar)$ is hard to obtain but will drop out of the quantization condition and is just a normalization of the spectral determinant. Thus for the inspection of the above conjecture it is negligible.

$J_{\text{WS}}(\mu, \hbar)$ denotes the worldsheet instanton part of the modified grand potential which has an analogous interpretation in the unrefined free energy of the topological string. It is defined by [26, 42]

$$J_{\text{WS}}(\mu, m_i, \hbar) = \sum_{g \geq 0} \sum_{\vec{d}, v} n_g^{\vec{d}} \frac{1}{v} \left(2 \sin \frac{2\pi^2 v}{\hbar} \right)^{2g-2} (-1)^{v\vec{d} \cdot \vec{K}} e^{-v\vec{d} \cdot \vec{t} \frac{2\pi}{\hbar}}. \quad (3.156)$$

Here $\vec{K} = \vec{c}$ with c_i defined in (3.161) denotes the canonical class of the geometry X and the relation between μ and t is given by (3.161) and (3.163). It is a generalization of the B-field for geometries with additional non-normalizable moduli m_i . The worldsheet instanton part of the modified grand potential only depends on the unrefined instanton numbers $n_g^{\vec{d}}$ and not on the instanton numbers in the NS limit or general refined instanton numbers.

The third part of the modified grand potential $J_{\text{M2}}(\mu_{\text{eff}}, \hbar)$ on the other hand does depend on the refined invariants. In the ABJM slice of local $\mathbb{P}^1 \times \mathbb{P}^1$ it can be interpreted as the instanton contributions coming from M2-branes in the lift of ABJM theory with coupling k to M-theory on $AdS_4 \times S_7/\mathbb{Z}_k$. From the non-perturbative completion conjectured in [25]

$$J_{\text{M2}}(\mu, \hbar) = -\frac{1}{2\pi} \frac{\partial}{\partial \lambda_s} \left(\lambda_s F_{\text{NS}}^{\text{inst}}(\vec{T}, \lambda_s) \right) \Big|_{\lambda_s = \frac{2\pi}{\hbar}}, \quad (3.157)$$

we can find the general structure of J_{M2} . We find [26]

$$J_{\text{M2}}(\mu_{\text{eff}}, m_i, \hbar) = \mu_{\text{eff}} \tilde{J}_b(\mu_{\text{eff}}, m_i, \hbar) + \tilde{J}_c(\mu_{\text{eff}}, m_i, \hbar), \quad (3.158)$$

with

$$\tilde{J}_b(\mu_{\text{eff}}, m_i, \hbar) = -\frac{1}{2\pi} \sum_{j_L, j_R} \sum_{w, \vec{d}} (\vec{c} \cdot \vec{d}) N_{j_L, j_R}^{\vec{d}} \frac{\sin \frac{\hbar w}{2} (2j_L + 1) \sin \frac{\hbar w}{2} (2j_R + 1)}{2w \sin^3 \frac{\hbar w}{2}} e^{-w\vec{d} \cdot \vec{r}}, \quad (3.159)$$

$$\begin{aligned} \tilde{J}_c(\mu_{\text{eff}}, m_i, \hbar) &= \frac{1}{2\pi} \sum_{i, j} \sum_{j_L, j_R} \sum_{w, \vec{d}} d_i \alpha_{ij} \log Q_{m_j} N_{j_L, j_R}^{\vec{d}} \frac{\sin \frac{\hbar w}{2} (2j_L + 1) \sin \frac{\hbar w}{2} (2j_R + 1)}{2w \sin^3 \frac{\hbar w}{2}} e^{-w\vec{d} \cdot \vec{r}} \\ &+ \frac{1}{2\pi} \sum_{j_L, j_R} \sum_{w, \vec{d}} \hbar^2 \frac{\partial}{\partial \hbar} \left[\frac{\sin \frac{\hbar w}{2} (2j_L + 1) \sin \frac{\hbar w}{2} (2j_R + 1)}{2\hbar w^2 \sin^3 \frac{\hbar w}{2}} \right] N_{j_L, j_R}^{\vec{d}} e^{-w\vec{d} \cdot \vec{r}}. \end{aligned} \quad (3.160)$$

Both in J_{WS} and J_{M2} the Kähler parameters t_i appear. These are the Kähler parameters in an arbitrary basis (for example fixed by the Batyrev coordinates (3.86)). They can be translated to the Kähler parameters of the normalizable and non-normalizable moduli $t_u = -\log Q_u$ and $t_{m_i} = -\log Q_{m_i}$. Our notation for the coefficients occurring in the transformation are

$$t_i = c_i \mu_{\text{eff}} - \alpha_{ij} \log Q_{m_j}. \quad (3.161)$$

Here we have already identified the proper modulus t_u of the geometry with the effective chemical potential $t_u = r\mu_{\text{eff}}$.

The effective chemical potential

In the definition of the modified grand potential occurred the effective chemical potential μ_{eff} . Let us introduce this quantity and clarify its connection to the energy and the chemical potential.

We introduced the chemical potential by $\kappa = e^\mu$. Since the spectral trace has zeros at the points

$$\kappa = -e^E, \quad (3.162)$$

we can identify $\mu = E + i\pi$.

The effective chemical potential is then defined as

$$\mu_{\text{eff}} = E_{\text{eff}} + i\pi = \mu - \frac{1}{r} \sum_{m \geq 1} (-1)^{rm} a_m(\hbar) e^{-rm\mu}. \quad (3.163)$$

Here $a_m(\hbar)$ are the coefficients appearing in the quantum A-period of the dynamical modulus of the geometry

$$-t_u = \log(u) + \sum_{m \geq 1} a_m(\hbar) u^m. \quad (3.164)$$

On the other hand r is given by the definition of the variable u in terms of \tilde{u}

$$u = \frac{1}{\tilde{u}^r}. \quad (3.165)$$

The generalized theta function

The generalized theta function $\theta_X(\mu, \hbar)$ in (3.148) is given by

$$\begin{aligned} \Theta_X(\mu, \hbar) = \sum_{n \in \mathbb{Z}} \exp \left(-4\pi^2 n^2 C(\hbar) \mu_{\text{eff}} + 2\pi i n \left(C(\hbar) \mu_{\text{eff}}^2 + B(\hbar) \right) - \frac{8\pi^3 i n^3}{3} C(\hbar) \right. \\ \left. + 2\pi i n \tilde{J}_b(\mu_{\text{eff}}, \hbar) + J_{\text{WS}}(\mu_{\text{eff}} + 2\pi i n, \hbar) - J_{\text{WS}}(\mu_{\text{eff}}, \hbar) \right). \end{aligned} \quad (3.166)$$

It is called generalized theta function since it reduces in the maximally supersymmetric case (see Sub-section 3.3.4) to a normal theta function.

3.3.3 The quantization condition

Next we will derive a non-perturbative quantization condition for the phase space volume as in [26]. This allows to test the numerical calculation of the energy levels of the Hamiltonian obtained from the spectral curve (3.138).

To derive the quantization condition we note that the energy levels of the quantum mechanical system can be obtained from the zeros of the spectral determinant (3.142). From the conjecture of [26] (3.148) we see that the zeros can only stem from the second factor Θ_X since the first one behaves as an exponential. The generalized theta function on the other hand is an oscillating function and thus has in general zeros. Using the connection between the energy of the system E and the chemical potential μ we can reformulate the generalized theta function in terms of the energy. We find [26]

$$\begin{aligned} \Theta_X(E + \pi i, \hbar) = e^\zeta \sum_{n \in \mathbb{Z}} \exp \left(-4\pi^2 \left(n + \frac{1}{2} \right)^2 C(\hbar) E_{\text{eff}} - \frac{8\pi^3 i \left(n + \frac{1}{2} \right)^3}{3} C(\hbar) + f_{\text{WS}}(E_{\text{eff}} + \pi i, n) \right. \\ \left. - \frac{1}{2} f_{\text{WS}}(E_{\text{eff}} + \pi i, -1) + 2\pi i \left(n + \frac{1}{2} \right) \left(C(\hbar) E_{\text{eff}}^2 + B(\hbar) + \tilde{J}_b(E_{\text{eff}} + \pi i, \hbar) \right) \right). \end{aligned} \quad (3.167)$$

Here we have factored out the overall factor

$$\zeta = \pi^2 C(\hbar) E_{\text{eff}} - \pi i \left(C(\hbar) E_{\text{eff}}^2 + B(\hbar) + \tilde{J}_b(E_{\text{eff}} + \pi i, \hbar) \right) + \frac{1}{2} f_{\text{WS}}(E_{\text{eff}} + \pi i, -1) + \frac{\pi^3 i C(\hbar)}{3}. \quad (3.168)$$

Additionally we have introduced the functions

$$\begin{aligned} f_{\text{WS}}(\mu, n) &= J_{\text{WS}}(\mu + 2\pi i n, \hbar) - J_{\text{WS}}(\mu, \hbar) \\ &= \sum_{v \geq 1} \sum_{g \geq 0} \sum_{\vec{d}} n_g^{\vec{d}} \frac{1}{v} \left(2 \sin \frac{2\pi^2 v}{\hbar} \right)^{2g-2} \left(e^{-4\pi^2 i v d_{i,c} n / \hbar} - 1 \right) (-1)^{v \vec{K} \cdot \vec{d}} e^{-2\pi v d_{i,c} \mu / \hbar}. \end{aligned} \quad (3.169)$$

The sum in (3.167) can be evaluated perturbatively since higher orders are exponentially suppressed. Taking only the lowest orders $n = 0, -1$ we find that (3.167) reduces to [26]

$$\Theta_X(E + \pi i, \hbar) \approx \exp \left(\zeta - \pi^2 C(\hbar) E_{\text{eff}}^2 \right) \cos(\pi \Omega(E)). \quad (3.170)$$

The occurring phase space volume $\Omega(E)$ can be split into a perturbative and a non-perturbative part

$$\Omega(E) = \Omega_p(E) + \Omega_{np}(E), \quad (3.171)$$

with

$$\begin{aligned} \Omega_p(E) &= C(\hbar)E_{\text{eff}}^2 + B(\hbar) - \frac{\pi^2}{3}C(\hbar) + \tilde{J}_b(E_{\text{eff}} + \pi i), \\ \Omega_{np}(E) &= -\frac{1}{\pi} \sum_{v \geq 1} \sum_{g \geq 0} \sum_{\vec{d}} n_g^{\vec{d}} \frac{1}{v} \left(2 \sin \frac{2\pi^2 v}{\hbar} \right)^{2g-2} \sin \frac{2\pi^2 v d_i c_i}{\hbar} (-1)^{v \vec{K} \cdot \vec{d}} e^{-2\pi v c_i d_i E_{\text{eff}} / \hbar}. \end{aligned} \quad (3.172)$$

The perturbative part can also be found from the refined topological string in the NS limit [105]. The non-perturbative part was first proposed in [24] in the case of ABJM theory by considering a generalized HMO cancelation procedure for the poles of the perturbative part for $\hbar = 2\pi n$, $n \in \mathbb{Z}$, stemming from \tilde{J}_b .

The zeros of the spectral determinant Θ_X can then be found as the zeros of the resulting cosine which are found by quantizing the non-perturbative phase space volume (3.171)

$$\Omega(E) = s + \frac{1}{2}, \quad s = 0, 1, 2, \dots \quad (3.173)$$

For a general treatment we have to include more terms in the series expansion of (3.167). This leads to a change of the non-perturbative phase space volume (3.171) [26]. Taking the additional terms into account agrees with the numerical results of [121]. Since the change in the non-perturbative phase space volume vanishes for the maximally supersymmetric case $\hbar = 2\pi$, which we will constrain ourselves to, we omit the discussion here and refer to [26].

3.3.4 The maximally supersymmetric case

In the following we will concentrate on the case $\hbar = 2\pi$ and simplify the quantization condition and the proposed expression for the spectral determinant (3.173) and (3.148) respectively. In [26, 122] this case was phrased the maximally supersymmetric case since in ABJM theory it leads to an enhancement of supersymmetry from $\mathcal{N} = 6$ to $\mathcal{N} = 8$.

Let us first analyze the simplifications occurring in the modified grand canonical potential. In (3.156) the terms with $g \geq 2$ vanish. The singular part will cancel against the singular parts of \tilde{J}_b and \tilde{J}_c in J_{M2} [26]. Calculation of the finite part leads to

$$\begin{aligned} J_{\text{WS}} &\xrightarrow{\hbar \rightarrow 2\pi} \frac{1}{8\pi^2} \sum_{i,j} (c_i \mu_{\text{eff}} - \alpha_{ik} \log Q_{m_k}) (c_j \mu_{\text{eff}} - \alpha_{jl} \log Q_{m_l}) \frac{\partial F_0^{\text{inst}}}{\partial t_i \partial t_j} \\ &\quad - \frac{1}{4\pi^2} \sum_i (c_i \mu_{\text{eff}} - \alpha_{ij} \log Q_{m_j}) \frac{\partial F_0^{\text{inst}}}{\partial t_i} + \frac{1}{4\pi^2} F_0^{\text{inst}}(t) + F_1^{\text{inst}}(t), \end{aligned} \quad (3.174)$$

with the instanton parts of the free energy

$$F_0^{\text{inst}}(\vec{t}) = \sum_{w, \vec{d} \geq 1} n^{\vec{d}_0} \frac{(-1)^{w \vec{d} \cdot \vec{K}}}{w^3} e^{-w \vec{d} \cdot \vec{t}}, \quad F_1^{\text{inst}}(t) = \sum_{w, \vec{d} \geq 1} \left(\frac{n_0^{\vec{d}}}{12} + n_1^{\vec{d}} \right) \frac{(-1)^{w \vec{d} \cdot \vec{K}}}{w} e^{-w \vec{d} \cdot \vec{t}}. \quad (3.175)$$

Looking at the non-perturbative part coming from M2-branes (3.158) we observe that the finite con-

tribution of \tilde{J}_b (3.159) vanishes for $\hbar \rightarrow 2\pi$ [26]. The part coming from \tilde{J}_c (3.160) can be expressed by the instanton part of the free energy in the NS limit [26]

$$\begin{aligned}\tilde{J}_b(\mu_{\text{eff}}, m_i, \hbar) &\xrightarrow{\hbar \rightarrow 2\pi} 0 \\ \tilde{J}_c(\mu_{\text{eff}}, m_i, \hbar) &\xrightarrow{\hbar \rightarrow 2\pi} F_1^{\text{NS, inst}}(\vec{t} + i\pi).\end{aligned}\quad (3.176)$$

In total we then find for the modified grand potential in the maximally supersymmetric case

$$\begin{aligned}J_X(\mu, \hbar = 2\pi) &= J^{(p)}(\mu_{\text{eff}}, 2\pi) + \frac{1}{8\pi^2} \sum_{i,j} (c_i \mu_{\text{eff}} - \alpha_{ik} \log Q_{m_k}) (c_j \mu_{\text{eff}} - \alpha_{jl} \log Q_{m_l}) \frac{\partial F_0^{\text{inst}}}{\partial t_i \partial t_j} \\ &\quad - \frac{1}{4\pi^2} \sum_i (c_i \mu_{\text{eff}} - \alpha_{ij} \log Q_{m_j}) \frac{\partial F_0^{\text{inst}}}{\partial t_i} + \frac{1}{4\pi^2} F_0^{\text{inst}}(t) + F_1^{\text{inst}}(t) + F_1^{\text{NS, inst}}(t).\end{aligned}\quad (3.177)$$

Next we have a more detailed look at the generalized theta function (3.166). Using (3.161) and the results obtained above for J_{WS} and \tilde{J}_b we observe that it can be brought to the form [26]

$$\Theta_X(\mu, 2\pi) = \sum_{n \in \mathbb{Z}} \exp\left(\frac{\pi i n^2 r^2}{4} \tau + 2\pi i n (\xi + B(2\pi)) - \frac{2\pi i n^3 C}{3}\right), \quad (3.178)$$

with

$$\begin{aligned}\tau &= \frac{2i}{\pi} \partial_t^2 F_0(t), \\ \xi &= \frac{r}{4\pi^2} (t \partial_t^2 F_0(t) - \partial_t F_0(t)).\end{aligned}\quad (3.179)$$

In the whole we then find the quantization condition [42]

$$\begin{aligned}CE_{\text{eff}}^2 + 4\pi^2 B(2\pi) - \frac{\pi^2 C}{3} - \sum_i c_i \frac{\partial F_0^{\text{inst}}}{\partial t_i} + E_{\text{eff}} \sum_{i,j} c_i c_j \frac{\partial F_0^{\text{inst}}}{\partial t_i \partial t_j} - \sum_{i,j,k} c_k \alpha_{ij} \log Q_{m_j} \frac{\partial^2 F_0^{\text{inst}}}{\partial t_i \partial t_k} \\ = 4\pi^2 \left(s + \frac{1}{2}\right), \quad s = 0, 1, 2, \dots\end{aligned}\quad (3.180)$$

3.3.5 Example: local \mathbb{F}_2

In the following we want to discuss the non-perturbative corrections proposed in the last subsection for an explicit example. We will consider the example of local \mathbb{F}_2 . The quantum periods and free energies in the NS limit for this geometry are calculated in Subsection 3.2.4. For this discussion it is useful to take another parametrization of the spectral curve which takes a similar form as in [26]. A convenient choice is

$$W_X(e^x, e^p) = e^x + m e^{-x} + e^p + m^{-2} e^{-p+2x} - e^E, \quad (3.181)$$

where we introduced $u = e^{-2E}$. This translates to the Hamilton operator

$$\hat{H}_X = \log\left(e^x + m e^{-x} + e^p + m^{-2} e^{-p+2x}\right). \quad (3.182)$$

Calculating the constants

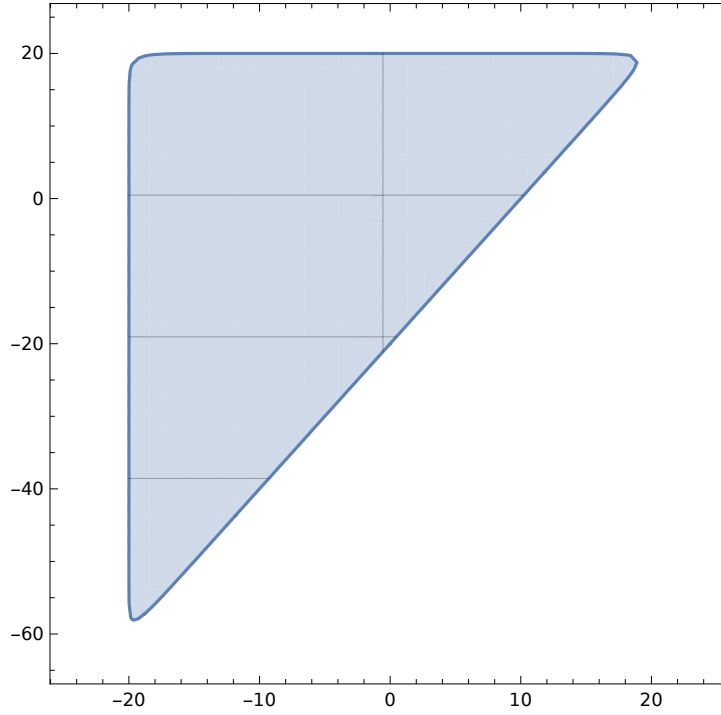


Figure 3.4: The phase space of the operator (3.182) for $E = 20$ and $m = 1$ in the $x - p$ plane. The associated toric diagram is up to an $SL(2, \mathbb{Z})$ transformation identical to polyhedron F_{13} in Figure 2.2 which is the dual polytope of the toric diagram of \mathbb{F}_2 .

We begin the discussion by first calculating the constants C , B_0 and B_1 of the perturbative part of the grand potential (3.149). In this course we follow the discussion in [26, 121].

To find the constants C , B_0 and B_1 we calculate the quantum phase space volume of local \mathbb{F}_2 analogous to the calculation in [121] for \mathbb{P}^2 . In Figure 3.4 we have depicted the phase space for the fixed values $E = 20$ and $m = 1$ numerically. In order to find it in general we solve the spectral curve (3.181) for p and find the two solutions

$$p^\pm = \log \left(e^E \frac{1 - e^{x-E} - me^{-x-E} \pm \sqrt{(1 - e^{x-E} - me^{-x-E})^2 - 4m^{-2}e^{2x-2E}}}{2} \right). \quad (3.183)$$

The two curves intersect at the zeros of the discriminant of the square root

$$\Delta_{\text{root}} = (1 - e^{x-E} - me^{-x-E})^2 - 4m^{-2}e^{2x-2E}. \quad (3.184)$$

The area which is enclosed by the two curves gives the phase space volume for energies smaller than E . To calculate its classical part we solve $\Delta_{\text{root}} = 0$ neglecting instanton contributions $O(e^{-E})$. We find the two solutions

$$x^- = -E + \log m, \quad x^+ = E + \log(m) - \log(m + 2), \quad (3.185)$$

which give the range of integration for the calculation of the phase space volume. We then find for the

zeroth order phase space volume

$$\begin{aligned}
 \text{vol}_0(E) &= \int_{x^-}^{x^+} (p^+(x) - p^-(x)) dx \\
 &= 4E^2 - \log^2(m+2) - \frac{\pi^2}{3} \\
 &\quad + \int_0^{m/(m+2)} \frac{2}{u} \log \frac{1-u + \sqrt{(1-u)^2 - 4m^{-2}u^2}}{2} du + \mathcal{O}(e^{-E}).
 \end{aligned} \tag{3.186}$$

Here we used an intermediate value x_0 with $-2x_0 + 2E \sim E \sim E - x_0$ as in [121] to split up the integral. This can be evaluated via comparison with the quite similar geometry of local \mathbb{F}_0 [42] and we find

$$\text{vol}_0(E) = 4E^2 - \frac{2}{3}\pi^2 - \left(\log \frac{m \pm \sqrt{m^2 - 4}}{2} \right)^2 + \mathcal{O}(e^{-E}). \tag{3.187}$$

Comparing to (3.154) we find the constants

$$C = 4, \quad B_0 = \frac{\pi}{3} - \frac{1}{2\pi} \log^2 \left(\frac{m + \sqrt{m^2 - 4}}{2} \right). \tag{3.188}$$

Since the phase space volume equals a linear combination of the B-periods we can use the quantum operators in (3.118) to calculate the higher order corrections in \hbar [26, 121]. Translating the first operator in (3.118) to the energy variable using $u = e^{-2E}$ we find up to instanton corrections $\mathcal{O}(e^{-E})$

$$\text{Leading}(\text{vol}_1)(E) = -\frac{1}{48} \partial_E^2 \text{Leading}(\text{vol}_0)(E). \tag{3.189}$$

Thus we find for the leading order of vol_1

$$\text{vol}_1(E) = -\frac{1}{24} C + \mathcal{O}(e^{-E}). \tag{3.190}$$

Comparing with (3.155) we can read off

$$B_1 = -\frac{1}{12\pi}. \tag{3.191}$$

Numerical calculation

To numerically calculate the energies E_n of the operator (3.181) we use the method described in [121].

The idea is to take an orthonormal basis of L^2 functions and calculate the matrix elements of the Hamilton operator. Since the functions are in general not the eigenfunctions of the operator the resulting matrix will not be diagonal. By diagonalizing the matrix we obtain the eigenfunctions expressed in terms of the basis as well as the eigenvalues. Since in practice we can only choose a finite subset of the infinite set of basis functions the eigenfunctions and eigenvalues are not exact. Nevertheless the accuracy increases with the number of basis functions [26].

In particular we take as a basis for the space of functions the eigenfunctions of the harmonic oscillator

with mass m_0 and frequency ω_0 [121]

$$\psi_n(x) = \frac{1}{\sqrt{2^n n!}} \left(\frac{m_0 \omega_0}{\pi \hbar} \right)^{\frac{1}{4}} e^{-\frac{m_0 \omega_0 x^2}{2\hbar}} H_n \left(\sqrt{\frac{m_0 \omega_0}{\hbar}} x \right). \quad (3.192)$$

Here $H_n(x)$ are the Hermite polynomials. The obtained numerical values are independent of the chosen values for m_0 and ω_0 . We choose $m_0 \omega_0 = 1$. We find the numerical values for local \mathbb{F}_2 given in Tables 3.5, 3.6 and 3.7 for $m = 1$, $m = 2$ and $m = \frac{5}{2}$ respectively and the maximal supersymmetric case $\hbar = 2\pi$. To improve the numerical efficiency we performed a symplectic transformation in x and p to symmetrize the Hamiltonian.

matrix size	E_0	E_1	E_2
460	2.82859221870841 ...	4.22189119858874 ...	5.2621635156509 ...
480	2.82859221870830 ...	4.22189119858845 ...	5.2621635156502 ...
500	2.82859221870824 ...	4.22189119858831 ...	5.2621635156498 ...

Table 3.5: Numerical energy spectrum for the operator of local \mathbb{F}_2 in (3.181) for $m = 1$ and $\hbar = 2\pi$. Here we give the values for three different matrix sizes in order to find the numerical precision.

matrix size	E_0	E_1	E_2
460	2.88181542992648 ...	4.25459152858252 ...	5.28819530714533 ...
480	2.88181542992638 ...	4.25459152858225 ...	5.28819530714475 ...
500	2.88181542992634 ...	4.25459152858212 ...	5.28819530714446 ...

Table 3.6: Numerical energy spectrum for the operator of local \mathbb{F}_2 in (3.181) for $m = 2$ and $\hbar = 2\pi$. Here we give the values for three different matrix sizes in order to find the numerical precision.

matrix size	E_0	E_1	E_2
460	2.90483664037330 ...	4.26884642187458 ...	5.29956136206400 ...
480	2.90483664037321 ...	4.26884642187432 ...	5.29956136206343 ...
500	2.90483664037316 ...	4.26884642187420 ...	5.29956136206316 ...

Table 3.7: Numerical energy spectrum for the operator of local \mathbb{F}_2 in (3.181) for $m = \frac{5}{2}$ and $\hbar = 2\pi$. Here we give the values for three different matrix sizes in order to find the numerical precision.

From (3.141) we can then calculate numerically the spectral traces and using (3.146) we can translate these to the first canonical partition functions $Z(N, \hbar)$. We find [42]

$$\begin{aligned} Z(1, 2\pi) &= \frac{\sqrt{2}}{16} - m \left(\frac{1}{8\sqrt{2}\pi} - \frac{1}{32\sqrt{2}} \right) \\ Z(2, 2\pi) &= \frac{3}{256} - \frac{1}{32\pi}. \end{aligned} \quad (3.193)$$

Analytical calculation of energy levels

To analytically calculate the energy spectrum of the operator (3.182) we need to use the quantization condition (3.173). In the maximally supersymmetric case with $\hbar = 2\pi$ this translates into (3.180). To specify this for the case of local \mathbb{F}_2 we observe from (3.122) and (3.123) that

$$t_1 = 2t_u - \frac{1}{2} \log(Q_2), \quad t_2 = -\log(Q_2). \quad (3.194)$$

From these equations and (3.161) we can read off the nonzero constants α_{ij} and c_i for local \mathbb{F}_2

$$c_1 = 2, \quad c_2 = 0, \quad \alpha_{12} = -\frac{1}{2}, \quad \alpha_{22} = 1. \quad (3.195)$$

This leads to the quantization condition

$$\begin{aligned} 4E_{\text{eff}}^2 - \frac{4\pi^2}{3} - \log^2 \left[\frac{m + \sqrt{m^2 - 4}}{2} \right] - 2 \frac{\partial F_0^{\text{inst}}}{\partial t_1} + 4E_{\text{eff}} \frac{\partial^2 F_0^{\text{inst}}}{\partial t_1^2} - 2 \log Q_2 \left(\frac{\partial^2 F_0^{\text{inst}}}{\partial t_1 \partial t_2} - \frac{1}{2} \frac{\partial^2 F_0^{\text{inst}}}{\partial t_1^2} \right) \\ = 4\pi^2 \left(s + \frac{1}{2} \right), \quad s = 0, 1, 2, \dots \end{aligned} \quad (3.196)$$

Where we have to plug in $t_i \rightarrow c_i E_{\text{eff}} + c_i \pi i - \alpha_{ij} \log Q_{m_j}$. Here the effective energy can be calculated via (3.163). The needed prepotential part of the free energy F_0^{inst} is the free energy $F^{0,0}$ and can be constructed from the instanton numbers in Table 3.3. Additionally we need the classical A-period of \mathbb{F}_2 which can be obtained from (3.119) by setting $\hbar = 0$.

After using that fixing a value for m also fixes a value for Q_2 via (3.122) we find the lowest energy levels listed in Table 3.8.

Degree	$E_0(m=1)$	$E_0(m=2)$	$E_0\left(m=\frac{5}{2}\right)$
1	2.82843403020660...	2.88162738944221...	2.90462518397322...
4	2.82859221734474...	2.88181542693385...	2.90483663616878...
7	2.82859221870816...	2.88181542992617...	2.90483664037291...
10	2.82859221870819...	2.88181542992629...	2.90483664037312...
Numerical value	2.82859221870824...	2.88181542992634...	2.90483664037316...

Table 3.8: First energy levels calculated analytically from the quantization condition (3.196). We use $\hbar = 2\pi$ and $m = 1$, $m = 2$ and $m = \frac{5}{2}$. The degree denotes the order of expansion for the periods and the free energy. The numerical values were given in Table 3.5, 3.6 and 3.7 for a matrix size of 500.

Analytical calculation of the spectral determinant

Next we want to check the proposal of [26] for the spectral determinant in more detail. For this we calculate the spectral determinant (3.148) analytically. By a series expansion we can then extract the partition functions $Z(N, \hbar)$ and compare to the numerical values. We will again only consider the maximal supersymmetric case $\hbar = 2\pi$.

To obtain the spectral determinant (3.148) we have to calculate the grand potential $J_X(\mu, \hbar)$ and the generalized theta function $\theta_X(\mu, \hbar)$. The spectral determinant has to be expanded around $\kappa = 0$ to find the canonical partition functions (3.145). Due to the relation $\kappa \sim e^E$ the expansion leads us for $m = 0$ to

the \mathbb{Z}_4 orbifold point of local \mathbb{F}_2 . This means that we need the periods and free energies around the \mathbb{Z}_4 orbifold point. To do the analytic continuation we use the exact representation of the derivatives of the periods in terms of elliptic integrals [123]

$$\frac{\partial t}{\partial u} = -\frac{2}{\pi u \sqrt{1-4(2+m)u}} K\left(\frac{16u}{4(2+m)u-1}\right) \quad (3.197)$$

$$\frac{\partial^2 F_0}{\partial u \partial t} = -\frac{2}{u \sqrt{1-4(m-2)u}} K\left(\frac{4(m+2)u-1}{4(m-2)u-1}\right). \quad (3.198)$$

Then we analytically continue to the orbifold coordinates \tilde{v} and \tilde{m}

$$u = -i\frac{1}{\tilde{v}^2}, \quad m = i\tilde{m}. \quad (3.199)$$

Here we did not only go to the orbifold point at $\frac{1}{u^2}$ but also included a rotation around $e^{-ir\theta\pi}$ with $\theta = \frac{1}{4}$. The reason for the rotation is as in [26] to circumvent a conifold point in the moduli space. The rotation angle $\theta = \frac{1}{4}$ is chosen such that the prepotential is real near the orbifold point [42] which simplifies the calculations. This rotation also requires a rotation in the other quantities: Namely due to $u = e^{-r\mu}$ we find $\mu = \tilde{\mu} + \theta\pi i$ and similar for μ_{eff} . Also $t = \tilde{t} + r\theta\pi i$. The rotated free energies are defined to be equal to their previous values

$$\begin{aligned} \tilde{F}_0^{\text{inst}}(\tilde{t}) &:= F_0^{\text{inst}}(t) = F_0^{\text{inst}}(\tilde{t} + r\theta\pi i) \\ \tilde{F}_1^{\text{inst}}(\tilde{t}) + \tilde{F}_1^{\text{NS, inst}}(\tilde{t}) &:= F_1^{\text{inst}}(t) + F_1^{\text{NS, inst}}(t) = F_1^{\text{inst}}(\tilde{t} + r\theta\pi i) + F_1^{\text{NS, inst}}(\tilde{t} + r\theta\pi i). \end{aligned} \quad (3.200)$$

We then find the orbifold periods to be

$$\begin{aligned} \frac{\partial \tilde{t}}{\partial \tilde{v}} &= -\frac{4i}{\pi} \left(\frac{K\left(\frac{4i(2+i\tilde{m})+\tilde{v}^2}{4i(-2+i\tilde{m})+\tilde{v}^2}\right)}{\sqrt{4i(-2+i\tilde{m})+\tilde{v}^2}} - \frac{K\left(\frac{4i(-2+i\tilde{m})+\tilde{v}^2}{4i(2+i\tilde{m})+\tilde{v}^2}\right)}{\sqrt{4i(2+i\tilde{m})+\tilde{v}^2}} \right) \\ \frac{\partial \tilde{t}_D}{\partial \tilde{v}} &= 2 \left(\frac{K\left(\frac{4i(2+i\tilde{m})+\tilde{v}^2}{4i(-2+i\tilde{m})+\tilde{v}^2}\right)}{\sqrt{4i(-2+i\tilde{m})+\tilde{v}^2}} + \frac{K\left(\frac{4i(-2+i\tilde{m})+\tilde{v}^2}{4i(2+i\tilde{m})+\tilde{v}^2}\right)}{\sqrt{4i(2+i\tilde{m})+\tilde{v}^2}} \right). \end{aligned} \quad (3.201)$$

Here we continued the elliptic integrals via the formula

$$\frac{K\left(\frac{1+4i(i\tilde{m}+2)\tilde{u}}{1+4i(i\tilde{m}-2)\tilde{u}}\right)}{\sqrt{1+4i(i\tilde{m}-2)\tilde{u}}} = \frac{K\left(\frac{1+4i(i\tilde{m}-2)\tilde{u}}{1+4i(i\tilde{m}+2)\tilde{u}}\right)}{\sqrt{1+4i(i\tilde{m}+2)\tilde{u}}} + i \frac{K\left(\frac{16i\tilde{u}}{1+4i(i\tilde{m}+2)\tilde{u}}\right)}{\sqrt{1+4i(i\tilde{m}+2)\tilde{u}}}. \quad (3.202)$$

These periods can then be combined to the flat coordinates at the \mathbb{Z}_4 orbifold point and compared to the results in [123]. Here we just want to do an analytic continuation and keep the large radius flat coordinates. Thus we want to calculate exactly the large radius periods at the orbifold point.

To do this we additionally need to consider potential constant terms in \tilde{v} which can arise after integrating (3.201). We can find these pure \tilde{m} terms by calculating the periods numerically before and after the analytic continuation and comparing them at an intermediate point. We find that the periods at the orbifold point \tilde{t}^{orb} and \tilde{t}_D^{orb} obtained by integrating (3.201) differ from the rotated large radius coordinates

by

$$\begin{aligned}\tilde{r}^{\text{orb}} &= \tilde{t} + \log\left(\frac{\tilde{m} + \sqrt{\tilde{m}^2 + 4}}{2}\right) \\ \tilde{t}_D^{\text{orb}} &= \tilde{t}_D + \frac{\pi^2}{6} - \frac{1}{2}\left(\log\frac{\tilde{m} + \sqrt{\tilde{m}^2 + 4}}{2}\right)^2.\end{aligned}\tag{3.203}$$

Appart from the periods and the prepotential we need in the maximal supersymmetric case the free energies at genus one F_1 and F_1^{NS} . These can be calculated via the exact formulas [102]

$$\begin{aligned}F_1 &= -\frac{1}{2}\log\left(G_{u\bar{u}}|\Delta u^{a_0}\prod_i m_i^{a_i}\right)^{\frac{1}{3}} \\ F_1^{\text{NS}} &= \frac{1}{24}\log(\Delta u^{b_0}\prod_i m_i^{b_i}),\end{aligned}\tag{3.204}$$

where the powers a_0 , b_0 , a_i and b_i can be fixed by constant genus-one maps and requiring regularity at infinity. Δ denotes the discriminant of the geometry which can be calculated from the elliptic functions given in (3.116).

The phase rotation (3.199) also affects the generalized theta function $\theta(\mu, 2\pi)$ as described in [26, 42] by a shift in the summation index and an extra prefactor. This prefactor exactly cancels the change of the grand potential under the phase rotation (3.199) as in [26]. Neglecting the prefactor the two functions can then be simplified to

$$\begin{aligned}\tilde{J}_X(\tilde{\mu}, 2\pi) &= A(2\pi) + \frac{B(2\pi)}{r}\tilde{t} + \tilde{F}_1 + \tilde{F}_1^{\text{NS}} + \frac{\tilde{F}_0(\tilde{t}, \tilde{m})}{4\pi^2} - \frac{1}{4\pi^2}\left(\tilde{t}\frac{\partial}{\partial\tilde{t}} - e^{-r\theta\pi i}\pi\frac{\partial}{\partial\tilde{m}}\right)\tilde{F}_0(\tilde{t}, \tilde{m}) \\ &\quad + \frac{1}{8\pi^2}\left(\tilde{t}^2\frac{\partial^2}{\partial\tilde{t}^2} - e^{-r\theta\pi i}2\pi\tilde{t}\frac{\partial^2}{\partial\tilde{m}\partial\tilde{t}} + e^{-2r\theta\pi i}\pi^2\frac{\partial^2}{\partial\tilde{m}^2}\right)\tilde{F}_0(\tilde{t}, \tilde{m})\end{aligned}\tag{3.205}$$

$$\tilde{\Theta}(\tilde{\mu}, 2\pi) = \sum_{n \in \mathbb{Z}} \exp\left(\pi i(n + \frac{\theta}{2})^2 \tilde{\tau} + 2\pi i(n + \frac{\theta}{2})(\tilde{\xi} + B(2\pi)) - \frac{2\pi i}{3}(n + \frac{\theta}{2})^3 C\right),\tag{3.206}$$

with

$$\begin{aligned}\tilde{\tau} &= \frac{r^2}{4}\left(\frac{2i}{\pi}\frac{\partial^2}{\partial\tilde{t}^2}\tilde{F}_0(\tilde{t}, \tilde{m})\right) \\ \tilde{\xi} &= \frac{r}{4\pi^2}\left(\tilde{t}\frac{\partial^2}{\partial\tilde{t}^2}\tilde{F}_0(\tilde{t}, \tilde{m}) - \frac{\partial}{\partial\tilde{t}}\tilde{F}_0(\tilde{t}, \tilde{m}) - e^{-r\theta\pi i}\pi\frac{\partial^2\tilde{F}_0(\tilde{t}, \tilde{m})}{\partial\tilde{m}\partial\tilde{t}}\right).\end{aligned}\tag{3.207}$$

As a crosscheck we calculate that the elliptic j -invariant (3.92) is one at the orbifold point $m = 0$, $u \rightarrow \infty$. This leads to $\tau = i$ which is consistent with $\tilde{\tau} = i$ at the orbifold point.

The spectral determinant is then given by the product

$$\Xi(\mu, 2\pi) = e^{\tilde{J}_X(\tilde{\mu}, 2\pi)}\tilde{\Theta}(\tilde{\mu}, 2\pi).\tag{3.208}$$

Due to the rotation we find for the expansion of the spectral determinant (3.145) the rotated expansion

$$\Xi(\tilde{v}, \hbar) = e^{\tilde{J}_X(\tilde{\mu}, 2\pi)} \tilde{\Theta}(\tilde{\mu}, 2\pi) = 1 + \sum_{N \geq 1} Z(N, \hbar) e^{\frac{N\pi i}{4}} \tilde{v}^N. \quad (3.209)$$

Expanding the spectral determinant we then extract with $m = 0$ the values

$$Z(1, 2\pi) = \frac{\sqrt{2}}{16}, \quad Z(2, 2\pi) = \frac{3}{256} - \frac{1}{32\pi}, \quad (3.210)$$

which agree with the numerical values in (3.193).

Conclusion

In this thesis we have discussed two examples of non-perturbative physics where elliptic curves played a central role. In Chapter 2 we first discussed F-theory. We constructed two explicit compactification manifolds from a general base with the fiber being a hypersurface in a two dimensional toric variety. After finding the standard model and the Pati-Salam model as the complete gauge group calculated from the MW group and the codimension one singularities we also found the codimension two singularities giving the matter content and the codimension three singularities leading to Yukawa couplings in compactifications to four dimensions. Subsequently we have chosen the base \mathbb{P}^3 for compactifications to four dimensions and constructed the vertical G_4 flux. By imposing a family structure, D3-brane tadpole cancelation as well as integrality of the CS terms we found that the minimal amount of families is in each case three.

The two discussed examples are connected via a Higgsing which is reflected on the geometry side by a conifold transition. We generalized this to a complete network of all effective field theories stemming from compactifications where the fiber is a hypersurface in one of the 16 two dimensional toric fano varieties shown in Figure 2.2. This network led to interesting observations. For example we gave a prescription to calculate the charge transformations of the Higgsing from the geometry of the fiber. Additionally we have discussed different but equivalent Higgsings mediated by a vev in different representations (in the discussed example we had the two multiplets $(\mathbf{1}, \mathbf{2}, \mathbf{4})$ and $(\mathbf{2}, \mathbf{1}, \mathbf{4})$). The different equivalent Higgsings led to the necessity of a redefinition of the bundle structure. Last but not least we have found that the complete network of effective field theories as displayed in Figure 2.11 is mirror symmetric with respect to gauge groups with rank three. Together with the identification of discrete symmetries by Higgsing continuous symmetries this has led us to the conjecture that MW torsion and the TS group describing the discrete symmetries are mirror dual to each other.

We then discussed the occurrence of discrete symmetries in more detail in the example of X_{F_1} . First we discussed the gauge symmetries and spectrum of X_{F_3} which can subsequently be Higgsed to X_{F_1} . In the geometry of X_{F_3} we found a non-toric rational section leading to the first explicit example of a singlet with charge three. After completing the discussion of X_{F_3} by constructing the G_4 flux for a compactification to four dimensions with base \mathbb{P}^3 we have used the charge three singlet to Higgs to the geometry X_{F_1} . Since the singlet obtaining a vev is of non-minimal charge, this led to a discrete \mathbb{Z}_3 symmetry in X_{F_1} which is reflected on the geometry side by the non-existence of a rational section and the existence of a three-section. In [36] the occurrence of the \mathbb{Z}_3 TS group from the Higgsing was shown explicitly. We have then computed the matter content in a compactification to six dimensions. After finding a “discrete Shioda map” we commented on subtleties occurring in the comparison with the field content from the Higgsing process.

As a second example of non-perturbative physics from elliptic curves we discussed in Chapter 3 a possible non-perturbative completion of topological string theory. Since the proposal of [24–26] includes the periods of the geometries in the NS limit we first discussed a way of calculating the so-called

quantum periods. From a WKB expansion of brane wavefunctions we defined a quantum differential on the Riemann surface of the B-model geometry. This can in principle be integrated around the cycles of the respective geometry to obtain the quantum periods. Because the integration around the cycles is highly complicated we have circumvented this calculation by finding quantum operators which sent the classical differential to the quantum differential up to exact forms. From the examples studied so far we found that the operators are second order differential operators in the normalizable moduli u . Thus they are exact on the level of the periods. As a check for the quantum periods we used special geometry in the refined case to calculate the free energy in the NS limit. We then gave the first order operators, quantum periods and free energies for the examples of local \mathbb{F}_1 , local \mathbb{F}_2 and the resolution of $\mathbb{C}^3/\mathbb{Z}_5$.

Next we discussed the proposed non-perturbative completion for topological string theory. The proposal is based on defining a quantum mechanical problem from the spectral curve of the B-model geometry. From the proposed form of the spectral determinant as a product of a generalized theta function and the exponential of the modified grand potential we derived a non-perturbative phase space quantization condition. We have tested this quantization condition for the geometry of local \mathbb{F}_2 in the case of $\hbar = 2\pi$.

Outlook

The results obtained in this thesis are the starting point for a number of interesting questions. One possible future direction of research starting from our results in F-theory is related to model building. One can use tops to construct further non-Abelian gauge symmetries additional to the symmetries we already found. For example the discussion in [124] could be combined with one of the polytopes F_1 , F_2 or F_4 to obtain the standard model gauge group with an additional discrete gauge symmetry. The additional discrete gauge symmetry might then for example be able to forbid proton decay operators.

A second line of research is based on the conjectured duality of MW torsion and discrete symmetries. We conjectured this duality on the basis of three examples. In [89] another example for this duality was found. Based on the calculation of torsional groups for complete intersection fibers in [89] one could try to check this duality in more cases.

If the conjecture turns out to be true this would not only connect discrete symmetry and MW torsion. Since discrete symmetries in theories of quantum gravity are always remnants of continuous symmetries the duality also connects MW torsion with multiplets of corresponding non-minimal charge. By classifying the possible MW torsions for elliptic fibrations analogous to Mazur's Lemma for elliptic curves [48] this would also allow a classification of non-minimal charges analogous to the classification of non-Abelian gauge symmetries by Kodaira.

From a phenomenological point of view the duality allows a more systematic construction of discrete symmetries by constructing elliptic curves with a given MW torsion as in [54]. The problem in this explicit application of the duality is the application of mirror symmetry on a family of tori since we fiber a family of tori over the base and need to find the fibration of the dual family over the same base.

In the calculation of quantum periods we used second order differential operators in the normalizable moduli u to calculate the corrections to the classical periods of the geometry. Here arises the question if one can prove that the operators are in general of this form. Therefore a proof that the exact forms which need to be added in the derivation of the quantum operators (see Appendix A.3) are of the form given in (A.17) would be helpful. Insights in this directions could also lead to a way of calculating the quantum operators directly from the elliptic parameters of the spectral curve of the geometry. Another interesting idea is if one can find an extended PF system which directly computes the quantum periods.

Concerning the non-perturbative completion of topological string theory proposed by [24–26] there are the following open questions. First of all the conjecture needs to be checked for other geometries as for example the local geometries constructed from the Hirzebruch surfaces or the del Pezzo surfaces.

These checks must also include calculations away from the maximal supersymmetric case $\hbar = 2\pi$ since at other points in \hbar additional corrections do appear as first found in [121]. The proposed form of these terms [26] also needs to be checked.

A second point is the relation to other propositions of non-perturbative completions of topological string theory. It seems that the proposal from [125] is equivalent to the proposal discussed in this thesis. In contrast the relation to the proposal of [3, 4] is unclear. In [3] the holomorphic anomaly equation was brought to a form such that it can be solved with a trans-series ansatz instead of a series ansatz. This allowed to use resurgence methods to calculate the higher instanton sectors.

Last but not least from the topological string point of view there is no conceptual problem in going to higher genus spectral curves. This can be directly seen from the calculation of the free energies in the NS limit of the resolution of $\mathbb{C}^3/\mathbb{Z}^5$ in this thesis or the discussion in [119]. Nevertheless the interpretation in terms of the discussion of [26] is unclear. For the case of a genus two spectral curve one has two normalizable moduli u_1 and u_2 which need to be interpreted according to [26] as energies. This would probably also lead to two phase space quantization conditions. In the moment the generalization is unclear.

A.1 Addition law on elliptic curves

In this appendix we want to define an addition law for rational or marked points on elliptic curves \mathcal{E} . The addition law is important since it is an important ingredient in the definition of elliptic curves and the MW group which gives the Abelian gauge group in F-theory.

To define an addition law which has a group structure for rational points on elliptic curves we first introduce the *chord-tangent* composition law.

A rational line intersects the cubic rational curve in three points. If two of these are rational then the third intersection point is also rational [48]. Using this one assigns to the two rational points P and Q of the rational curve \mathcal{E} the third intersection point (PQ) of the line through P and Q with \mathcal{E} , see Figure A.1 for an illustration with a real curve. One obviously sees that this composition law is commutative. But

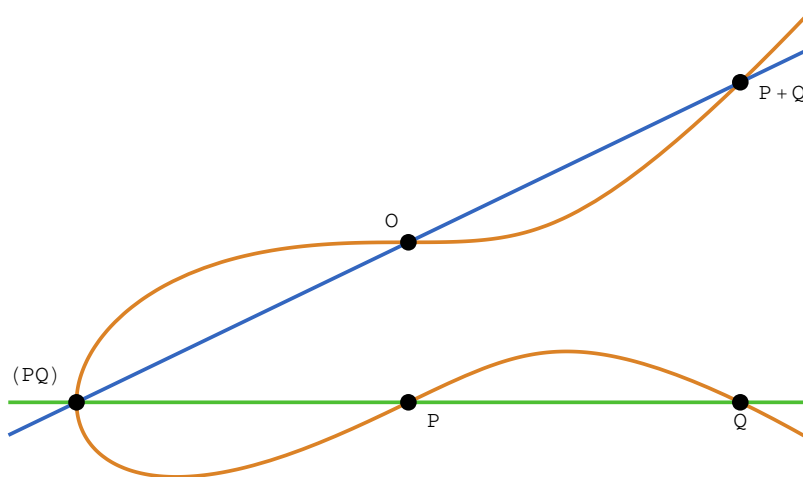


Figure A.1: Example of an elliptic curve over the field \mathbb{R} with zero point O . The third rational intersection point of the green line intersecting the curve \mathcal{E} at the rational points P and Q is the chord-tangent composition (PQ) . The third intersection point of the blue line through the composed rational point (PQ) and the zero point O with the elliptic curve \mathcal{E} gives the added point $P + Q$.

it does not have a neutral element and thus does not define a group.

The group law then uses the chord-tangent composition law and an additional rational point O as the zero point. It is defined by the third intersection point of the line through the zero point O and the

composed point (PQ)

$$P + Q = O(PQ). \tag{A.1}$$

For a better demonstration of this see Figure A.1 where we have used a curve over the field \mathbb{R} .

The addition law defined in (A.1) has the neutral element O . This can be seen since the third intersection point of the line through O and (OP) is again P , see Figure A.2. To construct the inverse element $(-P)$ we need the tangent at the zero point. The second intersection point of this tangent gives the point (OO) . The inverse element $(-P)$ is then given as the third intersection point of the line through P and (OO) with the elliptic curve \mathcal{E} . We then have that $(P(-P))$ is (OO) and the third intersection point of the line through (OO) and O is O since the line has a double intersection with the elliptic curve \mathcal{E} at O . For an example see Figure A.2.

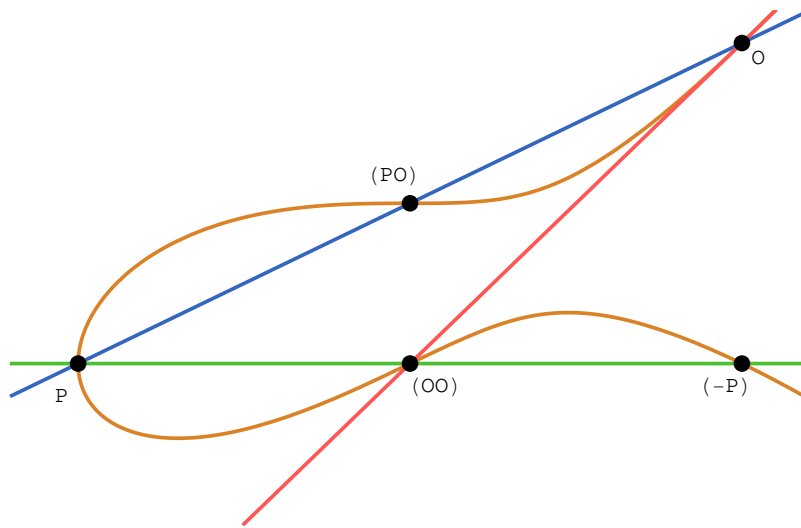


Figure A.2: Illustration of the inverse element $(-P)$ and the neutral element O of an elliptic curve \mathcal{E} with zero point O . The inverse element $(-P)$ is constructed as the third intersection point of the line through (OO) and P with the elliptic curve \mathcal{E} (green line). The point (OO) in this construction is the second intersection point of the tangent to the elliptic curve at the zero point O with the elliptic curve \mathcal{E} (red line). The composition of the point P with the neutral element O under the chord-tangent composition law leads to the point (PO) (blue line).

We omit here the explicit prove of associativity and refer to text books as for example [48].

A.2 Nagell algorithm

In this appendix we want to discuss the Nagell algorithm. With the Nagell algorithm one can calculate the Weierstrass or Tate form of an irreducible nonsingular cubic curve C in \mathbb{P}^2 . For the algorithm to work one needs a rational point. We will follow the discussion in [37, 49].

Let us first explain the basic idea before diving into the details. The basic idea of the algorithm [37] is to take all lines through a rational point, see Figure A.3. Each of these lines intersects the cubic C in two more points giving a double cover of \mathbb{P}^1 . Among these lines there are four where the two additional intersection points agree. In the course of our analysis we can shift one of these to infinity. This results

¹ The \mathbb{P}^1 can be seen in this picture as all the possible slopes of the lines through the rational point.

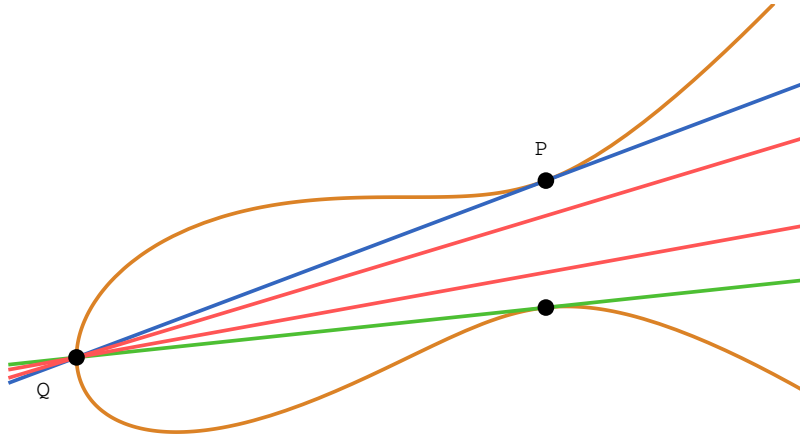


Figure A.3: Basic idea of the Nagell algorithm [37]. A cubic with a rational point Q . In general one can construct four lines through Q whose other two intersection points with the cubic agree (see (A.9)). All lines through Q give a double cover of the rational curve.

in an order three polynomial which determines the coordinates of the tangential points. This polynomial then gives the right hand side of the Weierstrass form.

We start with the following cubic C in \mathbb{P}^2

$$p = s_1u^3 + s_2u^2v + s_3uw^2 + s_4v^3 + s_5u^2w + s_6uvw + s_7v^2w + s_8uw^2 + s_9vw^2. \quad (\text{A.2})$$

This is not the most general cubic in \mathbb{P}^2 (see Section 2.5.2 for a discussion of the most general cubic). The reason why we do not choose the most general cubic is that we need a rational point which is not present in the general case. In this form we have the rational point $P = [0, 0, 1]$. Additionally we choose the coordinates u and v such that s_9 is unequal to zero. If this is not possible the curve is singular at P which we excluded.

In a first step we want to construct an additional rational point Q such that the line through Q and P is a tangent to C at P . To do this we split the cubic such that

$$p = F_3(u, v) + F_2(u, v)w + F_1(u, v)w^2. \quad (\text{A.3})$$

The point P becomes a tangent that means a double intersection point of a line with the cubic iff $F_1 = 0$ along the line [37, 49]. This can be seen easily in the patch $w = 1$. Thus the tangent is described by

$$F_1 = s_8u + s_9v = 0. \quad (\text{A.4})$$

The third intersection point of this line with the cubic can be found by plugging (A.4) into the polynomial (A.3). After using the scaling relation of \mathbb{P}^2 to clear denominators we find the other intersection point [37, 49]

$$Q = [-b_2s_9 : b_2s_8 : b_3]. \quad (\text{A.5})$$

Here we defined the quantities $b_i = F_i(s_9, -s_8)$.

We observe two special cases [37]: If $b_2 = 0$ the points Q and P are identical and thus a triple

intersection point of the cubic with a line. On the other hand if $b_3 = 0$ the new point $Q = [-s_9, s_8, 0]$ is shifted to infinity. The case where both b_2 and b_3 are equal to zero can obviously not exist since the point P is not at infinity. This can also be seen from the fact that in this case $p = 0$ along the line and p thus factorizes and does not give an elliptic curve.

Next we want to choose convenient coordinates $[u', v', w']$ such that $Q = [u' = 0, v' = 0, w']$. The reason for this choice is that we focus now on the point Q through which we construct all lines. To perform the coordinate transformation we have to distinguish two cases. In each of these cases the coordinate transformations are [37, 49]

$$\begin{aligned} b_3 \neq 0 : \quad u' &= u + s_9 \frac{b_2}{b_3} w, & v' &= v - s_8 \frac{b_2}{b_3} w, \\ b_3 = 0 : \quad u' &= u + s_9 w, & v' &= v - s_8 w. \end{aligned} \tag{A.6}$$

In this new coordinates the cubic C in \mathbb{P}^2 takes the form

$$p = f_3(u', v') + f_2(u', v')w + f_1(u', v')w^2. \tag{A.7}$$

We again used a split form to define the homogeneous functions $f_k(u', v')$ of degree k in (u', v') . This equation can now be reformulated in terms of the slopes $t = \frac{v'}{u'}$ of the lines through the point Q . To reformulate the cubic in terms of the slopes we factor out a u' and find [37, 49]

$$\phi_3(t)u'^2 + \phi_2(t)u'w + \phi_1(t)w^2 = 0. \tag{A.8}$$

Here we already canceled a factor of $u' = 0$ corresponding to the intersection point of the line with slope t and the point Q . Additionally we defined the polynomials $\phi_i(t) = f_i(1, t)$. The two remaining solutions for u' give the other two intersection points of the line with slope t and the cubic.

We can now solve (A.8) for the other two points u' . Since taking a square root might lead to a field extension we arrive after completing the square at [37]

$$(2\phi_3(t)u' + \phi_2(t)w)^2 = \delta(t)w^2, \quad \delta(t) = \phi_2^2(t) - 4\phi_1(t)\phi_3(t). \tag{A.9}$$

The square is a sign that we arrived at the double cover of \mathbb{P}^1 . The function $\delta(t)$ is in general of fourth order. Its zeros are the values of the slopes where the lines through Q are tangents at the cubic, see Figure A.3. Since we already know one of these slopes $t_0 = -\frac{s_8}{s_9}$ from the construction of Q we can change the coordinates such that this zero is shifted to infinity. This is done by the coordinate transformation $t = t_0 + \frac{1}{\tau}$. We then find the cubic polynomial [37, 49]

$$\rho(\tau) = \tau^4 \delta\left(t_0 + \frac{1}{\tau}\right) = c\tau^3 + d\tau^2 + e\tau + k. \tag{A.10}$$

Identifying the quadratic term in (A.9) with the quadratic variable of the Weierstrass form up to constants is equivalent to $\rho(\tau) = \frac{y^2}{c}$. This identification as well as $\tau = \frac{x}{c}$ then leads to the Tate form

$$y^2 = x^3 + dx^2 + ecx + kc^2. \tag{A.11}$$

To find the coordinates in this Tate form we can go backwards through the coordinate changes in

(A.6) and (A.10). With $p = 0$ in (A.7) we then find the two coordinates [37]

$$\begin{aligned} x &= c \frac{u + s_9 \frac{b_2}{b_3} w}{v + \frac{s_8}{s_9} u}, \\ y &= c \frac{-f_2 \left(u + s_9 \frac{b_2}{b_3}, v - s_8 \frac{b_2}{b_3} \right) w - 2f_1 \left(u + s_9 \frac{b_2}{b_3}, v - s_8 \frac{b_2}{b_3} \right) w^2}{\left(v + \frac{s_8}{s_9} u \right)^2}. \end{aligned} \quad (\text{A.12})$$

In order to find the discriminant we can complete the cube on the right hand side of (A.11) to find the Weierstrass form

$$y^2 = \tilde{x}^3 + f\tilde{x} + g. \quad (\text{A.13})$$

The necessary coordinate redefinition and the corresponding constants are given by

$$\begin{aligned} \tilde{x} &= x + \frac{d}{3} \\ f &= ec - \frac{1}{3}d^2, \quad g = kc^2 + \frac{2}{27}d^3 - \frac{1}{3}ecd. \end{aligned} \quad (\text{A.14})$$

A.3 Calculation of quantum operators

The calculation of the quantum operators can be done via a partial integration of the WKB functions $S'_n(x)$ (3.68). If the functions $S'_m(x)$, $m = 0, \dots, n$ are given the operator \mathcal{D}_n can be calculated by the following method.

1. First one makes a general ansatz for the operator

$$\mathcal{D}_n S'_0(x) = c_{1,n}(u, \vec{m}) \Theta_u S'_0(x) + c_{2,n}(u, \vec{m}) \Theta_u^2 S'_0(x). \quad (\text{A.15})$$

2. The difference between the WKB function and the operator applied to $S'_0(x)$ (A.15) must then be a total derivative. The general structure of the WKB function is

$$S'_n(x) \sim \frac{n_1(x) + n_2(x) \sqrt{f(x)}}{d(x) f(x)^m}. \quad (\text{A.16})$$

Here the factors in $d(x) = \prod_k d_k(x)^{m_k}$ are usually much simpler than $f(x)$. An ansatz for the total derivative which reproduces this denominator structure is given by²

$$\begin{aligned} S'_n - \mathcal{D}_n S'_0(x) &= c + \frac{d}{dx} \left(\frac{\sum_k y_k e^{kx}}{f(x)^{m-1} \prod_k d_k(x)^{m_k-1}} \right) + \frac{d}{dx} \left(\frac{\sum_k \tilde{y}_k e^{kx}}{f(x)^{m-3/2} \prod_k d_k(x)^{m_k-1}} \right) \\ &+ \sum_{m=0}^n \sum_{k=1}^{n-m} y_{m,k} \frac{d^k}{dx^k} S'_m(x). \end{aligned} \quad (\text{A.17})$$

3. In the next step one solves (A.17) order by order in e^{kx} and $e^{kx} \sqrt{f(x)}$ for the coefficients y_k , \tilde{y}_k and $y_{m,k}$. After eliminating these we are left with a system of equations for $c_{1,n}$ and $c_{2,n}$.

² The coefficients \tilde{y}_k could be set to zero in all our examples but are included in general to cancel the square root terms.

The speed of the above mentioned procedure can be increased by first cancelling the square roots occurring in $S'_n - \mathcal{D}_n S'_0(x)$ proportional to $c_{1,n}$, $c_{2,n}$ and 1 individually. Therefore one needs to add constant terms as well as terms of the form $\frac{d^k}{dx^k} S'_0(x)$ proportional to $c_{1,n}$ and $c_{2,n}$. For the terms proportional to 1 one has to additionally include $\frac{d^k}{dx^k} S'_m(x)$ for $m \neq 0$.

In the process of calculating the expressions for $S'_m(x)$ one encounters factors of the form

$$\frac{1}{(g(x) + \sqrt{f(x)})}. \quad (\text{A.18})$$

The occurring terms can be simplified considerably by multiplying with $\frac{(g(x) - \sqrt{f(x)})}{(g(x) + \sqrt{f(x)})}$.

Although this procedure worked in all examples it is not proven that the ansatz in (A.17) consists of a basis of functions which span the complete space of possible total derivatives necessary for the partial integration.

A.4 Refined matrix models

There are two main proposals for matrix models dual to the refined topological string analogously to the duality in the unrefined case [126–128]. The first one is the β ensemble proposed in [110] (see Section 3.2.2). The other proposal is the q -deformed matrix model introduced in [111] in a refinement of CS theory. In this Appendix we want to briefly introduce the q -deformed matrix model of [111] and mention some of its problems.

In [111] the q -deformed matrix model is derived for CS theory on the conifold by gluing the partition function of CS theory on two solid tori as was done in the unrefined case in [17]. The unrefined matrix model for CS theory on S^3 is given by

$$\begin{aligned} Z_{\text{unref}}(S^3) &= \frac{1}{\text{vol}(U(N))} \int \prod_{i=1}^N d\lambda_i \prod_{i<j} \left(2 \sinh \left(\frac{\lambda_i - \lambda_j}{2} \right) \right)^2 e^{-\frac{1}{2g_s} \sum_{i=1}^N \lambda_i^2} \\ &= \mathcal{N} \int d^N \lambda \prod_{i \neq j} \left(2 \sinh \left(\frac{\lambda_i - \lambda_j}{2} \right) \right) e^{-\frac{1}{2g_s} \sum_{i=1}^N \lambda_i^2}. \end{aligned} \quad (\text{A.19})$$

The q deformation is then introduced as a deformation of the measure

$$\prod_{i \neq j} \left(2 \sinh \left(\frac{\lambda_i - \lambda_j}{2} \right) \right) = \prod_{i \neq j} \left(\left(e^{\frac{\lambda_i - \lambda_j}{2}} - e^{-\frac{\lambda_i - \lambda_j}{2}} \right) \right) \longrightarrow \prod_{m=0}^{\beta-1} \prod_{i \neq j} \left(e^{\frac{\lambda_j - \lambda_i}{2}} - q^m e^{\frac{\lambda_i - \lambda_j}{2}} \right). \quad (\text{A.20})$$

Here we introduced the factor $q = e^{ig_s/\beta}$ ³. In the refined topological string we used the refined parameters ϵ_1 and ϵ_2 . In the case of matrix models one usually takes the parameters g_s and β . The connection between the corresponding sets of parameters is

$$\beta = -\frac{\epsilon_2}{\epsilon_1} \quad \text{and} \quad g_s = -i\epsilon_2. \quad (\text{A.21})$$

³ Note that we redefined $g_s \rightarrow \frac{g_s}{\beta}$ compared to [111].

Then the total partition function for the q -deformed matrix model on S^3 is given by

$$Z_q(S^3) = \mathcal{N} \int d^N \lambda \prod_{m=0}^{\beta-1} \prod_{i \neq j} \left(e^{\frac{\lambda_i - \lambda_j}{2}} - q^m e^{\frac{\lambda_i - \lambda_j}{2}} \right) e^{-\frac{\beta}{2g_s} \sum_{i=1}^N \lambda_i^2}. \quad (\text{A.22})$$

In [111] this partition function was rewritten as

$$Z(N, \beta) = \prod_{k=1}^{N-1} \prod_{m=0}^{\beta-1} \left(1 - t^{N-k} q^m \right)^k, \quad (\text{A.23})$$

where we defined the parameter $t = q^\beta$. Starting from this expression for the partition function one can calculate the free energy

$$\begin{aligned} F(N, \beta) &= \log(Z(N, \beta)) = \sum_{k=1}^{N-1} \sum_{m=0}^{\beta-1} k \log \left(1 - t^{N-k} q^m \right) \\ &= - \sum_{\ell=1}^{\infty} \sum_{k=1}^{N-1} \sum_{m=0}^{\beta-1} \frac{k}{\ell} t^{\ell N} t^{-\ell k} q^{\ell m} \\ &= - \sum_{\ell=1}^{\infty} \frac{t^\ell - 1}{q^\ell - 1} \frac{1}{\ell} \left(-t^{-\ell N} \left\{ \frac{t^\ell}{(t^\ell - 1)^2} + \frac{t^{\ell N}}{t^\ell - 1} - \frac{t^\ell t^{\ell N}}{(t^\ell - 1)^2} \right\} t^{\ell N} \right) \\ &= - \sum_{\ell=1}^{\infty} \frac{1}{\ell} \left(\frac{t^{\ell N} t^{\ell/2} q^{-\ell/2}}{(t^{\ell/2} - t^{-\ell/2})(q^{\ell/2} - q^{-\ell/2})} - \frac{t^{\ell/2} q^{-\ell/2}}{(t^{\ell/2} - t^{-\ell/2})(q^{\ell/2} - q^{-\ell/2})} - N \frac{t^\ell}{q^\ell - 1} \right). \end{aligned} \quad (\text{A.24})$$

Here we expanded the logarithm in the second line and then used the geometric series to resum the resulting expression. The first term in this series agrees with the conifold free energy derived with the refined topological vertex [103] after the identification

$$Q = t^N t^{\frac{1}{2}} q^{-\frac{1}{2}}. \quad (\text{A.25})$$

The second summand in the final expression of (A.24) which is independent of N can be neglected in the large N limit. But the third term in (A.24) can be expanded in a g_s expansion as

$$\begin{aligned} N \sum_{\ell=1}^{\infty} \frac{1}{\ell} \frac{t^\ell}{q^\ell - 1} &= N \sum_{\ell=1}^{\infty} \frac{1}{\ell} \frac{q^{\beta \ell}}{q^\ell - 1} = N \sum_{\ell=1}^{\infty} \sum_{m=0}^{\infty} B_m(\beta) \frac{(g_s \ell)^{m-1}}{\beta^{m-1} \ell m!} \\ &= N \sum_{m=0}^{\infty} B_m(\beta) \frac{g_s^{m-1}}{\beta^{m-1} m!} \sum_{\ell=1}^{\infty} \ell^{-(2-m)} \\ &= N \sum_{m=0}^{\infty} B_m(\beta) \zeta(2-m) \frac{g_s^{m-1}}{\beta^{m-1} m!} \\ &= N \left(g_s^{-1} \beta B_0(\beta) \zeta(2) + g_s^0 B_1(\beta) \zeta(1) + g_s \frac{\beta^{-1}}{2!} B_2(\beta) \zeta(0) \right. \\ &\quad \left. - \sum_{m=0}^{\infty} \beta^{-2(m+1)} B_{2m+3}(\beta) \frac{B_{2(m+1)}}{2(m+1)} \frac{g_s^{2(m+1)}}{(2m+3)!} \right). \end{aligned} \quad (\text{A.26})$$

Here we have used the Bernoulli polynomials $B_n(x)$ as well as the Riemann zeta function at odd negative values

$$\frac{te^{tx}}{e^t - 1} = \sum_{n=0}^{\infty} B_n(x) \frac{t^n}{n!}, \quad \zeta(n) = \sum_{k=1}^{\infty} \frac{1}{k^n} = -\frac{B_{1-n}}{1-n}, n = -1, -3, \dots \quad (\text{A.27})$$

These terms are apparently neglected in [111] although they contribute in general. Additionally the expansion of these neglected terms does not fit in the ϵ_1 and ϵ_2 expansion of the topological string.

Using the gluing procedures as used in [111] to derive the q-deformed matrix model for the conifold we can also use the same method and try to derive analogous to [17] q-deformed matrix models for Lens spaces. With these methods we arrive at the following q-deformed Lens space matrix model

$$Z = \int \prod_{j=1}^p \frac{d^{N_j} u^{(j)}}{N_j!} \Delta_1(u^{(j)}) \prod_{j < k} \Delta_2(u^{(j)}, u^{(k)}) e^{-\frac{p\beta}{2g_s} \sum_{j=1}^p \text{Tr}(u^{(j)})^2}, \quad (\text{A.28})$$

with

$$\begin{aligned} \Delta_1(u^{(j)}) &= \prod_{m=0}^{\beta-1} \prod_{k \neq n} \left(e^{\frac{u_k^{(j)} - u_n^{(j)}}{2}} - q^m e^{\frac{u_n^{(j)} - u_k^{(j)}}{2}} \right), \\ \Delta_2(u^{(j)}, u^{(k)}) &= \prod_{m=0}^{\beta-1} \prod_{i,n} \left(e^{\frac{u_i^{(j)} - u_n^{(k)} + d_{j,k}}{2}} - q^m e^{\frac{u_n^{(k)} - u_i^{(j)} + d_{j,k}}{2}} \right) \left(e^{\frac{u_i^{(j)} - u_n^{(k)} + d_{k,j}}{2}} - q^m e^{\frac{u_n^{(k)} - u_i^{(j)} + d_{k,j}}{2}} \right), \end{aligned} \quad (\text{A.29})$$

where $d_{j,k} = \frac{2\pi i(j-k)}{p}$. This however leads to inconsistencies with the calculations in the dual topological string theory [102, 129].

Bibliography

- [1] M. Mariño, *Lectures on non-perturbative effects in large N gauge theories, matrix models and strings*, Fortsch.Phys. **62** (2014) 455–540, arXiv:1206.6272 [hep-th] (cit. on p. 1).
- [2] J. Écalle, *Les fonctions resurgentes, I, II et III*, Publications Mathématiques d’Orsay, 1981 and 1985 (cit. on p. 1).
- [3] R. C. Santamaría et al., *Resurgent Transseries and the Holomorphic Anomaly* (2013), arXiv:1308.1695 [hep-th] (cit. on pp. 1, 89).
- [4] R. Couso-Santamaría et al., *Resurgent Transseries and the Holomorphic Anomaly: Nonperturbative Closed Strings in Local CP^2* (2014), arXiv:1407.4821 [hep-th] (cit. on pp. 1, 89).
- [5] R. Blumenhagen, D. Lüst, and S. Theisen, *Basic Concepts of String Theory*, Springer, 2013 (cit. on pp. 1, 51).
- [6] T. Kaluza, *On the Problem of Unity in Physics*, Sitzungsber.Preuss.Akad.Wiss.Berlin (Math.Phys.) **1921** (1921) 966–972 (cit. on p. 2).
- [7] O. Klein, *Quantum Theory and Five-Dimensional Theory of Relativity. (In German and English)*, Z.Phys. **37** (1926) 895–906 (cit. on p. 2).
- [8] H. P. Nilles, *Supersymmetry, Supergravity and Particle Physics*, Phys.Rept. **110** (1984) 1–162 (cit. on p. 2).
- [9] E. Witten, *String theory dynamics in various dimensions*, Nucl.Phys. **B443** (1995) 85–126, arXiv:hep-th/9503124 [hep-th] (cit. on p. 2).
- [10] P. Di Francesco, P. Mathieu, and D. Senechal, *Conformal field theory* (1997) (cit. on p. 3).
- [11] G. ’t Hooft, *A Planar Diagram Theory for Strong Interactions*, Nucl.Phys. **B72** (1974) 461 (cit. on p. 3).
- [12] J. M. Maldacena, *The Large N limit of superconformal field theories and supergravity*, Int.J.Theor.Phys. **38** (1999) 1113–1133, arXiv:hep-th/9711200 [hep-th] (cit. on p. 3).
- [13] J. Casalderrey-Solana et al., *Gauge/String Duality, Hot QCD and Heavy Ion Collisions* (2011), arXiv:1101.0618 [hep-th] (cit. on p. 3).
- [14] S. A. Hartnoll, *Lectures on holographic methods for condensed matter physics*, Class.Quant.Grav. **26** (2009) 224002, arXiv:0903.3246 [hep-th] (cit. on p. 3).
- [15] E. Witten, *Topological Sigma Models*, Commun.Math.Phys. **118** (1988) 411 (cit. on p. 3).
- [16] E. Witten, *On the Structure of the Topological Phase of Two-dimensional Gravity*, Nucl.Phys. **B340** (1990) 281–332 (cit. on pp. 3, 51).

- [17] M. Aganagic et al., *Matrix model as a mirror of Chern-Simons theory*, JHEP **0402** (2004) 010, arXiv:hep-th/0211098 [hep-th] (cit. on pp. 3, 96, 98).
- [18] M. Marino, *Chern-Simons theory, matrix models, and topological strings*, Int.Ser.Monogr.Phys. **131** (2005) 1–197 (cit. on pp. 3, 47).
- [19] K. Hori et al., *Mirror Symmetry*, Oxford University Press, 2003 (cit. on pp. 4, 17, 47).
- [20] O. Aharony et al., *$N=6$ superconformal Chern-Simons-matter theories, M2-branes and their gravity duals*, JHEP **0810** (2008) 091, arXiv:0806.1218 [hep-th] (cit. on p. 4).
- [21] M. Marino, *Lectures on localization and matrix models in supersymmetric Chern-Simons-matter theories*, J.Phys. **A44** (2011) 463001, arXiv:1104.0783 [hep-th] (cit. on p. 4).
- [22] I. R. Klebanov and A. A. Tseytlin, *Entropy of near extremal black p -branes*, Nucl.Phys. **B475** (1996) 164–178, arXiv:hep-th/9604089 [hep-th] (cit. on p. 4).
- [23] N. Drukker, M. Marino, and P. Putrov, *From weak to strong coupling in ABJM theory*, Commun.Math.Phys. **306** (2011) 511–563, arXiv:1007.3837 [hep-th] (cit. on p. 4).
- [24] J. Kallen and M. Marino, *Instanton effects and quantum spectral curves* (2013), arXiv:1308.6485 [hep-th] (cit. on pp. 4–6, 47, 71, 77, 87, 88).
- [25] Y. Hatsuda et al., *Non-perturbative effects and the refined topological string*, JHEP **1409** (2014) 168, arXiv:1306.1734 [hep-th] (cit. on pp. 4–6, 47, 56, 71, 74, 87, 88).
- [26] A. Grassi, Y. Hatsuda, and M. Marino, *Topological Strings from Quantum Mechanics* (2014), arXiv:1410.3382 [hep-th] (cit. on pp. 4–6, 47, 71–74, 76–80, 82–84, 87–89).
- [27] M. Marino and P. Putrov, *ABJM theory as a Fermi gas*, J.Stat.Mech. **1203** (2012) P03001, arXiv:1110.4066 [hep-th] (cit. on pp. 4, 72).
- [28] C. Vafa, *Evidence for F theory*, Nucl.Phys. **B469** (1996) 403–418, arXiv:hep-th/9602022 [hep-th] (cit. on p. 5).
- [29] V. Braun and D. R. Morrison, *F -theory on Genus-One Fibrations* (2014), arXiv:1401.7844 [hep-th] (cit. on pp. 5, 13).
- [30] D. R. Morrison and W. Taylor, *Sections, multisections, and $U(1)$ fields in F -theory* (2014), arXiv:1404.1527 [hep-th] (cit. on pp. 5, 13).
- [31] L. B. Anderson et al., *Physics of F -theory compactifications without section* (2014), arXiv:1406.5180 [hep-th] (cit. on pp. 5, 13).
- [32] D. Klevers et al., *F -Theory on all Toric Hypersurface Fibrations and its Higgs Branches*, JHEP **1501** (2015) 142, arXiv:1408.4808 [hep-th] (cit. on pp. 5–7, 10, 12–14, 17, 20, 23, 29, 35, 37).
- [33] I. García-Etxebarria, T. W. Grimm, and J. Keitel, *Yukawas and discrete symmetries in F -theory compactifications without section*, JHEP **1411** (2014) 125, arXiv:1408.6448 [hep-th] (cit. on pp. 5, 13).
- [34] C. Mayrhofer et al., *Discrete Gauge Symmetries by Higgsing in four-dimensional F -Theory Compactifications*, JHEP **1412** (2014) 068, arXiv:1408.6831 [hep-th] (cit. on pp. 5, 13).

- [35] C. Mayrhofer et al., *On Discrete Symmetries and Torsion Homology in F-Theory* (2014), arXiv:1410.7814 [hep-th] (cit. on pp. 5, 13).
- [36] M. Cvetič et al., *F-Theory Vacua with Z_3 Gauge Symmetry* (2015), arXiv:1502.06953 [hep-th] (cit. on pp. 5, 13, 45, 87).
- [37] M. Cvetič, D. Klevers, and H. Piragua, *F-Theory Compactifications with Multiple $U(1)$ -Factors: Constructing Elliptic Fibrations with Rational Sections*, JHEP **1306** (2013) 067, arXiv:1303.6970 [hep-th] (cit. on pp. 5, 12, 15, 41, 92–95).
- [38] J. Borchmann et al., *Elliptic fibrations for $SU(5) \times U(1) \times U(1)$ F-theory vacua*, Phys.Rev. **D88.4** (2013) 046005, arXiv:1303.5054 [hep-th] (cit. on p. 5).
- [39] M. Cvetič et al., *Chiral Four-Dimensional F-Theory Compactifications With $SU(5)$ and Multiple $U(1)$ -Factors*, JHEP **1404** (2014) 010, arXiv:1306.3987 [hep-th] (cit. on pp. 5, 15–17, 32).
- [40] M. Cvetič et al., *Three-Family Particle Physics Models from Global F-theory Compactifications* (2015), arXiv:1503.02068 [hep-th] (cit. on pp. 6, 7, 15, 17, 20).
- [41] M.-x. Huang et al., *Quantum geometry of del Pezzo surfaces in the Nekrasov-Shatashvili limit*, JHEP **1502** (2015) 031, arXiv:1401.4723 [hep-th] (cit. on pp. 6, 54, 56, 58, 61, 62, 64, 66–68).
- [42] J. Gu et al., *Exact solutions to quantum spectral curves by topological string theory* (2015), arXiv:1506.09176 [hep-th] (cit. on pp. 6, 71, 74, 78, 80, 81, 83, 84).
- [43] F. Denef, *Les Houches Lectures on Constructing String Vacua* (2008) 483–610, arXiv:0803.1194 [hep-th] (cit. on pp. 7, 8, 10, 13, 15).
- [44] T. Weigand, *Lectures on F-theory compactifications and model building*, Class.Quant.Grav. **27** (2010) 214004, arXiv:1009.3497 [hep-th] (cit. on pp. 7–10, 12–15).
- [45] W. Taylor, *TASI Lectures on Supergravity and String Vacua in Various Dimensions* (2011), arXiv:1104.2051 [hep-th] (cit. on pp. 7, 11–13, 23, 29).
- [46] K. Kodaira, *On compact analytic surfaces: II*, The Annals of Mathematics **77.3** (1963) 563–626 (cit. on pp. 10, 11).
- [47] J. Tate, *Algorithm for determining the type of a singular fiber in an elliptic pencil*, Modular functions of one variable IV (1975) 33–52 (cit. on p. 10).
- [48] D. Husemöller, *Elliptic Curves*, vol. 111, Graduate Texts in Mathematics, Springer, 1987 (cit. on pp. 11, 39, 41, 88, 91, 92).
- [49] I. Connell, *Elliptic Curve Handbook*, 1999 (cit. on pp. 11, 92–94).
- [50] J. H. Silverman, *The arithmetic of elliptic curves*, vol. 106, Springer, 2009 (cit. on p. 11).
- [51] S. Lang and A. Neron, *Rational points of abelian varieties over function fields*, American Journal of Mathematics (1959) 95–118 (cit. on p. 11).
- [52] B. Mazur, *Modular curves and the Eisenstein ideal*, Publications Mathématiques de l’Institut des Hautes Études Scientifiques **47.1** (1977) 33–186 (cit. on p. 11).
- [53] B. Mazur and D. Goldfeld, *Rational isogenies of prime degree*, Inventiones mathematicae **44.2** (1978) 129–162 (cit. on p. 11).

- [54] P. S. Aspinwall and D. R. Morrison, *Nonsimply connected gauge groups and rational points on elliptic curves*, JHEP **9807** (1998) 012, arXiv:hep-th/9805206 [hep-th] (cit. on pp. 12, 88).
- [55] D. R. Morrison and C. Vafa, *Compactifications of F theory on Calabi-Yau threefolds. 1*, Nucl.Phys. **B473** (1996) 74–92, arXiv:hep-th/9602114 [hep-th] (cit. on pp. 12, 14).
- [56] C. Mayrhofer et al., *Mordell-Weil Torsion and the Global Structure of Gauge Groups in F-theory* (2014), arXiv:1405.3656 [hep-th] (cit. on pp. 12, 28, 29, 37).
- [57] D. R. Morrison and D. S. Park, *F-Theory and the Mordell-Weil Group of Elliptically-Fibered Calabi-Yau Threefolds*, JHEP **1210** (2012) 128, arXiv:1208.2695 [hep-th] (cit. on pp. 12, 14, 15).
- [58] D. S. Park, *Anomaly Equations and Intersection Theory*, JHEP **1201** (2012) 093, arXiv:1111.2351 [hep-th] (cit. on pp. 12, 14, 45).
- [59] T. W. Grimm and T. Weigand, *On Abelian Gauge Symmetries and Proton Decay in Global F-theory GUTs*, Phys.Rev. **D82** (2010) 086009, arXiv:1006.0226 [hep-th] (cit. on p. 12).
- [60] P. Griffiths and J. Harris, *Principles of Algebraic Geometry*, John Wiley & Sons, 1978 (cit. on p. 13).
- [61] S. Y. An et al., *Jacobians of genus one curves*, Journal of Number Theory **90.2** (2001) 304–315 (cit. on pp. 13, 45).
- [62] D. R. Morrison and C. Vafa, *Compactifications of F theory on Calabi-Yau threefolds. 2.*, Nucl.Phys. **B476** (1996) 437–469, arXiv:hep-th/9603161 [hep-th] (cit. on p. 14).
- [63] T. W. Grimm et al., *Computing Brane and Flux Superpotentials in F-theory Compactifications*, JHEP **1004** (2010) 015, arXiv:0909.2025 [hep-th] (cit. on pp. 15, 17).
- [64] H. Jockers, P. Mayr, and J. Walcher, *On $N=1$ 4d Effective Couplings for F-theory and Heterotic Vacua*, Adv.Theor.Math.Phys. **14** (2010) 1433–1514, arXiv:0912.3265 [hep-th] (cit. on pp. 15, 17).
- [65] K. Intriligator et al., *Conifold Transitions in M-theory on Calabi-Yau Fourfolds with Background Fluxes*, Adv.Theor.Math.Phys. **17** (2013) 601–699, arXiv:1203.6662 [hep-th] (cit. on pp. 15, 26, 32).
- [66] N. C. Bizet, A. Klemm, and D. V. Lopes, *Landscaping with fluxes and the E8 Yukawa Point in F-theory* (), arXiv:1404.7645 [hep-th] (cit. on pp. 15, 17).
- [67] E. Witten, *On flux quantization in M theory and the effective action*, J.Geom.Phys. **22** (1997) 1–13, arXiv:hep-th/9609122 [hep-th] (cit. on pp. 16, 17, 26, 32).
- [68] S. Sethi, C. Vafa, and E. Witten, *Constraints on low dimensional string compactifications*, Nucl.Phys. **B480** (1996) 213–224, arXiv:hep-th/9606122 [hep-th] (cit. on p. 16).
- [69] S. Gukov, C. Vafa, and E. Witten, *CFT's from Calabi-Yau four folds*, Nucl.Phys. **B584** (2000) 69–108, arXiv:hep-th/9906070 [hep-th] (cit. on p. 16).

- [70] M. Haack and J. Louis, *M theory compactified on Calabi-Yau fourfolds with background flux*, Phys.Lett. **B507** (2001) 296–304, arXiv:hep-th/0103068 [hep-th] (cit. on p. 16).
- [71] T. W. Grimm and R. Savelli, *Gravitational Instantons and Fluxes from M/F-theory on Calabi-Yau fourfolds*, Phys.Rev. **D85** (2012) 026003, arXiv:1109.3191 [hep-th] (cit. on p. 16).
- [72] D. Belov and G. W. Moore, *Classification of Abelian spin Chern-Simons theories* (2005), arXiv:hep-th/0505235 [hep-th] (cit. on pp. 17, 26, 32).
- [73] A. Kapustin and N. Saulina, *Topological boundary conditions in abelian Chern-Simons theory*, Nucl.Phys. **B845** (2011) 393–435, arXiv:1008.0654 [hep-th] (cit. on pp. 17, 26, 32).
- [74] W. Fulton, *Introduction to toric varieties*, 131, Princeton University Press, 1993 (cit. on p. 17).
- [75] D. A. Cox and S. Katz, *Mirror Symmetry and Algebraic Geometry*, Oxford University Press, 1999 (cit. on pp. 17, 18).
- [76] V. Bouchard, *Lectures on complex geometry, Calabi-Yau manifolds and toric geometry* (2007), arXiv:hep-th/0702063 [HEP-TH] (cit. on pp. 17, 18).
- [77] E. Witten, *Phases of $N=2$ theories in two-dimensions*, Nucl.Phys. **B403** (1993) 159–222, arXiv:hep-th/9301042 [hep-th] (cit. on p. 18).
- [78] B. Haghighat, A. Klemm, and M. Rauch, *Integrability of the holomorphic anomaly equations*, JHEP **0810** (2008) 097, arXiv:0809.1674 [hep-th] (cit. on p. 18).
- [79] V. V. Batyrev, *Dual polyhedra and mirror symmetry for Calabi-Yau hypersurfaces in toric varieties*, J.Alg.Geom. **3** (1994) 493–545, arXiv:alg-geom/9310003 [alg-geom] (cit. on p. 18).
- [80] A. Grassi and V. Perduca, *Weierstrass models of elliptic toric K3 hypersurfaces and symplectic cuts* (2012), arXiv:1201.0930 [math.AG] (cit. on p. 19).
- [81] M. Kreuzer and H. Skarke, *On the classification of reflexive polyhedra*, Commun.Math.Phys. **185** (1997) 495–508, arXiv:hep-th/9512204 [hep-th] (cit. on p. 19).
- [82] W. P. Barth, C. A. M. Peters, and A. Van de Ven, *Compact Complex Surfaces*, Springer, 1984 (cit. on pp. 19, 55).
- [83] V. Braun, T. W. Grimm, and J. Keitel, *Geometric Engineering in Toric F-Theory and GUTs with $U(1)$ Gauge Factors*, JHEP **1312** (2013) 069, arXiv:1306.0577 [hep-th] (cit. on pp. 21, 28, 39).
- [84] F. Bonetti and T. W. Grimm, *Six-dimensional $(1,0)$ effective action of F-theory via M-theory on Calabi-Yau threefolds*, JHEP **1205** (2012) 019, arXiv:1112.1082 [hep-th] (cit. on p. 24).
- [85] M. Cvetič et al., *Elliptic fibrations with rank three Mordell-Weil group: F-theory with $U(1) \times U(1) \times U(1)$ gauge symmetry*, JHEP **1403** (2014) 021, arXiv:1310.0463 [hep-th] (cit. on pp. 26, 32).
- [86] M. Bershadsky et al., *Geometric singularities and enhanced gauge symmetries*, Nucl.Phys. **B481** (1996) 215–252, arXiv:hep-th/9605200 [hep-th] (cit. on p. 29).
- [87] G. Honecker and M. Trapletti, *Merging Heterotic Orbifolds and K3 Compactifications with Line Bundles*, JHEP **0701** (2007) 051, arXiv:hep-th/0612030 [hep-th] (cit. on p. 36).

- [88] T. Banks, *Effective Lagrangian Description of Discrete Gauge Symmetries*, Nucl.Phys. **B323** (1989) 90 (cit. on pp. 37, 38).
- [89] V. Braun, T. W. Grimm, and J. Keitel, *Complete Intersection Fibers in F-Theory* (2014), arXiv:1411.2615 [hep-th] (cit. on pp. 38, 88).
- [90] T. Banks and N. Seiberg, *Symmetries and Strings in Field Theory and Gravity*, Phys.Rev. **D83** (2011) 084019, arXiv:1011.5120 [hep-th] (cit. on p. 43).
- [91] S. Hosono, A. Klemm, and S. Theisen, *Lectures on mirror symmetry*, Lect.Notes Phys. **436** (1994) 235, arXiv:hep-th/9403096 [hep-th] (cit. on p. 47).
- [92] A. Neitzke and C. Vafa, *Topological strings and their physical applications* (2004), arXiv:hep-th/0410178 [hep-th] (cit. on p. 47).
- [93] M. Vonk, *A Mini-course on topological strings* (2005), arXiv:hep-th/0504147 [hep-th] (cit. on pp. 47–54).
- [94] A. Klemm, *Topological string theory on Calabi-Yau threefolds*, PoS RTN2005 (2005) 002 (cit. on p. 47).
- [95] M. Alim, *Lectures on Mirror Symmetry and Topological String Theory* (2012), arXiv:1207.0496 [hep-th] (cit. on p. 47).
- [96] M. E. Peskin and D. V. Schroeder, *An Introduction to quantum field theory* (1995) (cit. on p. 48).
- [97] E. Witten, *Mirror manifolds and topological field theory* (1991), arXiv:hep-th/9112056 [hep-th] (cit. on p. 48).
- [98] M. Bershadsky et al., *Kodaira-Spencer theory of gravity and exact results for quantum string amplitudes*, Commun.Math.Phys. **165** (1994) 311–428, arXiv:hep-th/9309140 [hep-th] (cit. on p. 52).
- [99] D. Krefl and J. Walcher, *Extended Holomorphic Anomaly in Gauge Theory*, Lett.Math.Phys. **95** (2011) 67–88, arXiv:1007.0263 [hep-th] (cit. on p. 54).
- [100] M.-x. Huang and A. Klemm, *Direct integration for general Ω backgrounds*, Adv.Theor.Math.Phys. **16.3** (2012) 805–849, arXiv:1009.1126 [hep-th] (cit. on p. 54).
- [101] M.-x. Huang, A.-K. Kashani-Poor, and A. Klemm, *The Ω deformed B-model for rigid $N = 2$ theories*, Annales Henri Poincare **14** (2013) 425–497, arXiv:1109.5728 [hep-th] (cit. on pp. 54, 63).
- [102] M.-X. Huang, A. Klemm, and M. Poretschkin, *Refined stable pair invariants for E-, M- and $[p, q]$ -strings*, JHEP **1311** (2013) 112, arXiv:1308.0619 [hep-th] (cit. on pp. 54, 63, 68, 84, 98).
- [103] A. Iqbal, C. Kozcaz, and C. Vafa, *The Refined topological vertex*, JHEP **0910** (2009) 069, arXiv:hep-th/0701156 [hep-th] (cit. on pp. 54, 68, 69, 97).
- [104] R. Dijkgraaf, C. Vafa, and E. Verlinde, *M-theory and a topological string duality* (2006), arXiv:hep-th/0602087 [hep-th] (cit. on p. 55).
- [105] M. Aganagic et al., *Quantum Geometry of Refined Topological Strings*, JHEP **1211** (2012) 019, arXiv:1105.0630 [hep-th] (cit. on pp. 55, 58–61, 77).
- [106] N. A. Nekrasov and S. L. Shatashvili, *Quantization of Integrable Systems and Four Dimensional Gauge Theories* (2009), arXiv:0908.4052 [hep-th] (cit. on p. 56).

- [107] S. H. Katz, A. Klemm, and C. Vafa, *Geometric engineering of quantum field theories*, Nucl.Phys. **B497** (1997) 173–195, arXiv:hep-th/9609239 [hep-th] (cit. on p. 58).
- [108] M. Aganagic et al., *Topological strings and integrable hierarchies*, Commun.Math.Phys. **261** (2006) 451–516, arXiv:hep-th/0312085 [hep-th] (cit. on pp. 58, 60, 61).
- [109] E. Witten, *Quantum background independence in string theory* (1993) 0257–275, arXiv:hep-th/9306122 [hep-th] (cit. on pp. 58, 60).
- [110] R. Dijkgraaf and C. Vafa, *Toda Theories, Matrix Models, Topological Strings, and N=2 Gauge Systems* (2009), arXiv:0909.2453 [hep-th] (cit. on pp. 58, 96).
- [111] M. Aganagic and S. Shakhmurov, *Knot Homology and Refined Chern-Simons Index*, Commun.Math.Phys. **333.1** (2015) 187–228, arXiv:1105.5117 [hep-th] (cit. on pp. 58, 96–98).
- [112] M. Marino, *Les Houches lectures on matrix models and topological strings* (2004), arXiv:hep-th/0410165 [hep-th] (cit. on p. 59).
- [113] J. Ambjorn, *Quantization of geometry* (1994), arXiv:hep-th/9411179 [hep-th] (cit. on p. 59).
- [114] A. Mironov and A. Morozov, *Nekrasov Functions and Exact Bohr-Zommerfeld Integrals*, JHEP **1004** (2010) 040, arXiv:0910.5670 [hep-th] (cit. on p. 61).
- [115] M.-x. Huang, *On Gauge Theory and Topological String in Nekrasov-Shatashvili Limit*, JHEP **1206** (2012) 152, arXiv:1205.3652 [hep-th] (cit. on p. 61).
- [116] M. Aganagic et al., *The Topological vertex*, Commun.Math.Phys. **254** (2005) 425–478, arXiv:hep-th/0305132 [hep-th] (cit. on pp. 68, 69).
- [117] T. Chiang et al., *Local mirror symmetry: Calculations and interpretations*, Adv.Theor.Math.Phys. **3** (1999) 495–565, arXiv:hep-th/9903053 [hep-th] (cit. on pp. 68, 69).
- [118] S. Hosono et al., *Mirror symmetry, mirror map and applications to Calabi-Yau hypersurfaces*, Commun.Math.Phys. **167** (1995) 301–350, arXiv:hep-th/9308122 [hep-th] (cit. on p. 70).
- [119] A. Klemm et al., *Direct Integration for Mirror Curves of Genus Two and an Almost Meromorphic Siegel Modular Form* (2015), arXiv:1502.00557 [hep-th] (cit. on pp. 71, 89).
- [120] R. Kashaev and M. Marino, *Operators from mirror curves and the quantum dilogarithm* (2015), arXiv:1501.01014 [hep-th] (cit. on p. 72).
- [121] M.-x. Huang and X.-f. Wang, *Topological Strings and Quantum Spectral Problems*, JHEP **1409** (2014) 150, arXiv:1406.6178 [hep-th] (cit. on pp. 74, 77, 79–81, 89).
- [122] S. Codesido, A. Grassi, and M. Marino, *Exact results in N=8 Chern-Simons-matter theories and quantum geometry* (2014), arXiv:1409.1799 [hep-th] (cit. on p. 77).
- [123] A. Brini and A. Tanzini, *Exact results for topological strings on resolved $Y^{**p,q}$ singularities*, Commun.Math.Phys. **289** (2009) 205–252, arXiv:0804.2598 [hep-th] (cit. on p. 83).
- [124] L. Lin and T. Weigand, *Towards the Standard Model in F-theory*, Fortsch.Phys. **63.2** (2015) 55–104, arXiv:1406.6071 [hep-th] (cit. on p. 88).

- [125] G. Lockhart and C. Vafa, *Superconformal Partition Functions and Non-perturbative Topological Strings* (2012), arXiv:1210.5909 [hep-th] (cit. on p. 89).
- [126] R. Dijkgraaf and C. Vafa, *Matrix models, topological strings, and supersymmetric gauge theories*, Nucl.Phys. **B644** (2002) 3–20, arXiv:hep-th/0206255 [hep-th] (cit. on p. 96).
- [127] R. Dijkgraaf and C. Vafa, *On geometry and matrix models*, Nucl.Phys. **B644** (2002) 21–39, arXiv:hep-th/0207106 [hep-th] (cit. on p. 96).
- [128] R. Dijkgraaf and C. Vafa, *A Perturbative window into nonperturbative physics* (2002), arXiv:hep-th/0208048 [hep-th] (cit. on p. 96).
- [129] J. Choi, S. Katz, and A. Klemm, *The refined BPS index from stable pair invariants*, Commun.Math.Phys. **328** (2014) 903–954, arXiv:1210.4403 [hep-th] (cit. on p. 98).

List of Figures

1.1	The M-Theory star indicating the string theory dualities between type I, type IIA, type IIB, heterotic SO(32) and heterotic $E_8 \times E_8$ string theories as well as eleven dimensional supergravity. These theories can all be interpreted as being limits of a central M-theory.	2
1.2	Illustration of the duality chain of topological string theory [17].	3
1.3	The quiver diagram of ABJM theory. The two nodes represent the two gauge groups and the lines between represent the connecting bifundamental matter [21].	4
2.1	Chain of dualities in the M/F-theory duality. M-theory compactified on a genus-one fibered CY manifold $X : C \rightarrow \mathcal{B}$ is equal to type IIA on the base of the fibration and one of the circles in the genus-one fiber $S^1_B \times \mathcal{B}$. Here we interpreted the other circle S^1_A in the genus-one fiber as the M-theory circle in the reduction to type IIA. Then we use T-duality on the left over circle S^1_B together with the limit $R_B \rightarrow 0 \Leftrightarrow \tilde{R}_B \rightarrow \infty$ to obtain type IIB compactified on \mathcal{B} . This is given by F-theory on the original manifold X	9
2.2	The 16 two dimensional reflexive polyhedra [80]. The polyhedron F_i and F_{17-i} are dual for $i = 1, \dots, 6$ and self-dual for $i = 7, \dots, 10$	19
2.3	The toric polytope of $X_{F_{11}}$ and its dual are given on the left along with a choice of toric coordinates as well as the corresponding Batyrev monomials, respectively. Here we marked the zero section by a dot. On the right we give the divisor classes of the fiber coordinates.	20
2.4	Codimension one fibers of $X_{F_{11}}$. The crosses denote the intersections with the two sections.	22
2.5	Possible values for (n_7, n_9) for the elliptically fibered CY fourfold $X_{F_{11}}$ with base $\mathcal{B} = \mathbb{P}^3$. The yellow dots denote bulk parts of the allowed region where all matter multiplets given in Table 2.2 are present. The blue dots denote the boundaries of the allowed region where generally not all matter multiplets from Table 2.2 are present. Thus the family solution (2.64) is not possible and diverges.	25
2.6	The toric polytope of $X_{F_{13}}$ and its dual are given on the left along with a choice of toric coordinates as well as the corresponding Batyrev monomials, respectively. Here we marked the zero section by a dot. On the right we give the divisor classes of the fiber coordinates.	27
2.7	Codimension one fibers of $X_{F_{13}}$. The crosses denote the intersections with the zero section.	28
2.8	Allowed region for (n_7, n_9) for the elliptically fibered CY fourfold $X_{F_{13}}$ with base $\mathcal{B} = \mathbb{P}^3$. The yellow dots denote bulk parts of the allowed region where all matter multiplets given in Table 2.2 are present. The blue dots denote the boundaries of the allowed region where generally not all matter multiplets from Table 2.2 are present. Thus the family solution (2.83) is not possible and thus diverges.	31
2.9	(a) Polyhedron F_{13} and its dual polyhedron F_4 . Blue denotes the locus of $(\mathbf{2}, \mathbf{1}, \mathbf{4})$ and red the locus of $(\mathbf{1}, \mathbf{2}, \mathbf{4})$. The transitions to $X_{F_{11}}$ can be triggered by Higgs fields in the representation $(\mathbf{2}, \mathbf{1}, \mathbf{4})$ (b) and $(\mathbf{1}, \mathbf{2}, \mathbf{4})$ (c).	34

2.10	Allowed region of $X_{F_{13}}$. The values for (n_7, n_9) which are not in the allowed region of $X_{F_{11}}$ are colored blue. At the green dots the $SU(4)$ is not present. At the yellow dots the $SU(2)_1$ is not present and at the orange dot both $SU(2)$'s are not present.	36
2.11	The network of Higgsings between all F-theory compactifications on toric hypersurface fibrations X_{F_i} . The axes show the rank of the MW group and the total rank of the gauge group of X_{F_i} . Each CY X_{F_i} is abbreviated by F_i and its corresponding gauge group is shown. The arrows indicate the existence of a toric Higgsing between two CY manifolds.	38
2.12	The toric diagram of polyhedron F_3 and its dual. The toric zero section is indicated by the dot. In the accompanying table we indicate the divisor classes of the fiber coordinates.	39
2.13	Allowed region for (n_7, n_9) for the elliptically fibered CY fourfold X_{F_3} with base \mathbb{P}^3 . The blue dots denote the boundary of the allowed region and the orange dots denote the bulk part where all matter given in Table 2.9 is present.	42
2.14	The toric diagram of polyhedron F_1 and its dual F_{16} with coordinate assignment and the monomials corresponding to the nodes via the Batyrev formula (2.39) respectively. By brevity of notation we set $e_i = 1$ in the Batyrev monomials. In the accompanying table we indicate the divisor classes of the fiber coordinates.	44
3.1	Toric diagram of \mathbb{F}_1 and toric data of local \mathbb{F}_1 . The toric diagram of local \mathbb{F}_1 is three dimensional and can be projected to the given two dimensional polytope.	62
3.2	Toric diagram of \mathbb{F}_2 and toric data of local \mathbb{F}_2 . The toric diagram of local \mathbb{F}_2 is three dimensional and can be projected to the given two dimensional polytope.	67
3.3	Toric diagram and data of resolved $\mathbb{C}^3/\mathbb{Z}_5$. The toric diagram of the resolution of $\mathbb{C}^3/\mathbb{Z}_5$ is three dimensional and can be projected to the given two dimensional polytope.	69
3.4	The phase space of the operator (3.182) for $E = 20$ and $m = 1$ in the $x - p$ plane. The associated toric diagram is up to an $SL(2, \mathbb{Z})$ transformation identical to polyhedron F_{13} in Figure 2.2 which is the dual polytope of the toric diagram of \mathbb{F}_2	79
A.1	Example of an elliptic curve over the field \mathbb{R} with zero point O . The third rational intersection point of the green line intersecting the curve \mathcal{E} at the rational points P and Q is the chord-tangent composition (PQ) . The third intersection point of the blue line through the composed rational point (PQ) and the zero point O with the elliptic curve \mathcal{E} gives the added point $P + Q$	91
A.2	Illustration of the inverse element $(-P)$ and the neutral element O of an elliptic curve \mathcal{E} with zero point O . The inverse element $(-P)$ is constructed as the third intersection point of the line through (OO) and P with the elliptic curve \mathcal{E} (green line). The point (OO) in this construction is the second intersection point of the tangent to the elliptic curve at the zero point O with the elliptic curve \mathcal{E} (red line). The composition of the point P with the neutral element O under the chord-tangent composition law leads to the point (PO) (blue line).	92
A.3	Basic idea of the Nagell algorithm [37]. A cubic with a rational point Q . In general one can construct four lines through Q whose other two intersection points with the cubic agree (see (A.9)). All lines through Q give a double cover of the rational curve.	93

List of Tables

2.1	Classification of different singularities due to Kodaira [45, 46].	11
2.2	Codimension two singular loci of $X_{F_{11}}$, corresponding fiber degenerations and charged matter representations under $SU(3) \times SU(2) \times U(1)$. The multiplicities of the matter representations are calculated from the homology classes of the divisors. The adjoint matter is included for completeness.	23
2.3	Codimension three singular loci and respective Yukawa couplings for $X_{F_{11}}$	24
2.4	(b, n_{D3}) gives the minimal possible number of families b which allows for a cancelation of the D3-brane tadpole (2.27) with the positive and integral number n_{D3} of D3-branes. Here we additionally impose that the CS terms are integral which is an indirect check of the quantization condition (2.26). The points where there is no number of families fulfilling these constraints are marked by "-".	27
2.5	Codimension two singular loci of $X_{F_{13}}$, corresponding fiber degenerations and charged matter representations under $(SU(4) \times SU(2)^2)/\mathbb{Z}_2$. The multiplicities of the matter representations are calculated from the homology classes of the divisors. The adjoint matter is included for completeness.	30
2.6	Codimension three singular loci and respective Yukawa couplings for $X_{F_{13}}$	31
2.7	The entries $(b; n_{D3})$ give the minimal number of families b for which the number of D3-branes n_{D3} is integral and positive for integral CS terms. At the points marked with "-" the number of D3-branes is not a positive integer.	33
2.8	The nodes which have to be identified for a proper matching of the theories after the Higgsing with a multiplet in the $(\mathbf{1}, \mathbf{2}, \mathbf{4})$ representation.	35
2.9	Charged matter representations under $U(1)$ and codimension two fibers of X_{F_3}	41
2.10	Codimension three loci and corresponding Yukawa couplings for X_{F_3}	41
2.11	The entries $\begin{pmatrix} \chi_3 & \chi_2 \\ \chi_1 & n_{D3} \end{pmatrix}$ give chiralities χ_1, χ_2 and χ_3 for which the number of D3-branes n_{D3} is integer and positive while the CS terms are also integral. The fluxes were parametrized by the chiralities χ_2 and χ_3 . At the allowed points for (n_7, n_9) marked as "-" the flux coefficients a_2 and a_4 diverge for the choosen parametrization.	44
2.12	Charged matter representation under \mathbb{Z}_3 and corresponding codimension two fiber of X_{F_1} . The given multiplicity is obtained field theoretically by the Higgsing from X_{F_3}	46
2.13	Codimension three locus and corresponding Yukawa coupling for X_{F_1}	46
3.1	Instanton numbers for local \mathbb{F}_1 at order \hbar^0 and \hbar^2	65
3.2	Instanton numbers for local \mathbb{F}_1 at order \hbar^4 and \hbar^6	65
3.3	Instanton numbers for local \mathbb{F}_2 at order \hbar^0 and \hbar^2 . Note the difference in $n^{0,1}$ for \hbar^0 compared to topological vertex calculations [103, 116]. This discrepancy has also been found and discussed in [117].	69
3.4	Instanton numbers for local \mathbb{F}_2 at order \hbar^4 and \hbar^6	69

3.5	Numerical energy spectrum for the operator of local \mathbb{F}_2 in (3.181) for $m = 1$ and $\hbar = 2\pi$. Here we give the values for three different matrix sizes in order to find the numerical precision.	81
3.6	Numerical energy spectrum for the operator of local \mathbb{F}_2 in (3.181) for $m = 2$ and $\hbar = 2\pi$. Here we give the values for three different matrix sizes in order to find the numerical precision.	81
3.7	Numerical energy spectrum for the operator of local \mathbb{F}_2 in (3.181) for $m = \frac{5}{2}$ and $\hbar = 2\pi$. Here we give the values for three different matrix sizes in order to find the numerical precision.	81
3.8	First energy levels calculated analytically from the quantization condition (3.196). We use $\hbar = 2\pi$ and $m = 1$, $m = 2$ and $m = \frac{5}{2}$. The degree denotes the order of expansion for the periods and the free energy. The numerical values were given in Table 3.5, 3.6 and 3.7 for a matrix size of 500.	82

Acronyms

- ABJM** Aharony-Bergman-Jafferis-Maldacena. 4, 5, 76, 79, 81
- BPS** Bogomol'nyi-Prasad-Sommerfield. 16
- CFT** conformal field theory. 3, 4
- CS** Chern-Simons. 3, 18, 19, 28–30, 35, 36, 45–47, 51, 91, 100
- CY** Calabi-Yau. 2–6, 9, 11–13, 15, 18–21, 28, 29, 34–36, 39–42, 45, 46, 53, 56, 58–62, 76, 77
- FI** Fayet-Iliopoulos. 20
- GW** Gromov-Witten. 57
- MW** Mordell-Weil. 5, 13, 14, 21, 23, 24, 31, 32, 40, 41, 43, 48, 91, 92, 95
- NS** Nekrasov-Shatashvili. 6, 58, 60, 63, 65, 68, 72, 75, 79, 81–83, 91–93
- NS-NS** Neveu-Schwarz-Neveu-Schwarz. 10
- PF** Picard-Fuchs. 74, 92
- QED** quantum electrodynamics. 1
- QFT** quantum field theory. 1, 2
- R-R** Ramond-Ramond. 9, 10
- SR** Stanley-Reisner. 20, 21, 23, 27, 31, 32, 42, 43, 45, 47
- TS** Tate-Shafarevich. 5, 15, 40, 41, 48, 91
- vev** vacuum expectation value. 20, 38, 39, 91
- WKB** Wentzel-Kramers-Brillouin. 62, 64, 68, 70, 72, 74, 92, 99